Master Thesis, Department of Geosciences

Sedimentological and reservoir geological developments of Triassic/Jurassic formations in Åsta Graben (well 17/3-1)

Kamran Javed

UNIVERSITY OF OSLO

FACULTY OF MATHEMATICS AND NATURAL SCIENCES

Sedimentological and reservoir geological developments of Triassic/Jurassic formations in Åsta Graben (well 17/3-1)

Kamran Javed

Master Thesis in Geosciences

Discipline: Petroleum Geology and Petroleum Geophysics

Department of Geosciences

Faculty of Mathematics and Natural Sciences

University of Oslo

June 3rd , 2013

Tutor(s) : Henning Dypvik and Lars Riber, UiO

This work is published digitally through DUO – Digitale Utgivelser ved UiO

http://www.duo.uio.no

It is also catalogued in BIBSYS (http://www.bibsys.no/english)

Abstract:

This study deals with the weathering of basement, resulting particle formation, depositional conditions, provenance and mode of transportation of Triassic/Jurassic strata in evolving rift basin setting in Stord Basin. Data from sedimentary core logging, XRD and petrographical analysis of cutting and core intervals from well 17/3-1 have been integrated to elucidate the depositional transition from basement to Triassic/Jurassic.

Fracture filling calcitic veins and striations are observed on basement indicating local basement has undergone different post Caledonian tectonic events. The low XRD% of kaolinite and high XRD% of plagioclase in studied section above basement indicates an absence of weathering profile. Lower part of the Smith Bank Formation is sourced by local basement identified on the basis of high amount of quartz and feldspar grains in mudclasts, high plagioclase XRD%, and high striated calcite percentage, deposited in alluvial fan settings. Mineralogical change observed by introduction of K-feldspar indicates another source than amphibolitic basement in middle part of the Smith Bank Formation. Mudclasts having more clayey content indicate sediments originated from distal source. High clay percentages, Gamma ray trends show deposition as channel sediments and floodplains by axially flowing meandering river. Structural settings of Utsira High makes it improbable provenance for sediments in study area. Uplifted hinterland of Fennoscandian shield is main probable provenance for middle part. The progressive decrease in feldspars in uppermost part of Triassic sediments depicts that basin has achieved tectonic maturity.

On the basis of observed structures Bryne Formation is interpreted to be deposited in delta plain/tidal flat settings. Sandnes Formation is interpreted to be deposited dominantly in shallow marine settings. It is overlying the non-marine Bryne Formation, suggesting a rise in sea level. Feldspars have been transformed mostly to clays by late diagenetic alteration noticed by XRD results and thin section analysis. The presence of Saponite rich clay intervals indicates altered basic, ultra basic rocks as one of probable source for this formation or by alteration of nontronite.. The possible source for these formations can be volcanic rocks in south of study area or from mainland Norway.

Keywords: Stord Basin, Smith Bank Formation, provenance, depositional conditions, XRD, thin section.

Table of Contents

1. Introduction

This master thesis is part of 'Utsira Project' supported by Lundin A/S titled as 'Petrography and porosity development in reservoir formations on the Utsira High-Importance of provenance weathering vs diagenesis'.

The project study aims to explore and understand weathering, clastic particle formation, origin and deposition of particles derived from the basement in regards to their immense significance for reservoir evaluation. In differnt petroleum basins like Chesapeake Bay area and North Sea basin, the weathering of the basement and resulting deposition of good quality reservoirs are of great interest in recent studies e.g. Quartz provenance studies of southern Utsira High and Draupne sandstone proved that Draupne sandstone is a product of erosion and short distance transportation of weathered material (Fredin et al., 2013). In the North Sea fractured and weathered basement plays an important part in hydrocarbon play on southern Utsira high (Fredin et al., 2013).

The study of weathering of basement rocks has been of great importance and studied in this project. Weathering profiles are studied and analyzed in detail from the Precambrian gneisses and granites of southern Scandinavia i.e. Scania and Bornholm by other project members. The provenance of the weathered material, its deposition in evolving rift basins has also been studied.

This thesis will focus on the basement, its weathering and resulting particle formation, the possible source for Triassic sediments will be studied and transportation and deposition of these particles in the rift basins will be analyzed in detail.

In this thesis, cutting samples from basement and Smith Bank Formation along with the cores from basement, Bryne Formation and Sandnes Formation are studied in detail (Fig 1). The sample material is studied petrographically and mineralogically (thin sections and XRD). The main purpose of the thesis is to comprehend the weathering of basement and transition from basement to Triassic strata.

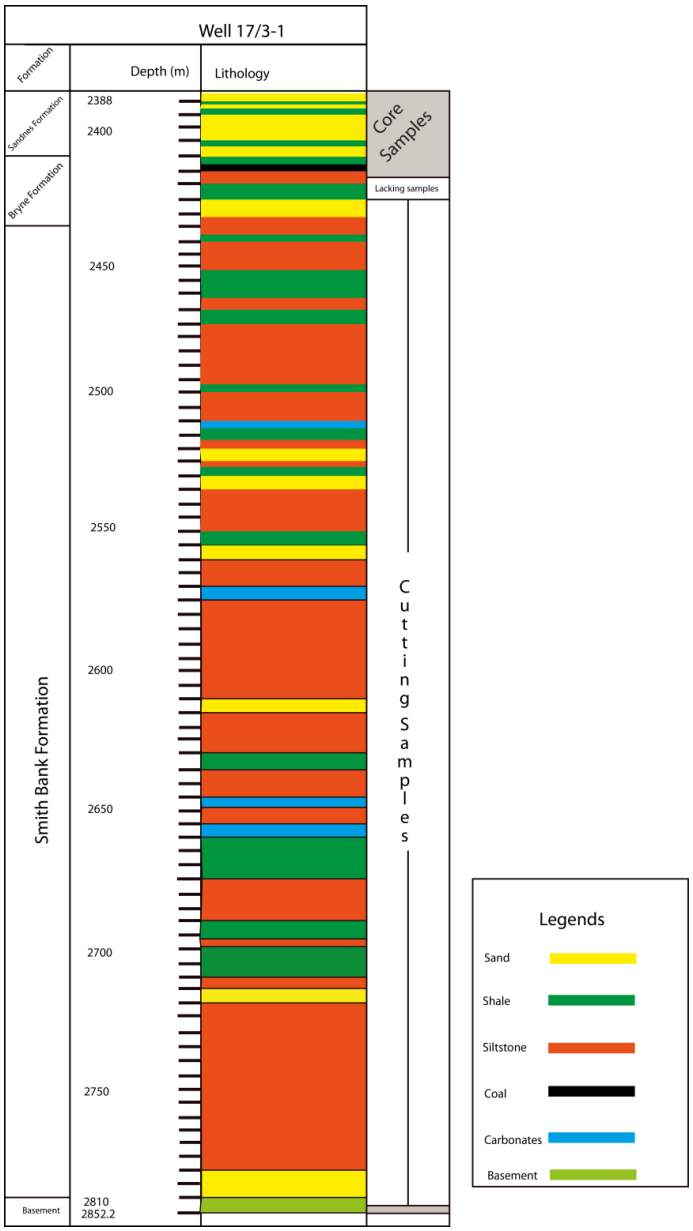

Fig 1: Showing lithostratigraphy of Well 17/3-1 and type of samples obtained.

1.1 Location of the study area

The study area is located in the Southern part of Stord Basin, North Sea, Norway (Fig 2). Well 17/3-1 is located on a horst structure (Fig 3). The Stord Basin lies to east of Viking Graben and it is an east-sloping extensional basin. This basin is also the result of normal faulting associated with Permo-Triassic extension in the North Sea. In the Stord Basin convincing evidence for major rifting in early Triassic is present (Mardsen et al., 1990, Steel and Ryseth, 1990).

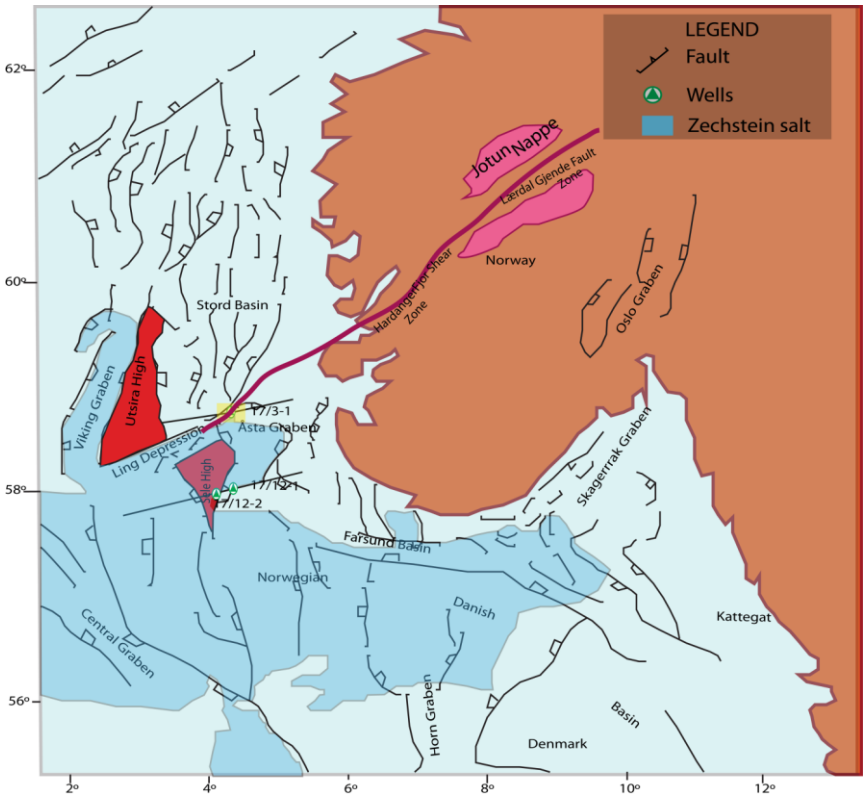

Figure 2: Structural map of North Sea. Location of study Well in yellow rectangle modified from Heerman and Faleide (2004) and Fossen & Hurich (2005).

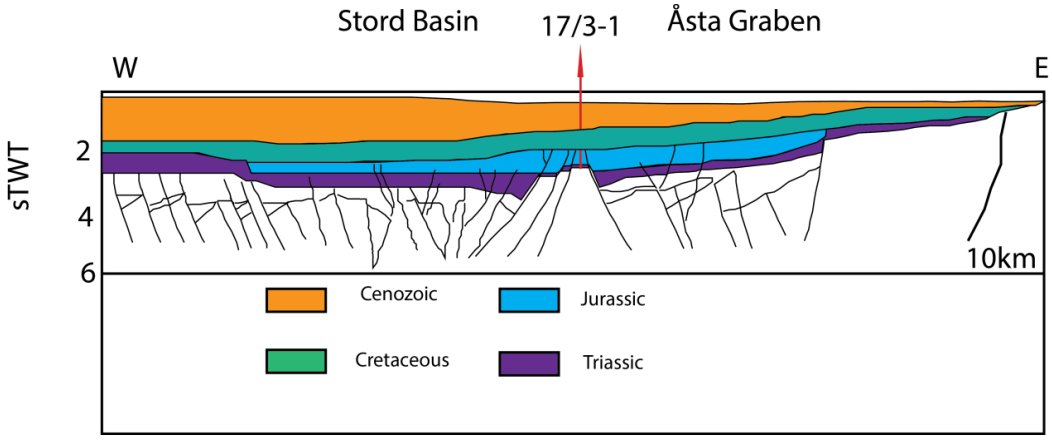

Fig 3: Profile across well 17/3-1modified from Heerman and Faleide (2004).

Well 17/3-1 is presumably located on a basement high, a high relief accommodation zone defined by Rosendahl, 1987. According to Faulds et al., 1998 this accommodation zone may be called as oblique synclinal accommodation zone. As this high hindered the further northward propagation of the Permian salt lakes e.g Heerman and Faleide, 2004. This part of the basin remained topographically elevated than neighboring grabens and basins during

permo-triassic rifting. From Fig 2 and Fig 3 it can also be seen that Well 17/3-1 is located on an intrabasinal horst present in oppositely dipping faults.

2. Tectonic History and Geological Evolution

The North Sea area is a part of north-west European continental shelf and has a long and complex geological history. North Sea developed through various geological evolutionary stages from Cambrian to recent times. The five main stages described by Ziegler 1975 are as follows

1) Caledonian stage (Cambrian-Devonian)

2) Variscan stage (Devonian to Carboniferous)

3) Permian-Triassic intracratonic stage

4) Rifting (Late Triassic to early Tertiary)

5) Postrifting stage (Tertiary)

Among the above mentioned five main phases shown in which played role in tectonic evolution of the North Sea area, first three will be discussed ahead. Fig 4 shows the main tectonic phases which occurred in the North Sea area.

2.1 Caledonian stage

The 'Caledonian Deformation Front' in the southeastern North Sea resulted from collision of micro-continent Avalonia and Baltica (Abramovitz & Thybo, 1998). Avalonia separated from Gondwana during Early Ordovician and collided with Baltica first at 440-435Ma. This collision led to closure of Tornquist Sea and formed Thor-Tornquist suture (Fig.5). Later Laurentia collided with Baltica and Avolania and caused in closure of Iapetus Ocean and formed Laurassia. These collisions resulted in the formation of Caledonian orogenic belt (van Staal et al., 1998).

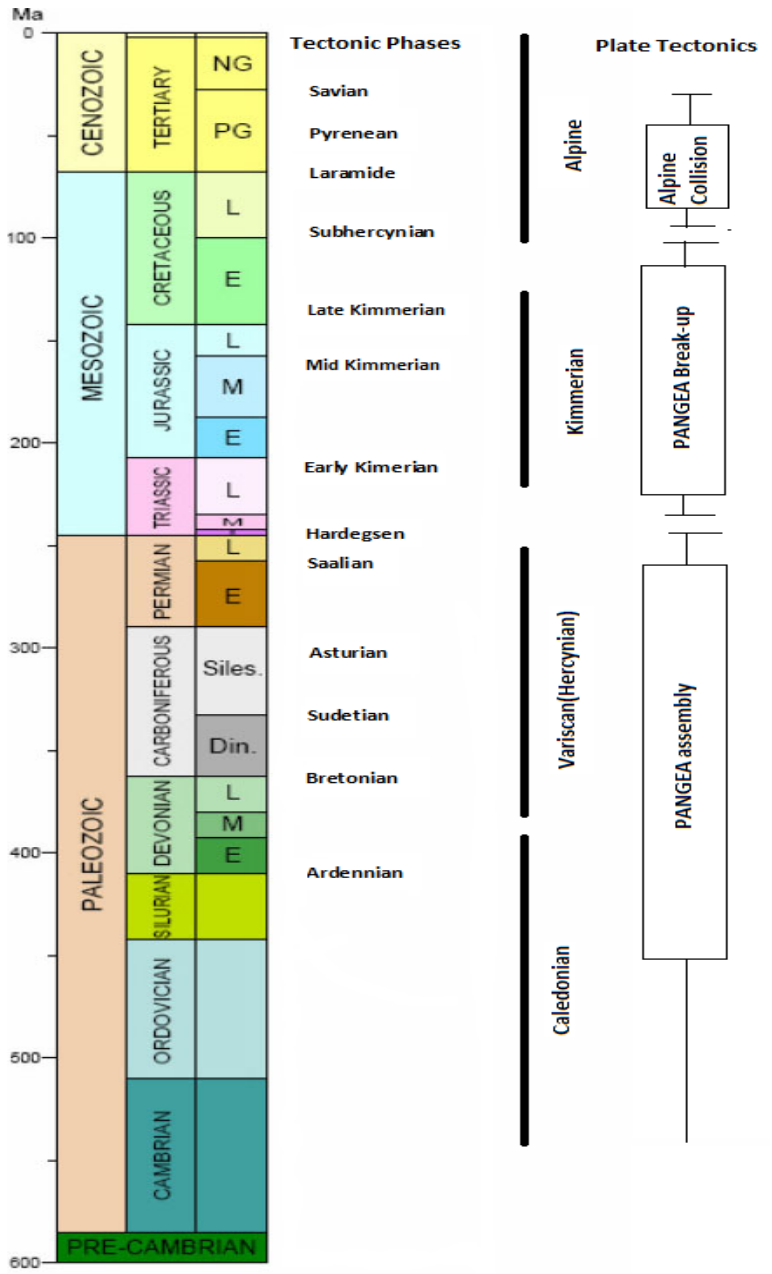

Fig 4: showing different tectonic phases and events occurring in the North Sea Area from Paleozoic to Cenozoic modified from epgeology.com.

The Caledonian orogeny resulted in rocks which act as basement in the North Sea and have varied composition and age. Accordingly two different sets of age groups can be recognized (Eide, 2001)

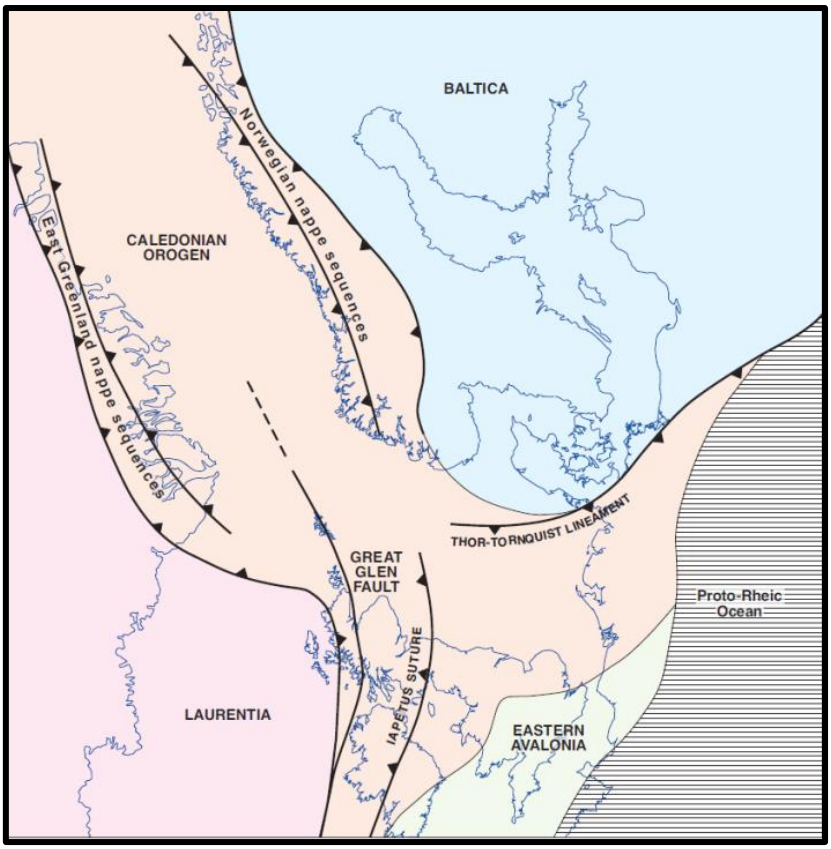

Figure 5: Showing early Paleozoic plate position and suture zones in North Sea region from Bassett (2003).

The older rocks which are identified in only few wells in Norwegian, Danish and UK sectors show dates of about 750 to 700Ma. The rocks are mostly granitic gneissose to hornblende. The younger suite of rocks is more widespread and their ages range in about 480Ma to 430 Ma (Frost et al., 1981). Medium to high grade metamorphic rocks were formed as a result of Early Ordovician to Early Silurian phases of Caledonian orogeny across whole of North Sea. In few wells (418-350 Ma) Late Silurian to Early or Mid-Devonian ages are reported, the result of early Acadian, terminal Caledonian tectonic coupling and associated age re-setting with granitic intrusion (Basset ,2003).

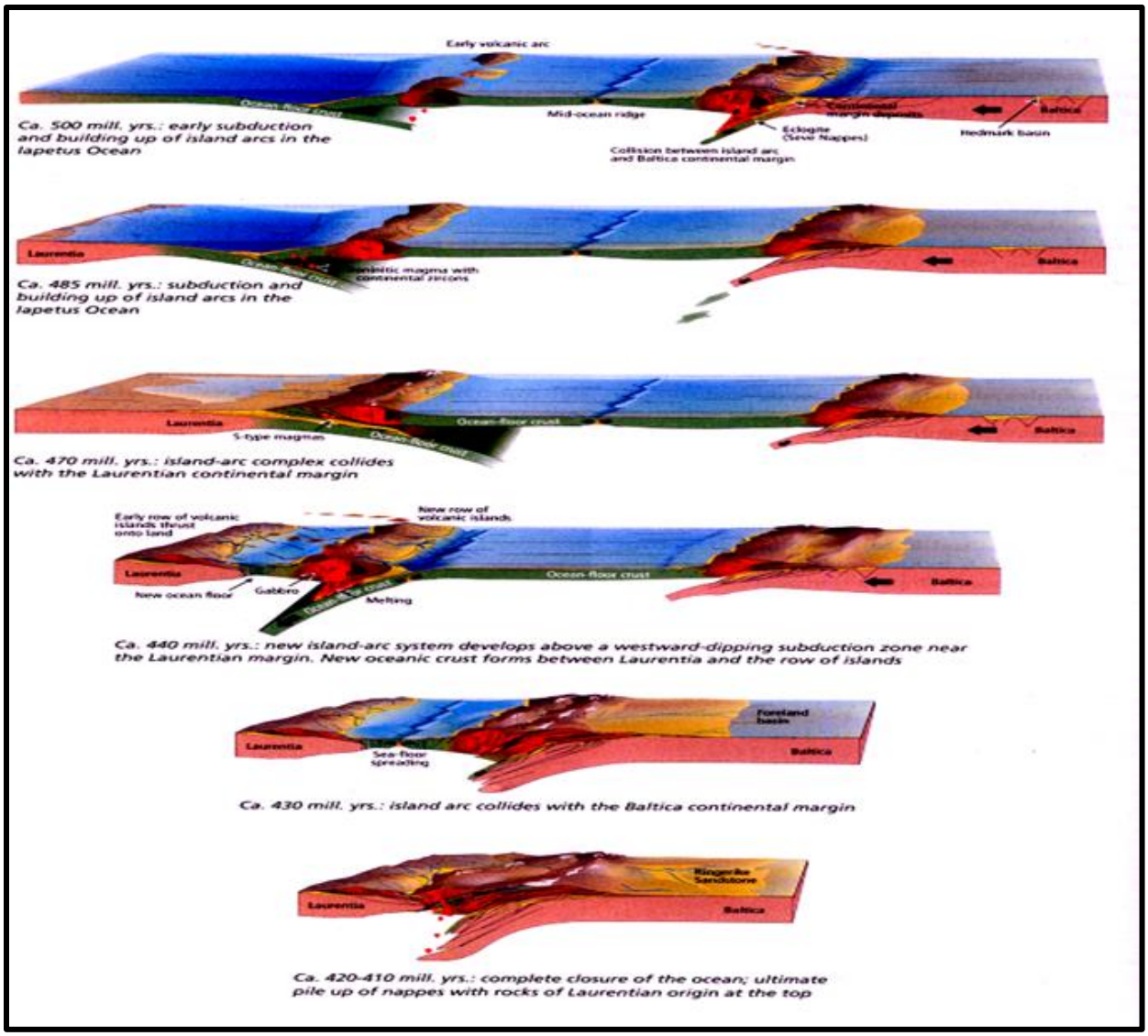

Fig 6: Showing evolutionary stages of Caledonian orogenic belt from the late Cambrian to transition from Silurian to Devonian from Fossen et al. (2002).

2.1.1 Generalized Composition of Caledonian Basement

North of lineament joining Hardangerfjord Shear Zone, Ling Graben and Highland Boundary Fault the North Sea has crystalline basement which is composed of metamorphic rocks of high grade along with intrusive igneous rocks. These rocks were deformed, showing that they have undergone retrogressive overprinting during 440-450 Ma. Various younger intrusions are present as well e.g 410Ma granite in well 16/2-1(Frost et al., 1981).

South of the lineament joining Hardangerfjord Shear Zone, Ling Graben and Highland Boundary Fault the rocks show low-grade metamorphism having age in between 440-450Ma.

The plutonic rocks which have not been deformed and Precambrian rocks in northeastern zone have been overprinted by late Caledonian events (Frost et al., 1981).

This varied basin substrate exerted a control on complex Mesozoic extensional sedimentary basin formed in latter ages (Færseth, 1996).

2.2 Variscan Orogeny

The Varsican orogeny is a Late Paleozoic collisional event starting in Devonian, having climax during the late Carboniferous and ended almost in Early Permian (Warr, 2012). The collision of Gondwana with the Laurassia during Carboniferous resulted in the formation of Variscan Mountains. Long periods of intracontinental deformation were associated with the collision of Laurassia and Gondwana, which rotated clockwise. This rotation added a SW-NE stress direction to Laurassia (McCann et al., 2008).

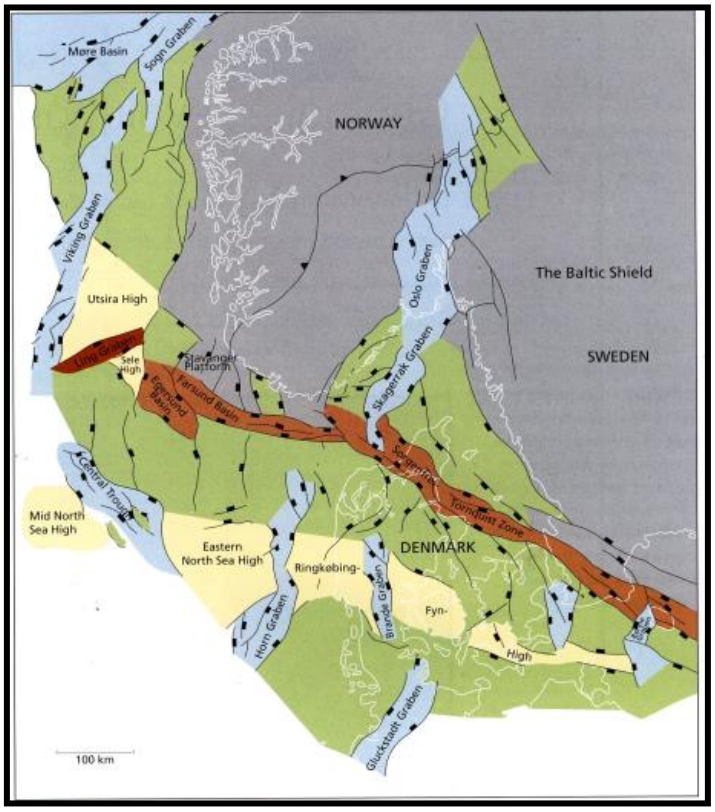

Figure 7: Showing structural elements of North Sea.Various extensional basin due to movement along Sorgenfrei-Tornquist zone (Varsican age) from Larsen et al. (2008).

The northernmost of the fracture zones is Sorgenfenfrie-Tornquist Zone displaying northwest-southeast trend (Fig 7). The lithosphere experienced both extension and shear displacements north and south of Sorgenfrei-Tornquist zone. The extensional features resulted in the

formation of grabens and rift structures, Oslo Rift being one of them (Fig 7) (Larsen et al., 2008).

2.3 Permian-Triassic rifting:

The Variscan compressive tectonics changed to an era of extension and collapse. Though the North Sea rift has a more prolonged history starting with the Devonian extension of thick Caledonides e.g. Hardangerfjord Shear Zone which experienced top to WNW Devonian extensional transport (Fossen, 1992) and Nordfjord-Sogn Detachment Zone dipping 25° to the north (Færseth, 1996) The lateral extent of these Devonian extensional zones are shown in (Fig.8)

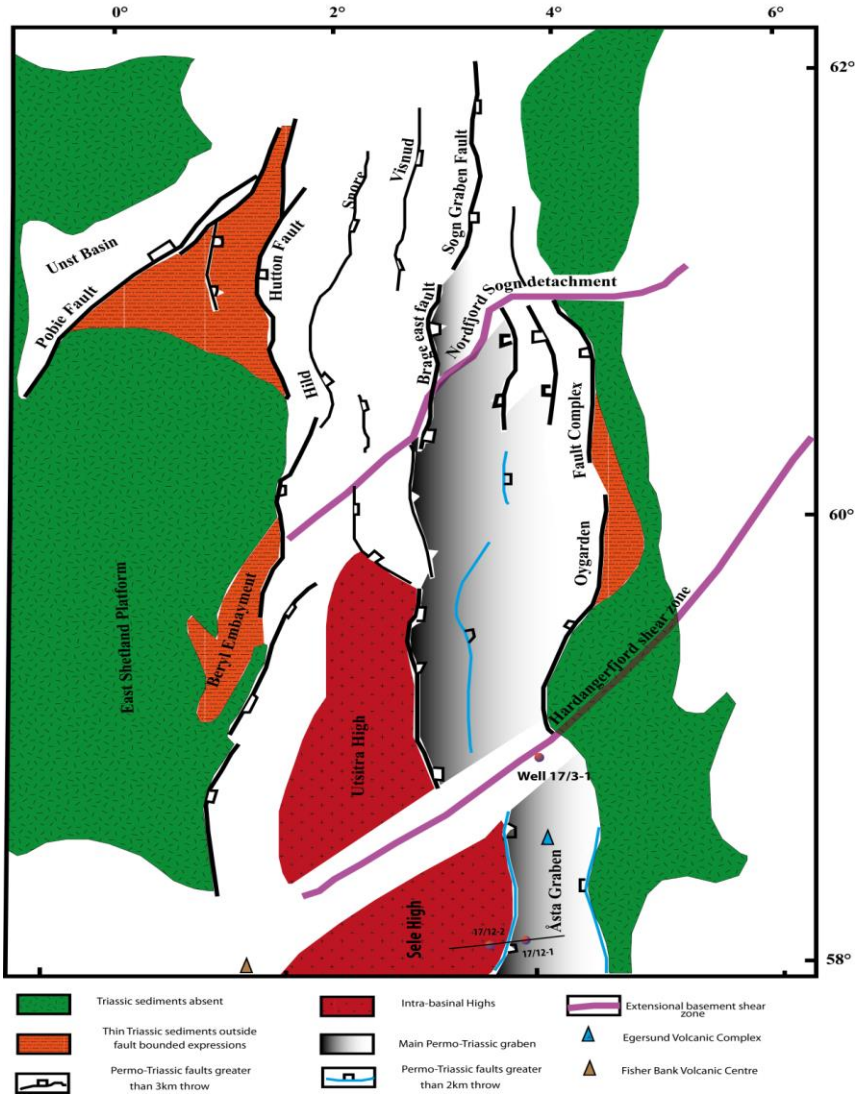

Figure 8: Main Permo-Triassic structural and tectonic features resulting from extensional tectonics modified from Færseth (1996) and Smith et al. (1993).

According to Gabrielsen et al. (1990) the rifting initiated in the North Sea in Permian and continued into the Scythian. This was supported by the presence of Permian dykes in the southwest Norwegian coastal area of intra-Permian age (c.260Ma) (Faerseth et al., 1995a). In the Nordfjord-Sogn Detachment Zone (Fig.8), the reactivation of brittle low angle faults and activation of Lærdal-Gjende Fault (Fig.2) show paleomagnetic age of 250-260Ma (Andersen et al., 1999). Block faulting below the Zechstein in southern Viking Graben and below Åsta Graben and Ling Depression also indicates initiation in Permian (Fig 9). The center for Permo-Triassic stretching was beneath Jurassic Viking Graben. (Færseth, 1996).

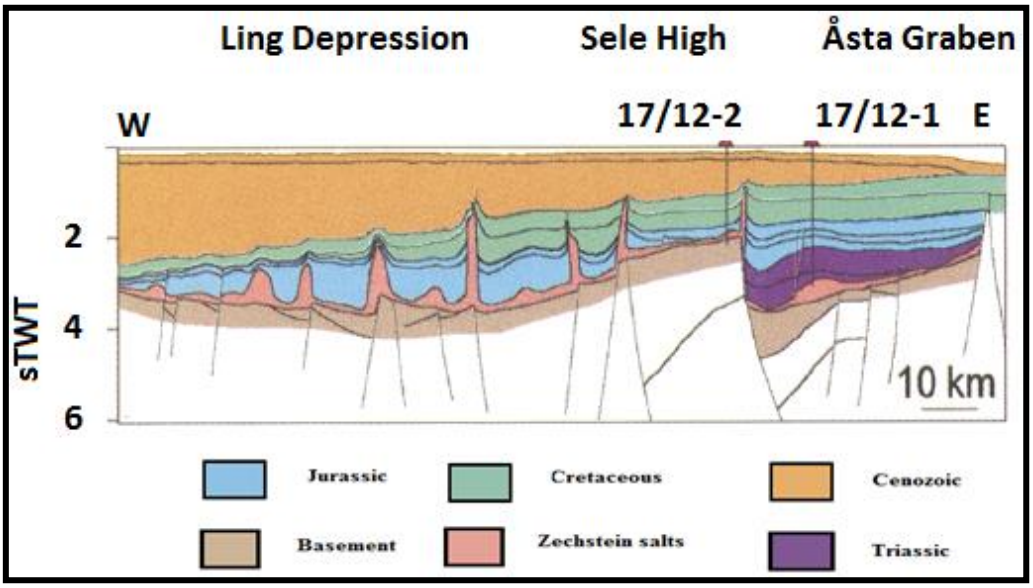

Figure 9: Pre-Zechstein block faulting, profile shown in Fig 2 and Fig 8 from Heerman and Faleide (2004).

2.3.1 Northern North Sea basin development in Permo-Triassic:

The northern part of the North Sea is an almost 170-200km wide basin and has a north trending extension, bounded by Norwegian mainland on East and Shetland Platform on West (Fig 8). It is an elongated, linked half graben system formed by almost E-W extension (Badley et al,. 1988).

Since the Early Permian the North Sea area represented an intraplate setting. North Sea basin has a very complex structure possibly due to reasons i.e

i) Due to varied Caledonian basin substrata upon which extensional events took place.
ii) Permo-Triassic extensional phase and Jurassic extensional regime and related subsidence.

The variation in Caledonian basement is both in terms of composition and grain across the basin (Færseth, 1996). Zeigler, 1990 suggested that start of Triassic rifting of North Sea was not accompanied with major lithospheric disturbance thus displayed low volcanic activity and only limited uplift of rift flanks.

In the Triassic the central and northern North Sea separated from southern North Sea Permian-Early Triassic rifting resulted in structures that can be observed on both sides of Viking Graben. The Triassic faults mostly have N-S strike (Fig.8). The fault activity in the North Sea resulted in formation of half graben with changing polarities along strike. The Permo-Triassic faults involving the basement have throws (4-5km) which is much higher than Jurassic reactivation of these faults (<300m) (Heeremans and and Faleide, 2004).

In early Triassic the basins formed were more distinct but towards the end of Triassic they subsided to form single broad alluvial plain (Nyusten et al., 2008).

2.3.2 Sedimentation in Triassic:

Triassic strata is present in most parts of the North Sea (Fig 11), in few places ranging upto 5-6 km thick e.g. the Stord Basin in the North Sea (Brekke et al., 2001). Most of the Triassic remained a period of thermal relaxation except late Permian-early Triassic extension. The rate of sedimentation was high enough to keep pace with the rate of subsidence. If the sedimentation rates would have been less in comparison to accomodation space being created then rift basins might have been converted to marine basins (Faleide et al,. 2010). The Triassic sediments are mainly red beds including alluvial fan, aeolian sabkha, and fluvial, shallow marine and lacustrine facies (Fig.10).

The Scandinavian Craton which is present along the eastern margin of the basin was uplifted in response to Permo-Triassic rifting and eroded throughout the Triassic. The uplifted Scandinavian Craton was major source of clastic sediments in Triassic (Coward, 1995). The thermal subsidence of basins formed due to rifting in Permian-Early Triassic resulted in uplift and erosion of mainland in the Middle Triassic-Early Jurassic times (Brekke et al., 2001).

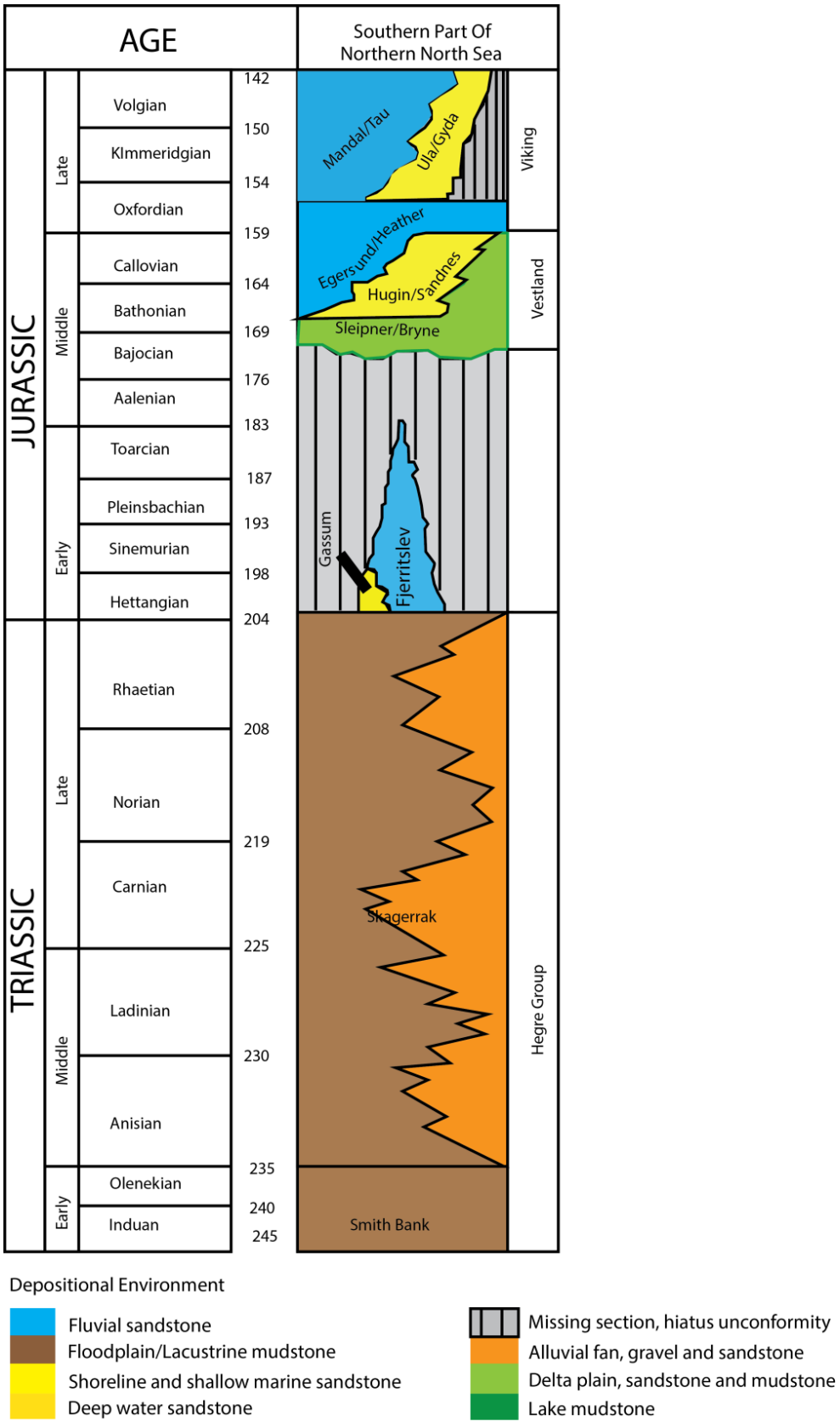

Figure 1: Stratigraphic sequence and depositonal environments in southern parts of North Sea modified from Nøttvedt et al. (2008)

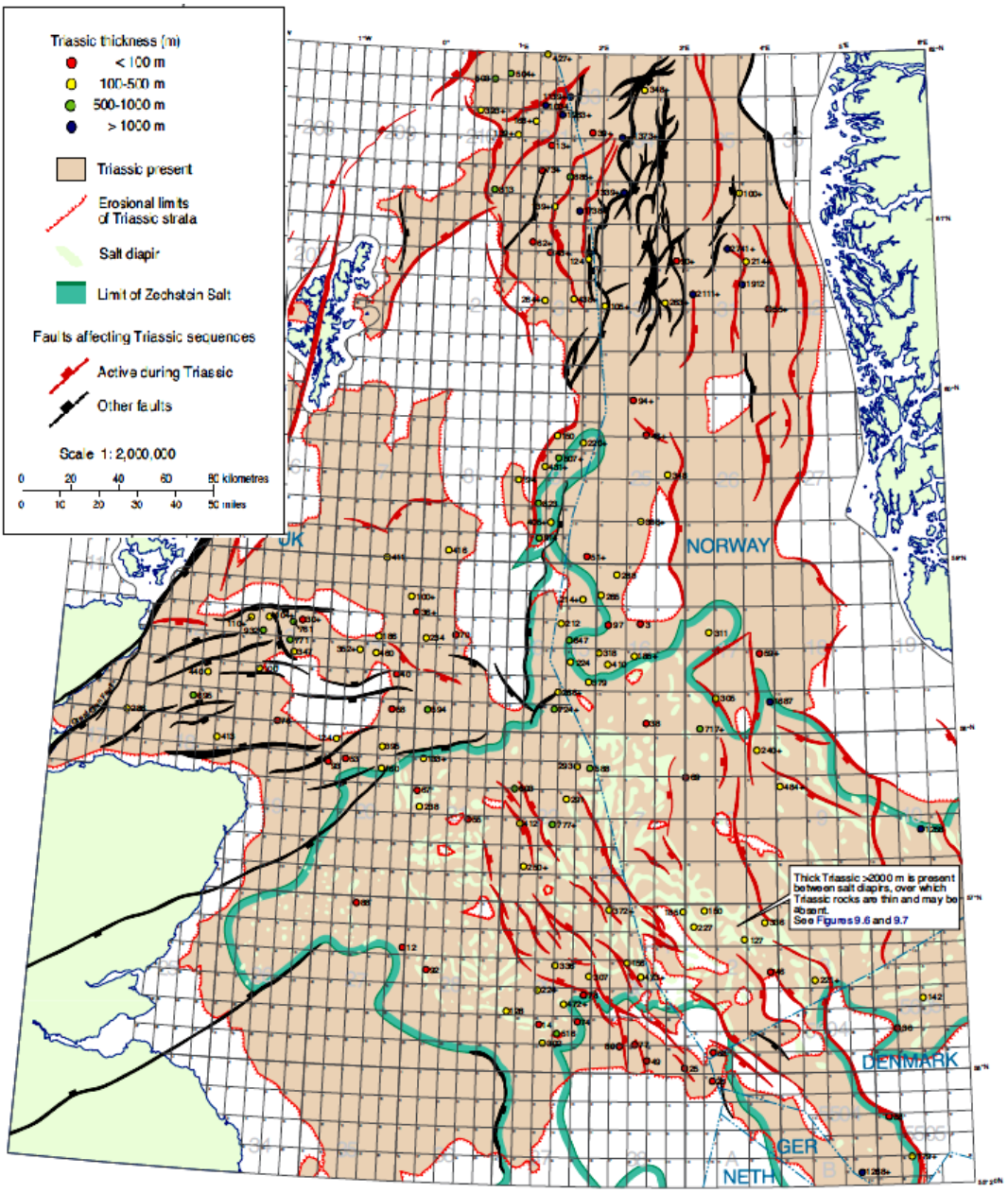

Figure 11: Triassic sediments in North Sea and major faults active in Triassic and Jurassic extensional episodes from Evans et al., 2003)

In early Triassic most of the sediment accumulation and extension occur along limited number of major rift boundary faults trending NNE to NNW. Alluvial fan deposits from fault scarps are found in active fault-bounded basins (Brekke et al., 2001).

2.3.3 Triassic stratigraphy in Well 17/3-1:

In well 17/3-1 Triassic deposits are named as Smith Bank Formation. According to Deegan and Scull (1977), the Smith Bank Formation is a repetitive sequence of brick red, silty claystone with ocassional sandstone streaks. In some areas sandy units may be present at base.

The mudstones are unfossiliferous and deposited in distal continental envrionments . The Smith Bank Formation deposited in possibly extensive lacustrine/floodplain environments under continental playa conditions or in a widespread lake in which sediment and fresh water supply surpassed evaporation (GOLDSMITH et al., 1995)(Fig.10).

The Permian sediments are absent in the Stord Basin. In Well 17/3-1 Triassic sediments are directly overlying amphibolitic basement. The measured thickness of Triassic sediments is 311m which is less compared to western part in Stord Basin and in east from Åsta Graben (Fig 3).

2.4 Paleogeography and Paleoclimate:

The Triassic paleogeography is quite unique. Pangea, the supercontinent existed and was centred almost on equator. Fig 12 showing the continents extending from 85°N to 90°S, surrounded by Panthallasa Ocean (Preto et al., 2010). At the start of Triassic, Norway was located in sub-tropical zone north of equator but due to northward movement of Pangaen plate the Norway and Northwest Europe entered into a temperate climatic zone.

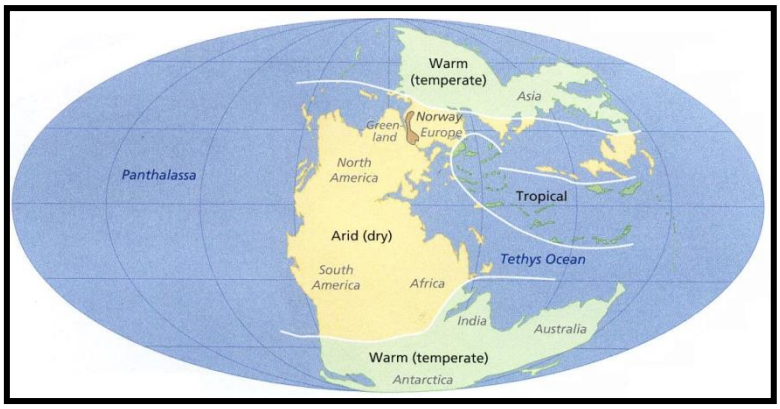

Figure 12: Reconstruction of climatic zones and extent of the continents from Nyusten et al. (2008).

In Early Triassic the intense hot climate persisted, continuing from the end-Permian. An indication of arid climate is the deposition of Red beds of Lower Triassic which have been widely distributed across central Europe. But the Red beds could probably be deposited under strongly seasonal climate as indicated by the presence of paleosols (Preto et al., 2010).

The Middle Triassic records an arid to semi-arid climate on the western end of Tethys. On the eastern Tethys more warm and temperate conditions prevailed. An increase in rainfall is described by Parrish et al. (1982) during Middle and Late Triassic.

The Late Triassic is usually considered as an era of intensified monsoonal rainfall. Various theories have been proposed by Preto et al. (2010) for this climatic change like:

i) Uplifting in the Tethys region resulted in changed atmospheric circulation
ii) Global climate change due to large masses of igneous eruption.
iii) Carnian Pluvial Event, which record the peak of mega-monsoon.

2.4.1 Positions of North Sea basins and climatic effects:

During Triassic time the North Sea basins were located approximately 20°N. Monsoonal or seasonal precipitation occurred, resulting into sheet floods, followed by periods of high temperature and drought throughout the year (Preto et al., 2010). Fluvial sedimentation was much more common throughout the Triassic in northern North Sea basin (Clemmensen 1979). Parrish et al. (1982) suggested that precipitation in later Triassic is much higher than Early Triassic in North Sea Basin and probably due to dispersal of Pangean plates, North Sea moved to 30°N. In latest Triassic i.e Norian-Rhateian times, there is a widespread marine trangression from Boreal Sea in North and Tethyan oceans in South. This transgression marked change to marine environment (Clemmensen et al., 1980).

2.5 Jurassic basin Development:

The Early Jurassic period was tectonically quiet, however in the Late Early Jurassic the North Sea suffered an uplift which resulted in so called Mid Cimmerian Unconformity (Ziegler 1982a). Middle Oxfordian to Early Kimmeridgian times marked the onset of major rifting phase which continued to earliest Cretaceous, followed by post rift subsidence characterized by N-W, S-E trending Viking Graben (Ziegler 1982a). The maximum stretching phase was in Late Jurassic. The extension which took place in Jurassic was much more concentrated along axis of Viking and Sogn Graben and is localized. The initial stages of Jurassic rifting affected the broader area than final stages of graben formation (Gabrielsen et al., 1990). A mosaic of smaller fault blocks and a marked compartmentalization of fault blocks were the result of Jurassic extension. Major faults of Permo-Triassic origin also show indication of Jurassic reactivation (Færseth, 1996).

2.5.1 Jurassic North Sea doming:

Another important event which affected the depositional architecture of North Sea was regional uplift and subsidence of the North Sea during Jurassic. In the Early Middle Jurassic,

the southern North Sea moved across a hot mantle plume, and this thermal anomaly resulted in uplift of the area. (Nøttvedt et al., 2008)

2.6 Lower to Middle Jurassic Stratigraphy:

The Jurassic stretching in the northern North Sea in general was quite confined and the sediments deposited during this age transgress the margins of Permo-Triassic basin (Færseth, 1996).

A rise in sea-level from Early to Middle Jurassic is reflected in shallow shelf clastic sediments in North Sea. The Lower Jurassic succession in the northern North Sea comprised mostly of mudstones and fluvial sandstone. These sediments show the southern extent of Boreal Sea during Lower Jurassic .Lower Jurassic sediments are not uniformly distributed south of Ling Depression (e.g. Hamar et al., 1982). The uplift due to mantle pluming resulted in the significant erosion during Middle Jurassic and as a result Lower Jurassic sediments are almost absent from southern part of the northern North Sea (Nøttvedt et al.2008) (Fig 10). Ziegler (1982a) suggested that the dome had lowlying but irregular regional relief which resulted in formation of paralic environment in areas which experienced differential subsidence.

A stratigraphic break termed ‘Mid- Cimmerian Unconformity’ marks the boundary between Middle and Lower Jurassic. Middle Jurassic times is characterized by progradation of clastic wedges resulting from erosion related updoming and associated building of the Middle Jurassic Brent Delta in central and northern parts of the North Sea. In the Late Jurassic times updomed areas collapsed and marine conditions occurred due to rising sea levels (Underhill and Partington, 1993).

2.6.1 Jurassic Stratigraphy in Well 17/3-1:

Bryne Formation and Sandnes Formation are part of the Vestland Group. Vestland Group is correlative to Middle Jurassic Brent Group (Deegan & Scull, 1977)(Fig 10). Vestland Group deposition resulted in response to uplift in south (Falt et al,. 1989) . The base of this group overlies the Intra-Aelenian Unconformity. In the Norwegian waters, there is an overall change observed from nonmarine to marine deposition in the Bryne, Sandnes, Haugesund and Egersund formations (Husmo et al., 2002)

In well 17/3-1 the Vestland Group consisting of Bryne Formation and Sandnes Formation are unconformably overlying the Triassic Smith Bank Formation (npd.no).

Bryne Formation mainly comprises interbedded sandstones, siltstone, coals and shales, predominantly of coastal plain origin. The age of Bryne formation is Bajocian to Bathonian (Vollset and Dore, 1984) (Fig 10).

Sandnes Formation consists of massive white, fine to coarse grained sandstone. It is friable, not well sorted. The shales are micaceous and occassionaly carbonaceous. The age of Sandnes is Callovian (Vollset and Dore, 1984) (Fig 10).

2.7 Geology of Southwest Norwegian Caledonides:

Fig 13 illustrates the distribution of metasupracrustal rocks of outer Hardangerfjorden area in western Norway which were subjected to polyphase deformation during tectonic evolution (Færeseth, 1982).

2.7.1 Lithological description of main units

The main lithological units exposed in Hardangerfjord area are discussed below:

Sunnhordland Precambrian Basement:

The Precambrian basement can be divided into three main units (Andersen and Færeseth, 1982).

i) Old complex of orthogneisses and paragneisses.
ii) Low grade supracrustal rocks.
iii) Sveconorwegian granites and gabbros .

Valen Mica Schists

This sequence comprises of monotonous, non-calcareous mica schists of deep water facies of shallow water autochthonous deposits (Andersen, 1978).

Halsnøy Complex

Halsnøy Complex has tectonic contact with Valen Mica Schist to the east and Hardangerfjorden group to the west. Halsnøy complex is predominantly quartzo feldspathic mylonite gneiss having amphibolitic bands and impure marble.

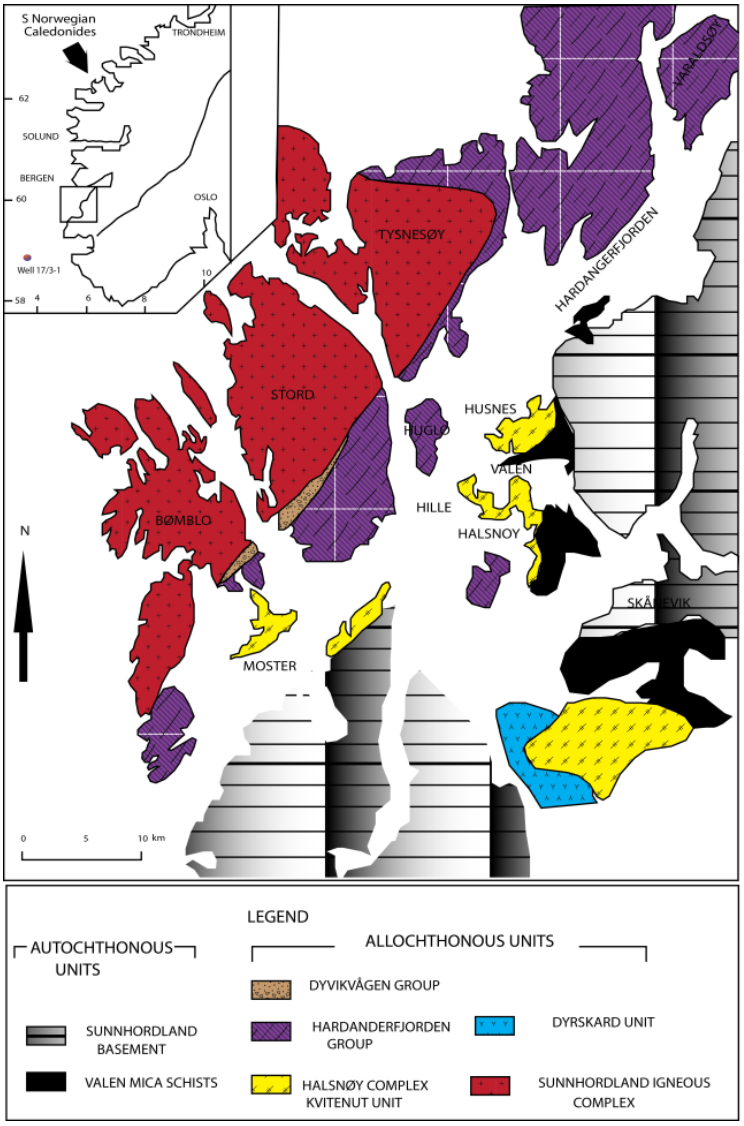

Figure 13: Generalized geological map of the Sunnhordland-outer Hardangerfjord area showing main litho structural units (Modified from Færeseth, 1982 and Andersen and Færeseth, 1982).

Sunnhordland Igneous Complex

The Sunnhordland Igneous Complex occupies the northern part of islands of Bømlo, Stord and Tysnesøy (Fig 13). A thick sequence of basalt and basaltic andesites occurs at base and passes upwards into thick sequence of rhyolitic lava flows (Andersen and Færeseth, 1982).

Hardangerfjordern Group

This group contains basic to acidic volcanic rocks with chert, psammite, pelites and marbles (Andersen and Færeseth, 1982). Basic volcanic rocks in the lower part are generated in early stage of island arc evolution while basic to intermediate volcanic rocks higher in group are

related to progressive development of an island arc (Færeseth, 1982). This group has been divided into five formations shown in Fig.14 from Lippard and Mitchell (1980).

Dyvikvågen Group

The rocks belonging to Dyvikvågen Group were deposited in late Ordovician to early Silurian time after first phase of Caledonian deformation (Andersen and Færeseth, 1982). This group is furthur divided (Fig.14).

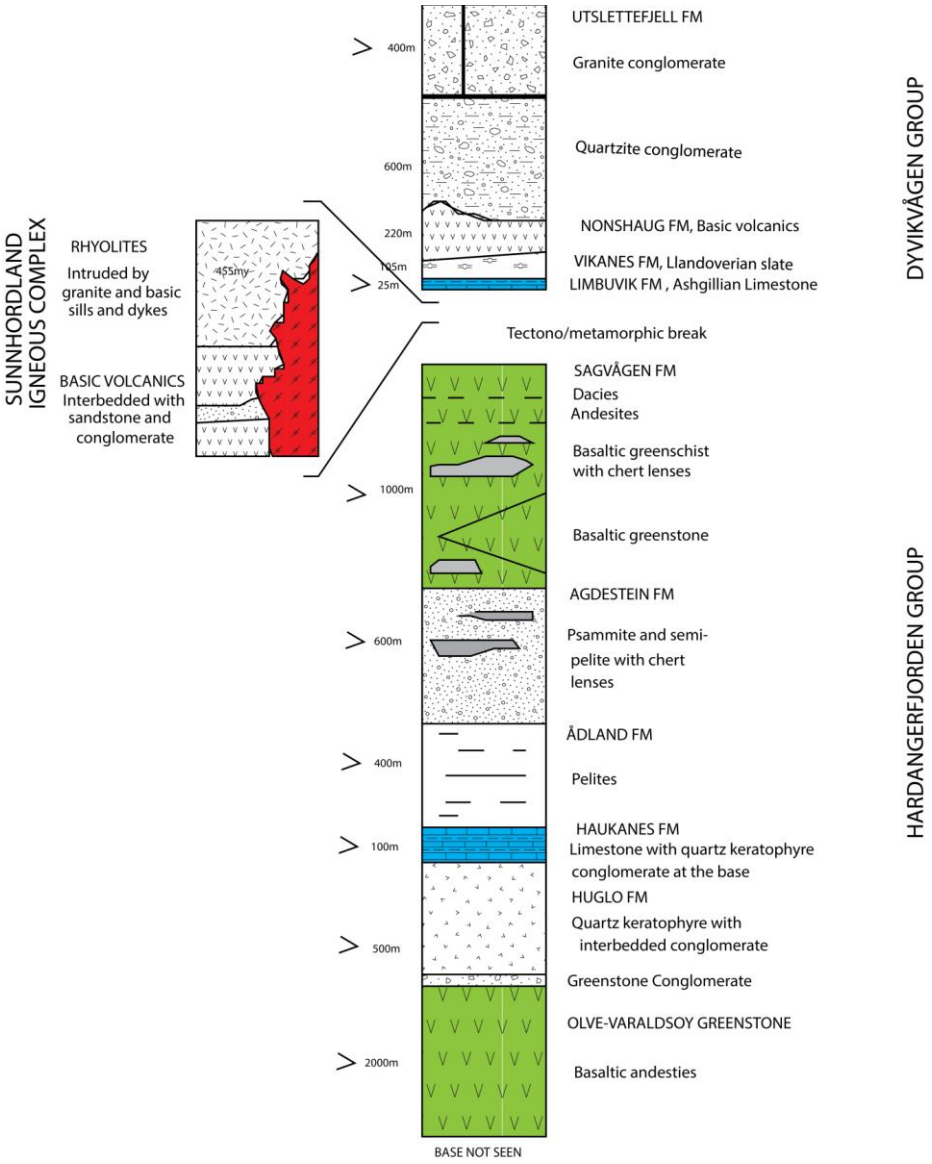

Figure 14: Stratigraphic coloumn for rocks in Hardangerfjord area. Stratigraphic column in eastern part of the Sunnhordland Igneous Complex on Stord modified from Lippard and Mitchell . (1980)

Composition of basement on Utsira High

The composition of basement on the Utsira High is summarized in the Table 1. The basement is mostly composed of granitic rocks.

Table 1 showing basement lithology encountered in different wells on Utsira high from the North Sea modified from Slagstad et al. (2011)

Sample No	Sample	Depth(m)	Rock Type	Age (Ma)
1	16/1-4	1937	Leucogabbro	420.8±2.9
2	16/6-1	2059.7	Dacite	429.8±5.5
3	16/3-2	2017.7	Granite	456.4±6.7
4	16/4-1	2908.6	Granite	460.0±7.7
5	16/5-1	1923.9	Granite	463±5.5

2.8 Rift Basin Development:

In the early stages of rift development various small isolated, fault bounded basins are formed, whereby in the rift climax stage dominant basin bounding fault develops (Watson et al. 1987). According to Schlische & Olsen (1990) the younger basins have smaller depocentres which helps sedimentation to keep pace with subsidence, while the fully developed basin have large depocentres so sedimentation is unable to keep pace with accommodation space been created. Tectonic slopes are produced by combination of footwall uplift and hangingwall subsidence. The footwall area is the main source of sediments in the adjacent basin, although in an assymetrical basin, hanging wall derived sediments may be more widely deposited (Leeder & Gawthorpe (1987). The displacement along the fault increases with time because of the relation between increased slip and fault length (Waterson 1986). Thus it can be inferred that if the sedimentation rate is constant, the potential for subsidence to outpace sedimentation will increase with increased fault movement. Depositional systems with varying rift stages (Leeder and Gawthorpe, 2000) are shown in Fig 15.

2.9 Sedimentary fills in Rift Basins:

The sedimentation in a rift basin is controlled by segmentation of faults and structural relief resulting due to extensional processes. Most of the subsidence occurs on major basin bounding faults. Various individual half grabens may conjoin to form incipient plate boundaries (Rosendahl, 1987). Within individual fault segment, the maximum subsidence of the hanging wall is observed near the centre of the fault segment similarly maximum footwall uplift is observed at centre of individual fault segment. Gravity flows, mass flows accompanied by small drainages are the characteristic of border fault margins (Gawthorpe and Leeder, 2000). Conversly hanging wall margins are less steep, large catchment areas and accomodation space is also limited.

The linkage geometry of adjacent fault segments may have cogent effect over developing drainage system. This affinity between fault segments results in new drainage basin which determines the sediment delivery pathways into basin depocenters and holds a control on syn-rift sedimentation. If the border faults have propogated to their maximum length, basin depostion can only be due to along-strike capture (Ebinger et al., 2011).

In most of extensional tectonic regimes,large river drainages enter in areas having lowest relief. As a result of this large drainage streams and rivers and coarse siliciclastic sediments deposited are found on the hanging wall blocks of individual half grabens, at the ends of linked half graben systems or where major bounding faults die out and foot wall relief is very low.(Ebinger et al., 2011).

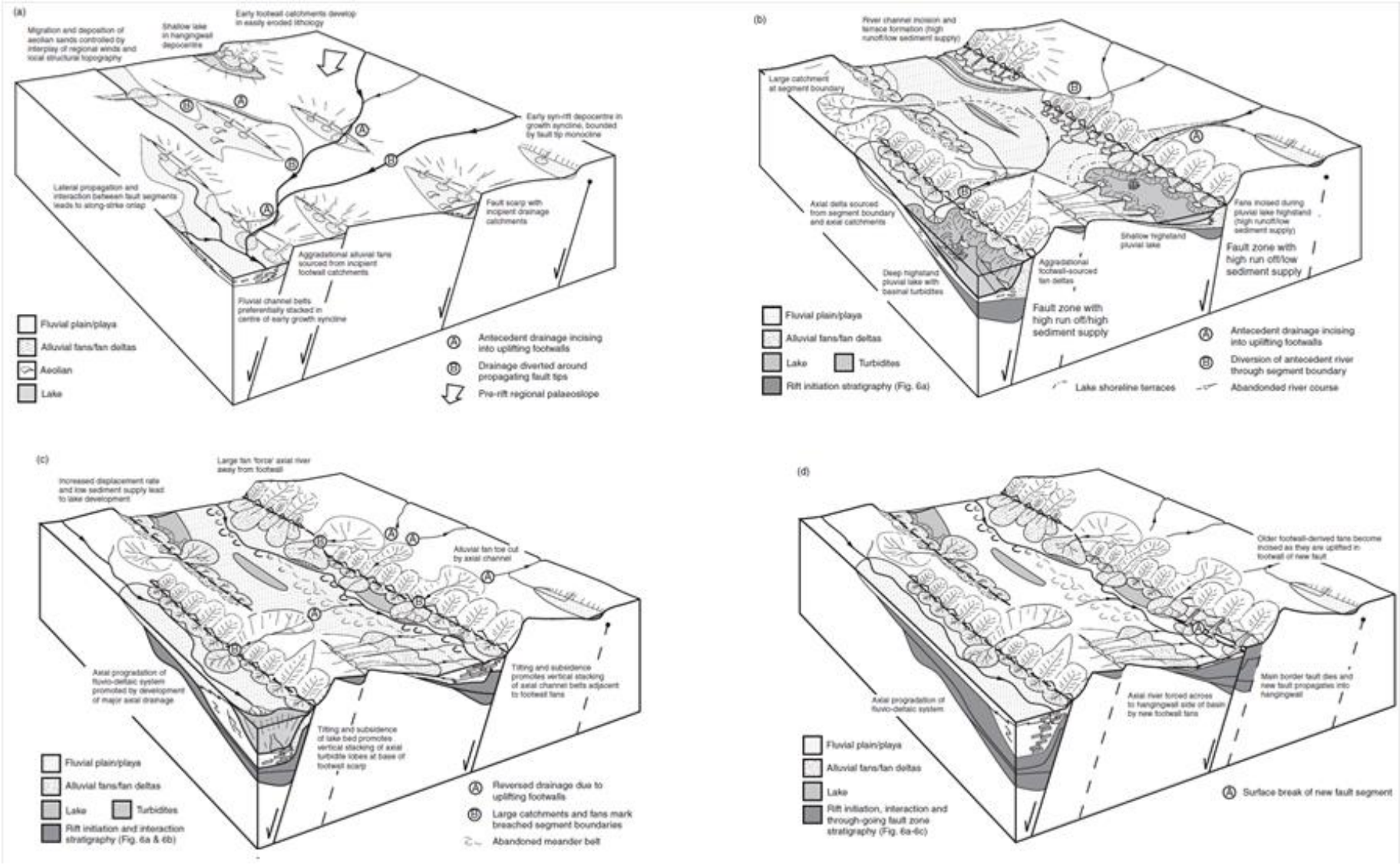

Figure 15: Showing depositional systems with varying rift stages from Gawthorpe and Leeder,(2000)

3. Material and Methodology

This chapter discusses the materials and methodologies used for analyzing the well cuttings and well cores of basement, Triassic and Middle Jurassic strata and encountered in Well 17/3-1.

3.1 Sedimentological core logging

The core logging of well 17/3-1(31m) was carried out in September, 2012 at Norwegian Petroleum Directorate core storage, Stavanger. The total core sample length was 32m but available for logging was 31m. The core was logged under the supervision of Professor Henning Dypvik. The core was logged at a scale of 1:10 on a standard logging sheet.

Core pieces of one meter length was cut and placed in core boxes which were made to contain five such units. Though in all the core boxes all five units were not stored.

Well 17/3-1 was logged from 2388 to 2390m, 2391 to 2417.85m and 2849 to 2852m. In addition to core logging, samples were also collected and pictures were taken of the core by the writer and by Professor Henning Dypvik.

3.2 Sampling

During core logging, samples were collected for analysis. Samples of cuttings were collected from depth 2425m to 2840m by Professor Henning Dypvik.

3.3 Mineralogical and petrographical analysis:

Mineralogical and petrographical analysis of the selected rock samples from the collection was done by optical study of thin sections and performing XRD analysis.

3.3.1 Thin sections

Samples from the cuttings were washed with water to get rid of any impurities due to drilling mud. These cutting samples were then dried and along with small slabs of rocks that were cut from the core samples sent to thin section lab for thin section preparation. The cutting and rock samples were impregnated in blue epoxy and polished.

Thin section description:

A total of 66 thin sections were prepared. 46 thin sections were collected from the cuttings which in total were 70. 20 samples were selected from the 24 samples collected from cores. The aim of thin section study was to understand and acquire detailed information of clast types, rock fragments and identifiable minerals in the cuttings and detailed information of lithology, grain shape and grain size and mineral identification in core samples. Table 1 shows the thin sections studied and Appendix 1 and 2 shows the summarized results.

Table 2: Analyzed Thin Sections. Point counted sections are shown in bold

Thin Section no.	Depth	Thin Section no.	Depth	Thin Section no.	Depth
Basement		Smith Bank Formation		Sandnes Formation	
1	2851,6	21	**2640**	41	2388,1
2	2849,5	22	2630	42	2389,8
3	2830	23	**2620**	43	2391,1
4	2820	24	2610	44	2395,9
Smith Bank Formation		25	**2600**	45	**2396**
5	**2810**	26	2590	46	2397,5
6	**2800**	27	**2580**	47	2398
7	**2790**	28	**2570**	48	**2399,6**
8	**2780**	29	**2560**	49	2399,9
9	2770	30	2550	50	2401,5
10	**2760**	31	**2540**	51	2401,9
11	2750	32	**2530**	52	2405,1
12	**2740**	33	2520	53	2406,4
13	2730	34	**2510**	54	2408
14	**2720**	35	**2490**	55	2409,3
15	2710	36	2485	Bryne Formation	
16	**2700**	37	2475	56	2411,7
17	2690	38	**2465**	57	**2412,9**
18	**2680**	39	2455	58	2417,4
19	2670	40	**2445**	59	**2417,6**
20	**2660**				

Mineral and clast counting

Mineral and clast counting has been done using a swift automatic brass made counter. A total of 20 thin sections from cuttings and 5 from core were counted using Nikon Optiphot-Pol petrographic microscope. Thin sections from core were counted for 400 points. However, the

thin sections from cuttings were counted for points between 150 and 200, due to less and larger clast fragments. Appendix 1 and 2 contain the results for mineral and clast counting.

3.3.2 X-Ray diffraction analysis

Powder X-ray diffraction is a tool for identifying and characterizing geological materials (William, 2007).XRD-analysis is done for qualitative and semi-quantitative analysis of minerals present in the cutting samples as well as in the core samples, using DIFFRAC.EVA V2.0. Diffrac.Eva software was used to calculate the XRD% by employing the simple peak height percentage calculation of each mineral. This provided the semi-quantitative analysis of minerals present in the cutting and core samples. It should be kept in mind that XRD% is not representing true volume percentages (P.C Henning Dypvik). Results of this analysis are displayed in Appendices 3, 4, and 5.

Table3: Bulk XRD samples with depth and XRD plate number

XRD no.	Depth	XRD no.	Depth	XRD no.	Depth	XRD no.	Depth
Basement		1194	2735	1221	2605	Bryne Formation	
1151	2852,15	1164	2730	1225	2600	1205	2417,7
1162	2849,5	1226	2725	1213	2595	1153	2411,7
1176	2840	1156	2720	1212	2590	Sandnes Formation	
1218	2835	1204	2715	1210	2585	1170	2408
1154	2830	1152	2700	1229	2580	1175	2405
1217	2825	1159	2690	1231	2575	1158	2401,9
1174	2820	1195	2685	1224	2570	1160	2399,6
1207	2815	1168	2680	1209	2565	1166	2398,8
Smith Bank Formation		1215	2675	1206	2560	1155	2398
1157	2810	1214	2670	1211	2555	1161	2392
1196	2805	1193	2665	1216	2550	1171	2391,5
1173	2800	1203	2660	1307	2540	1163	2388,1
1201	2795	1227	2655	1308	2520		
1172	2790	1192	2650	1303	2510		
1200	2785	1198	2645	1309	2500		
1167	2780	1197	2640	1312	2490		
1233	2775	1199	2635	1311	2480		
1232	2765	1228	2630	1306	2470		
1202	2755	1223	2625	1310	2460		
1208	2750	1222	2620	1305	2450		
1219	2745	1230	2615	1304	2440		
1165	2740	1220	2610	1302	2430		

Detection limit of XRD:

The XRD technique is useful for identification of major constituents of a mixture but usually it is unable to detect the substances which comprise less than 5% in a mixture (William, 2007).

The detection limit of a phase is highly dependent on mixture itself as well, in addition to the machine used. Multiphase samples show many diffraction peaks, some of which overlap to a certain degree. Therefore the detection limit of a certain phase is also dependent on other phases and if their respective peaks are interfering or not. Longer counting times will result in higher intensities; as a result small peaks are separated out from the background. Using a smaller step-size will result in higher resolution, making neighboring and overlapping peaks easier to notice. With the small step-size used in our analysis (0.01 degrees2theta, and the high sensitivity of Lynxeye detector, it is often stated that the detection limit is on the order of 1-2% in multiphase geological mixtures. However for the reasons mentioned above, detection limit can be lower for certain cases, and for other phases it can be higher. (P.C Maarten Aerts)

Bulk Analysis

Cuttings samples were crushed using crushing mill to fine powder. The core samples were crushed using micronizer to fine powder. These samples in the form of fine powder were then filled in sample holders. These holders were put in X-ray diffractometer (XRD) for bulk analysis. This crushing and sample preparation was done in sedimentology lab at University of Oslo. 63 samples were selected from cuttings and 13 from the core samples shown in Table 3.

Qualitative Analysis

The minerals are identified by X-ray diffractometer, which identifies minerals on the basis of X-rays reflection by characteristic atomic lattice planes within the crystals of minerals (Thorez, 1976). The resulting diffraction patterns increase the basal (001) reflection and help in identifing different minerals (Moore and Reynolds, 1989). X-ray diffractometer analysis aids to analyse all the constituent minerals in the sample. Diffrac.Eva software is used to identify various characteristic peaks for different minerals.

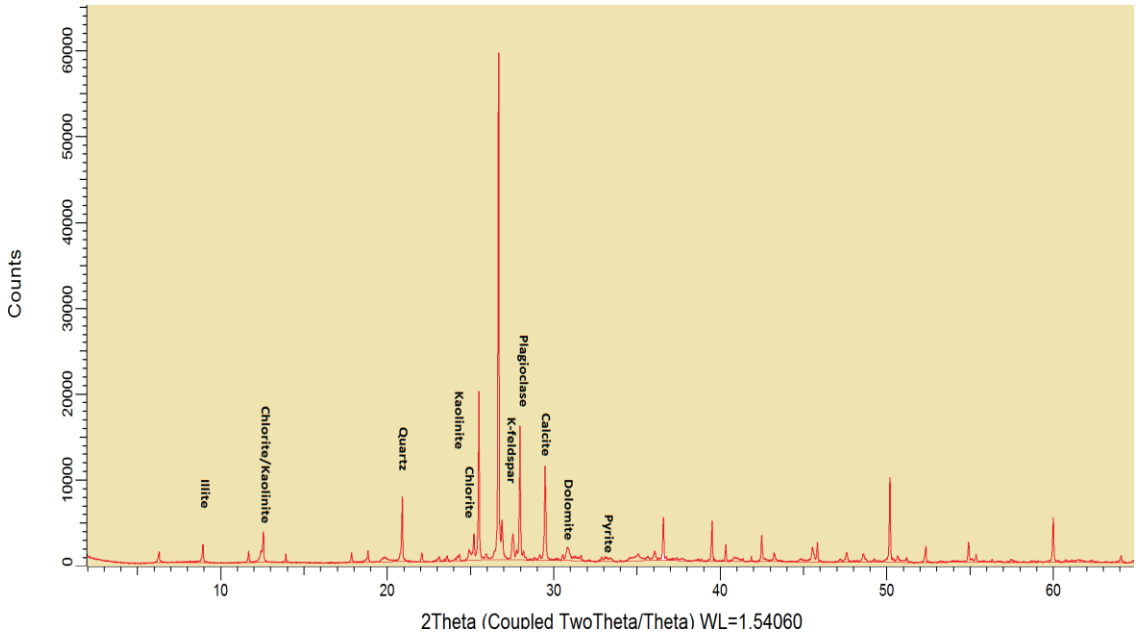

Figur 16: Diffractogram for bulk XRD analysis from 2775m in Smith Bank Formation (Diffrac.Eva software)

Following are the minerals which have been identified and quantified

Clay minerals

*Illite***:** 001 reflection identified at 10, 0 Å

Kaolinite/Chlorite: The 001 reflection for kaolinite and 002 reflection for chlorite are coinciding at about 7,00 Å. But kaolinite 002 reflection at 3, 58 Å and chlorite 004 reflection at 3, 54 Å are identified and the internal ratio is applied to 7,00 Å to get a semi-quantification of the kaolinite and chlorite.

Quartz: the 002 reflection at 4, 26 is utilized.

Feldspars:

K-feldspar: The 001 reflection at about 3, 24 Å is used.

Plagioclase: The 001 reflection at about 3, 19 Å is used.

Carbonates*:*

Calcite: 3, 03 Å reflections are used.

Dolomite: 2, 89 Å reflections are used.

Siderite: 2, 79 Å reflections are used.

Pyrite: Reflections at 2, 71 Å are used.

3.4 Petrophysical Approach

Petrel software is used for detailed study of geophysical logs. Well log data of 17/3-1 was imported in Petrel in the form of LAS files. Different geophysical logs were used simultaneously to interpret the lithologies, depositional sequences and process-response relationship in between the accommodation space and stratigraphic framework of rift basins. The applied logs studied in detail are given below

3.4.1 Gamma Ray Log:

Gamma ray log is the record of formation's radioactivity emanating from naturally occurring potassium, uranium and thorium. In sedimentary rocks gamma rays gives high values with increasing shaliness i.e. with fining grain size and vice versa. Gamma ray is used as a good lithology indicator (Rider, 2011).

3.4.2 Neutron Log:

Neutron log is the continuous record of formation's response to bombarding neutrons. It measures the hydrogen index which is the richness of hydrogen nuclei. Formations which have high hydrogen index modify neutrons by elastic scattering. The lithologies having higher water content have higher Hydrogen Index. Therefore it is also the measure of formation's water content (Rider, 2011).

3.4.3 Density Log:

The density log is the continuous record of formation's bulk density. Medium to high energy focused gamma rays are bombarded and the attenuation resulting due to Compton scattering is recorded between detector and source. If the lithology is denser, more gamma rays are attenuated so fewer reach the detector and vice versa (Rider, 2011).

3.5 Scanning electron microscopy (SEM)

SEM analysis has been done on samples using JEO JSM-6460LV Scanning Electron Microscope (SEM) with a LINK INCA Energy 300 Energy Dispersive X-Ray (EDX) system. Scanning Electron Microscopy (SEM) technique is used for high resolution analysis of carbon coated thin sections and gold coated stub mounted samples

The energies of emitted x-rays are displayed as series of peaks, spectra with the help of Energy dispersive X-Ray microanalysis (EDS). These peaks are distinct for individual elements.(Bishop et al., 1992).

Two different types of samples were studied under SEM. Thin sections coated with carbon and freshly fractured chips from cutting samples which were mounted over stubs and coated with gold. The main emphasis of the SEM was to analyze mineralogy and clay content of the Triassic strata.

Table 4 showing selected samples prepared for SEM examination

Well Name	Formation	Thin section	Carbon coated	Stubs
17/3-1	**Basement**	1	1	-
17/3-1	**Smith Bank**	6	6	4
17/3-1	**Bryne**	1	1	-
17/3-1	**Sandnes**	1	1	-

3.6 Uncertainties and Difficulties:

Cutting samples studied may not be the true representative of the depth. The 5-10m lag is expected in the cutting samples unlike the core samples which are representing true depths. Identification of minerals on their characteristic appearance during thin section study was difficult from cutting samples. Point counting cannot be done to 400 points due to large clast fragments. Cutting samples were heterogeneous mixture of minerals. In the SEM analysis it was difficult to identify and distinguish a pure mineral. The true representative energy spectrums of minerals were relatively difficult to observe, each having some impurity. Within a single clast different minerals having different energy spectrums were observed.

4 Sedimentological Description

This chapter presents the different sedimentological observations done during the logging of cores of basement, Bryne Formation and Sandnes Formation. Sedimentological core logging was done in the last week of September 2012. The sedimentological features, observed lithologies along with the photographs will be presented in the form of digitized logs.

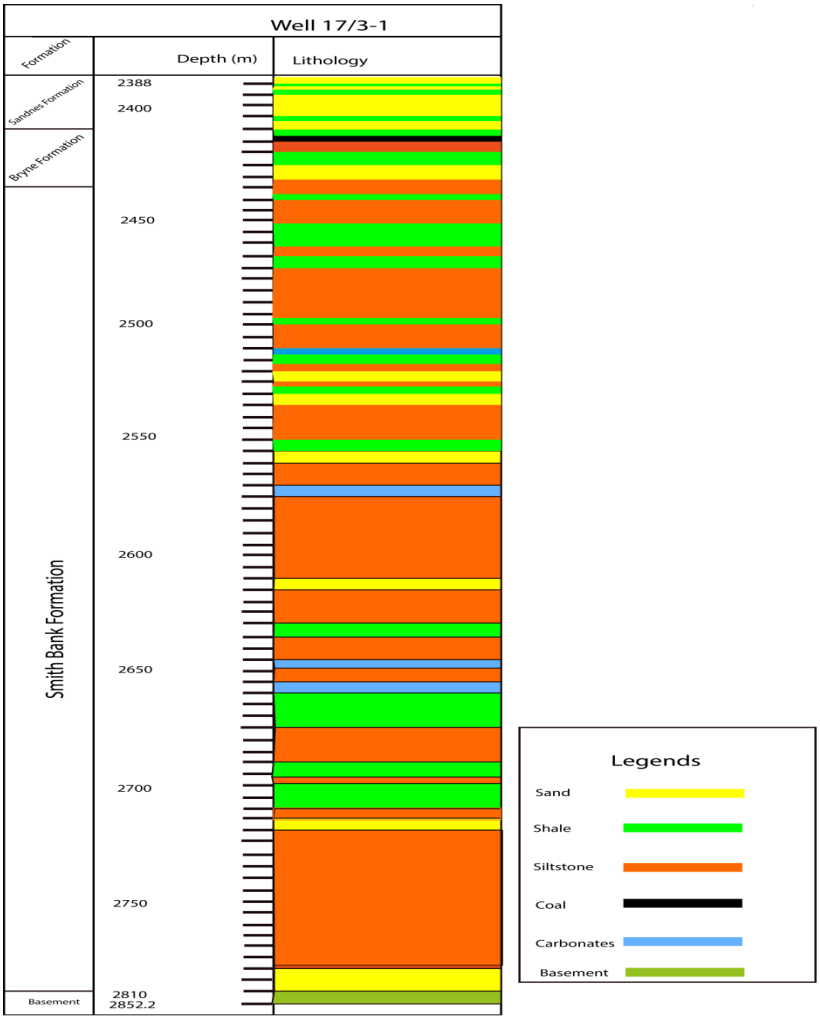

Figure 17: Lithology log of complete succession from Basement to Top Sandnes interpreted on the basis of geophysical logs and core logging.

4.1 Basement

Basement consists of amphibolite which has a green to dark green color. Amphibolite was intruded in places by calcite and quartz veins. The thickness of calcite veins is different i.e. varying from very thin veins less than 1mm thick to 0.7 cm thick vein. Calcite is found to be precipitated in fractures. Quartz precipitation is more thick compared to calcite, having 1 to 2cm thick vein. Few fractures observed at 2849.1m show no precipitation of calcite or quartz.

The other striking feature observed was the presence of striations or slickensides giving it a soapy,slippery touch (Fig.18). The striations were present on the calcite veins as well. Microfolds were also observed during core logging of the basement shown in Fig.18.

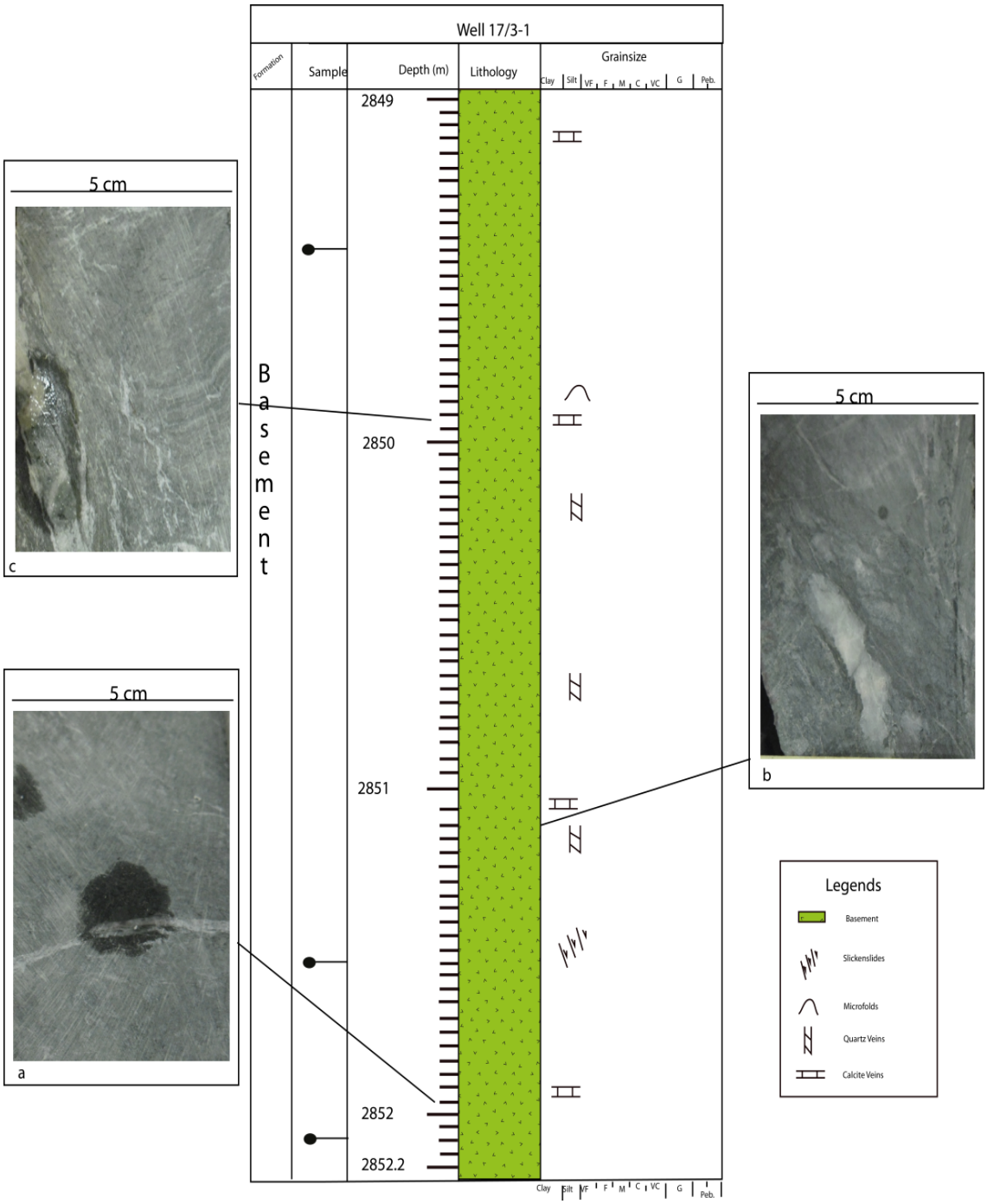

Figure 18 Sedimentological log of Basement showing lithology and structures observed.a) Calcite vein 2mm thick in striated, slickensided amphibolitic basement(2851.95m).b) Quartz precipitation 1-2 cm thick (2851.2m).c) Calcitic vein .

Bryne Formation and Sandnes Formation are part of Vestland Group. Vestland Group is correlative to Middle Jurassic Brent Group (Deegan & Scull, 1977). The base of this group overlies the Intra-Aalenian Unconformity. In the Norwegian waters, there is a overall change observed from nonmarine to marine deposition in the Bryne, Sandnes, Haugesund and Egersund formations (Husmo et al., 2002).

4.2 Bryne Formation:

The non-marine Bryne Formation is composed of interbedded sandstones, coals and shales and deposited on extensive alluvial/coastal plain (Husmo et al., 2002).

At 2417.7m wavy bedding is observed. The wavy bedding changes upward to fine sand size laminated layers with mud streaks at 2417m. Fine laminated sands with mica content and bioturbation is noticed at 2416.9 to 2416.7m. Small pieces of organic matter, rootlets 1-3mm is also present in this zone. Lenticular bedding is identified by the presence of sand lenses at 2415.9m. A 4.5cm thick zone of coal bed is lying above the fine sand with mud intercalated unit (Fig.19). Coaly shale unit of dark grey color is overlying the coal bed.

A small zone of coarsening upward sequence from 2414.7m to 2414.3m consisting of fine sands to alternating mudstones at base with increasing sand content at the top. This part is overlain by fine laminated sands with mostly clay content. From 2413m mostly the logged part has sand rich units with intermittent thin shale rich units. Soft sediment deformation structures like ball and pillow, flame structures and erosional scour are seen at the top of shale rich units overlain by sandy part(Fig.19c). Homogenous sand bed of 2cm thickness devoid of any bioturbation is noticed (Fig.19). In the sand rich zones above the 2413m ripple marks are the dominant sedimentary structures. The signs of bioturbation were minimal in the zones where ripple marks are present. Herring bone cross stratification is observed at the top of Bryne Formation at 2410.2m (Fig.20a).

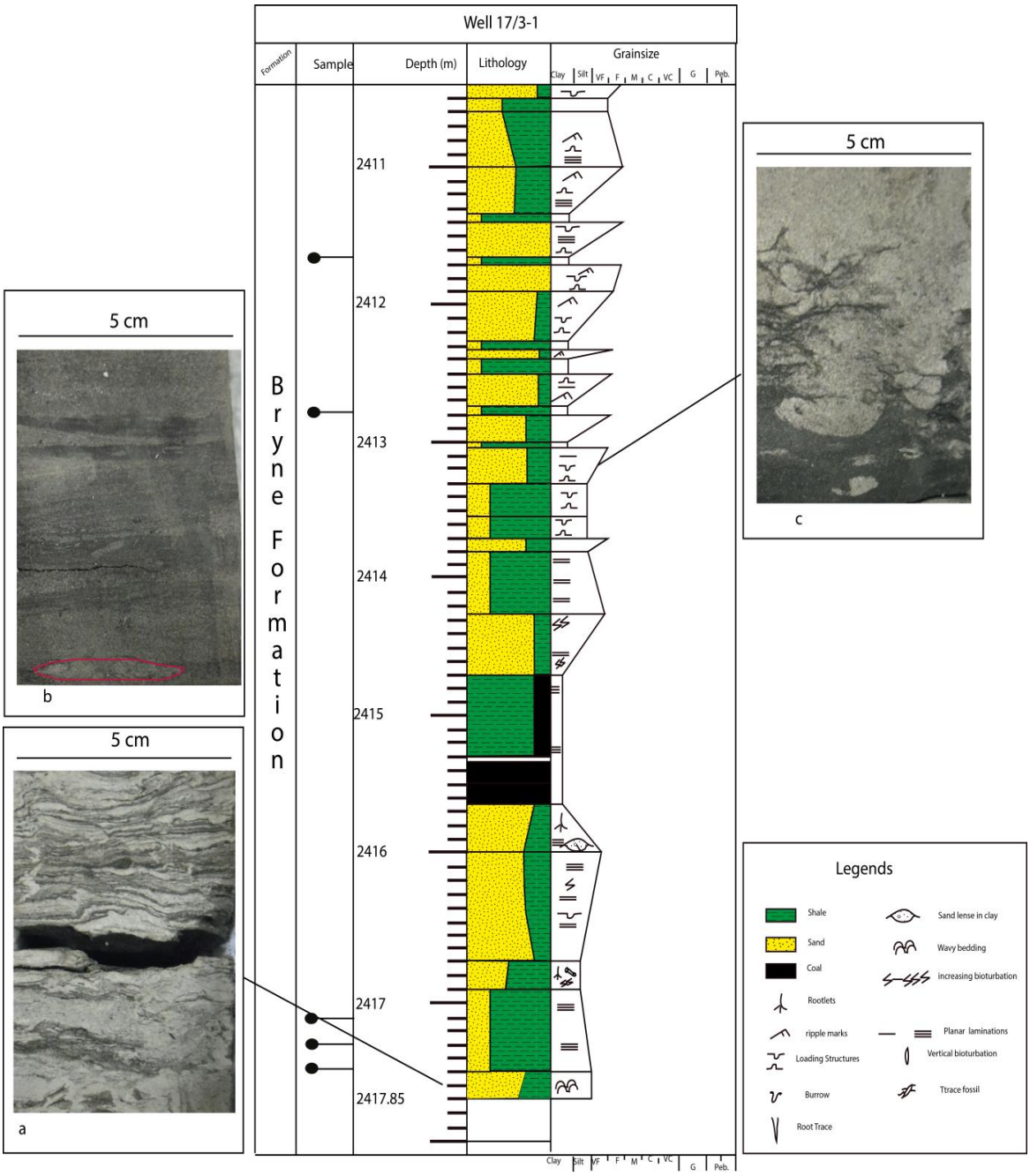

Figure 19: Sedimentological log of Bryne Formation showing lithology and the structures observed.a) Flaser bedding b) Sand lens in finely laminated alternating sand and shale layers resembling lenticular bedding.c) Loading structures at the base of sand unit.

4.3 Sandnes Formation:

The Sandnes Formation consists of shallow marine and coastal white sandstones and shale. (Husmo et al., 2002).

The base of the Sandnes Formation has cemented, bioturbated and homogenous sands at 2410m. This homogenous sand unit is coarsening upward (2410m-2409.1m), with very few

sedimentary structures like ripples. Bioturbation marks can be observed with thin clay laminae. Peat bed is observed at 2408.9m depth overlying a shale rich unit (Fig.20b). Alternating shale and sand rich intervals is observed above the peat bed (Fig.20). An erosional base is marked at 2406.3m.

A thick interval of homogenous sands is observed and logged from 2405m to 2399.4m (Fig. 20 and Fig.21). This unit is highly bioturbated at base. Upwards the bioturbation reduces and an increase in grain size and sand content is also observed. The sand size increases upwards showing coarsening upward sequence in this interval. This six metre thick sand is mostly friable and not well cemented.

A change in facies to more shale rich sands is noticed at 2399.4m. The sands are more mica rich. Various shell fragments and ripples marks are seen in fine to medium sands from 2399.4m to 2395m.

An abrupt change in lithology at 2395.1m from medium sand to sandy shale marks an erosional boundary. The sandy shale has high organic content. The shale content decreases upwards from 2395m to 2391.8m (Fig.22). Water escape structures and flame structures are observed in this zone at depths 2393.7m. At the top of this zone the sand rich interval is highly bioturbated and root trace of 3cm vertical length is observed (Fig.22b).

An abrupt change in lithology marks another erosional boundary at 2391.8m. A sandy shale with high organic content overlies coarsening upward sand unit. Fine to medium size sand units overlies the sandy shale. These sands are calcite cemented with ripple marks and very low bioturbation is noticed.

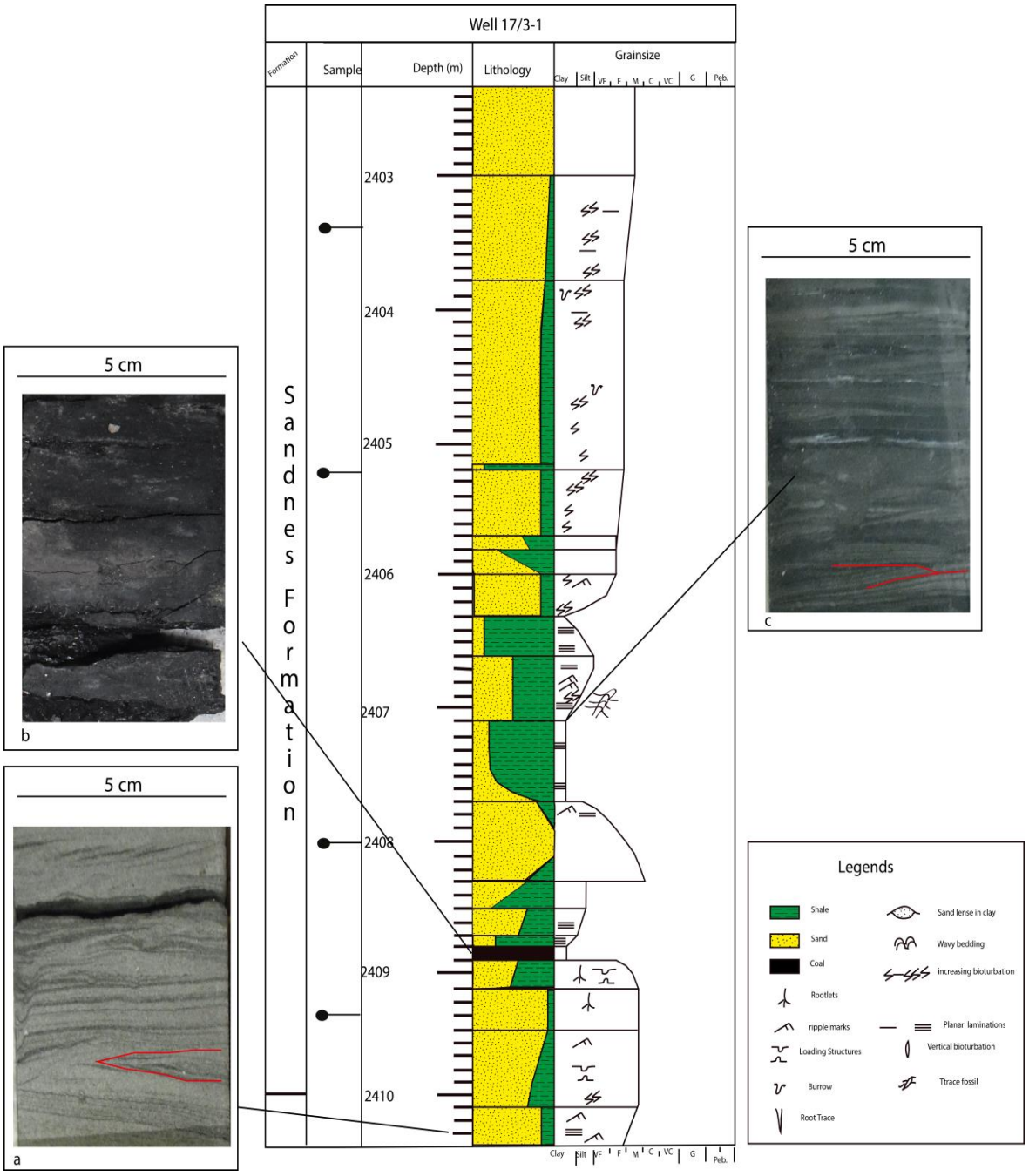

Figure 20: Sedimentological log of Sandnes Formation showing lithology and the structures observed.a) Ripple marks resembling Herring bone cross stratification. b) Peat bed interbedded between layers. c) Ripple marks in finely laminated sand and shale layers.

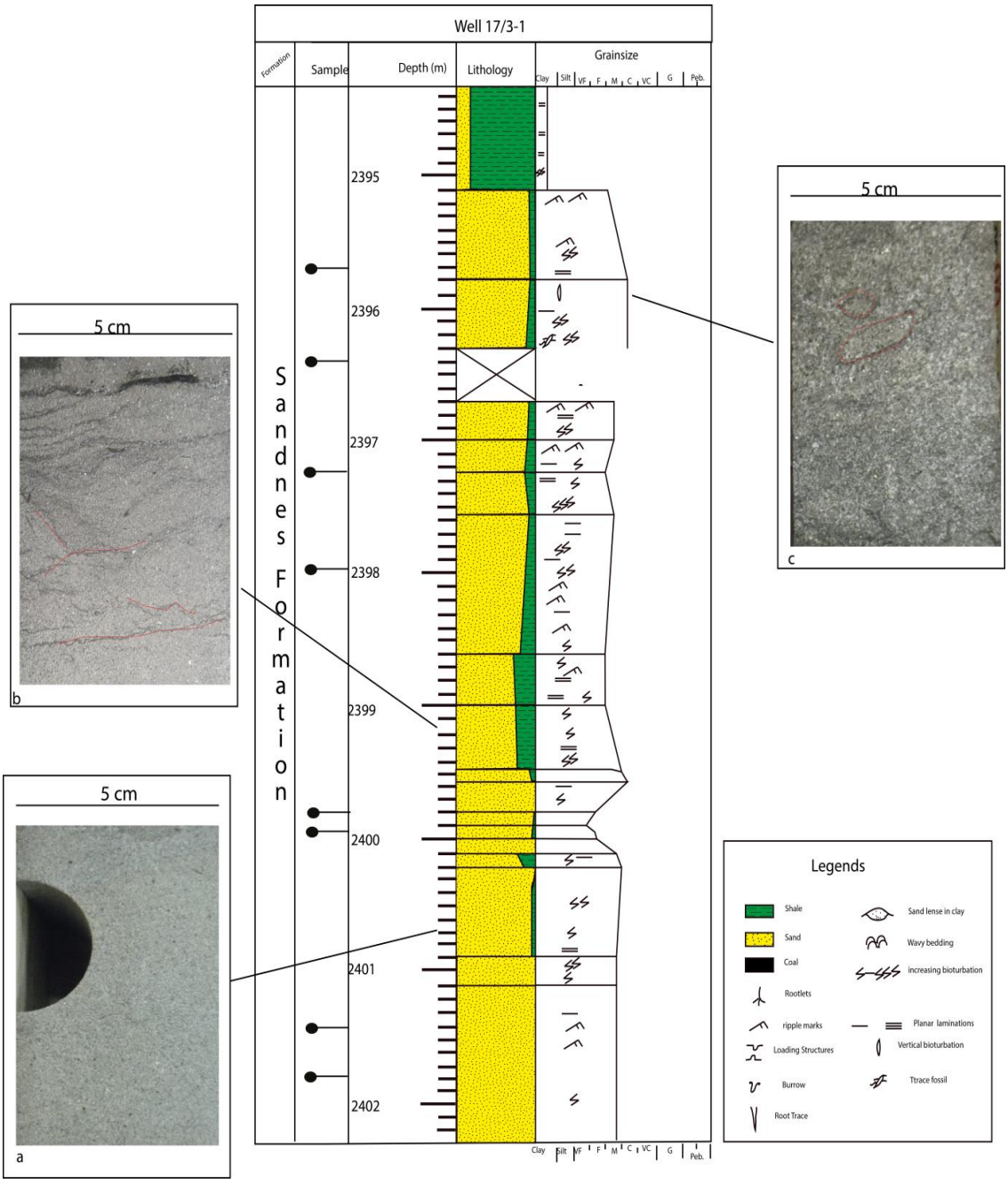

Figure 21: Sedimentological log of Sandnes Formation showing lithology and the structures observed. a) Homogenous sands of Sandnes Formation. b) Bioturbated sandstone, tracks marked with red lines. c) Shell fragments in sands.

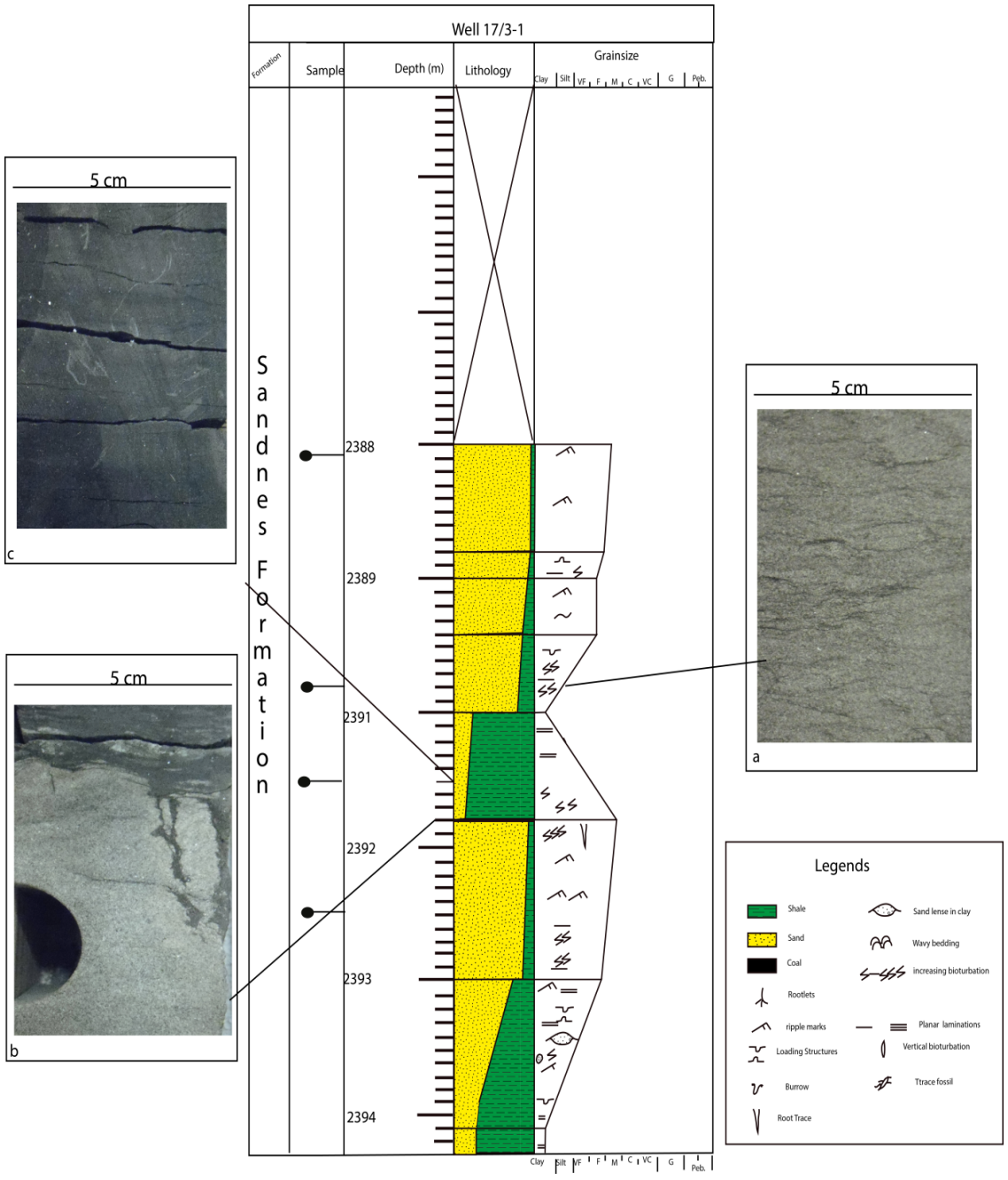

Figure 22: Sedimentological log of Sandnes Formation showing lithology and the structures observed. a) Highly bioturbated sand of Sandnes Formation.b) Rootlet showing bioturbation. c) Coaly shale

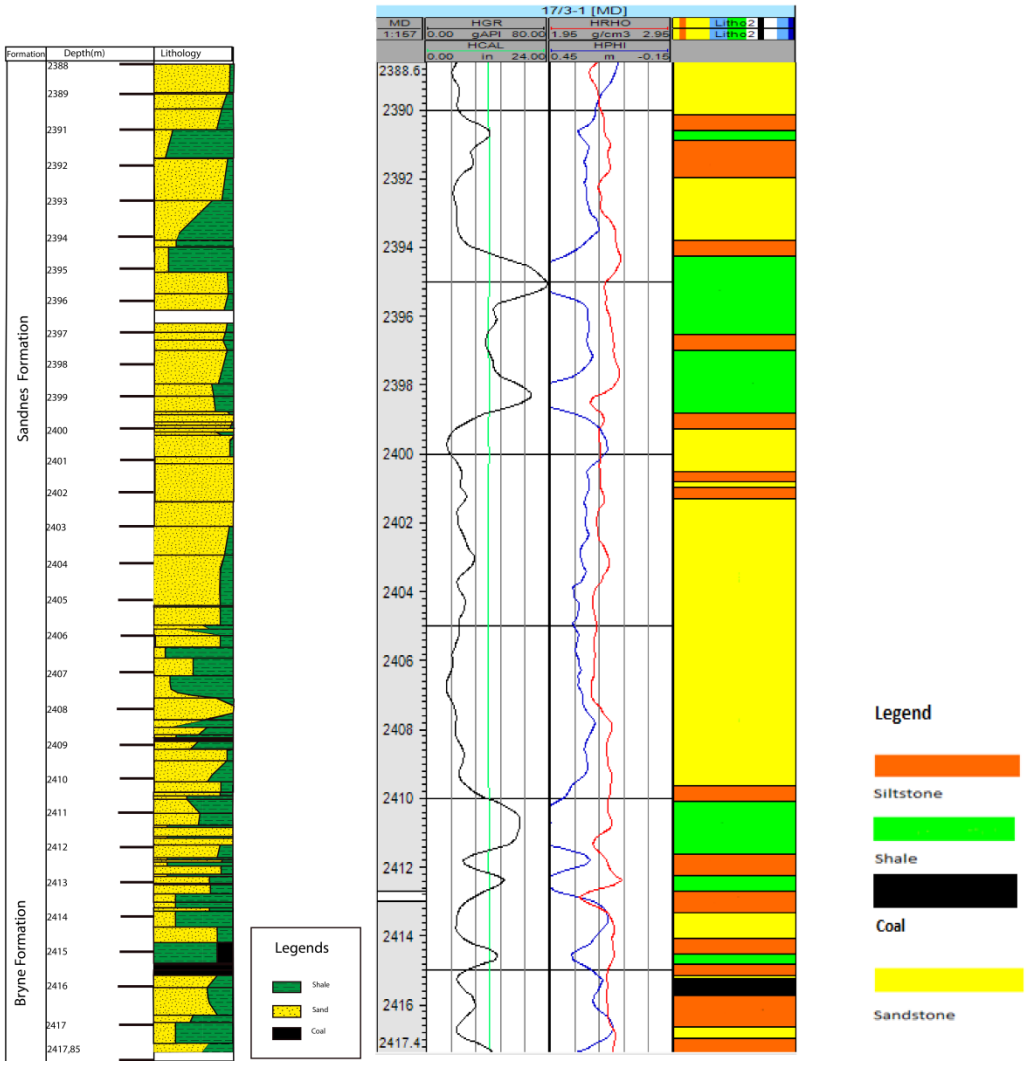

Figure 23: Comparison of observed lithology log and interpreted lithology from geophysical logs.

The figure above shows the comparison between the lithology log prepared during core logging and interpreted log using more indirect approach i.e geophysical logs. The sand rich and shale rich which are relatively thick intervals show resemblance on both the logs.

4.4 Smithbank Formation:

The lithology of Triassic Smith Bank formation was interpreted by importing the LAS files (Lundin A/S) to the Petrel software. Gamma ray values greater than 40API were used to identify the shales. Carbonate beds are identified by having gamma ray values below 13API. Similarly silts and sands are distinguished by having gamma ray values from 13 to 22API and 22 to 40API respectively.

But the lithologies interpreted on the basis of gamma ray log were further modified by more integrated approach using neutron porosity and density logs as well. Shales show high neutron porosity values due absorbed water. High neutron porosity in combination with high gamma ray confirm the presence of shales. Carbonates are distinguished with the help of neutron porosity log showing very low NPHI value as they retain less bound water and low GR values.

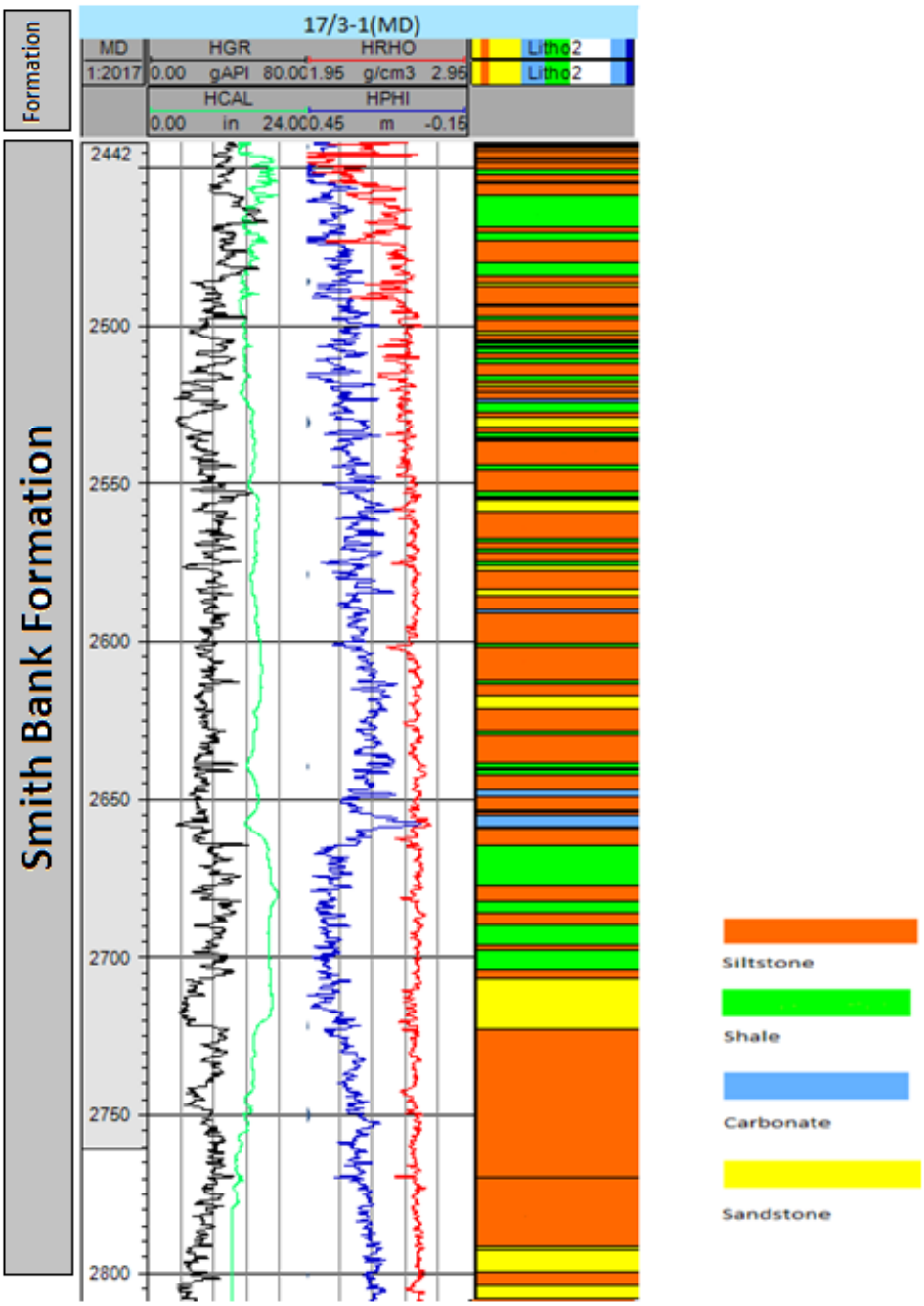

Figure 24: Lithology of Smith Bank Formation interpreted by geophysical logs using Petrel software.

5 Mineralogy and Petrography

5.1 Thin section analysis

5.1.1Basement

The basement is composed of feldspar and quartz grains embedded in fine grained matrix of chlorite. Calcite showing high interference colors and striations are observed on calcitic veins cross cutting the matrix (Fig.25a). The feldspar grains are sericitized showing birefringence. Chlorite is present as a very fine grained matrix showing pale yellow to green pleochroism when rotated under plane polarized light. Pyrite is also observed in the basement thin sections.

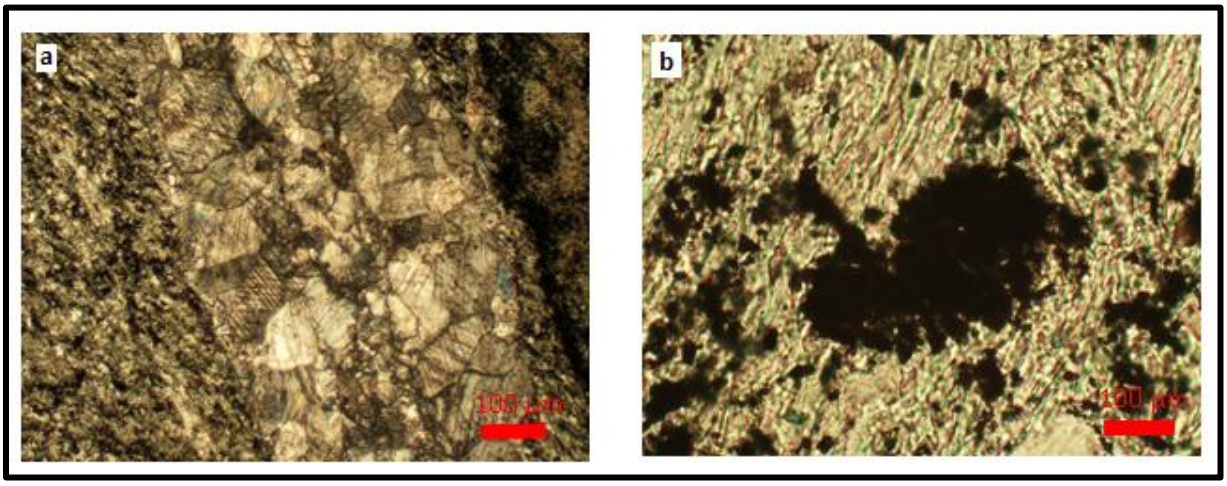

Figure: 25 a) Calcite vein in the amphibolite (2851, 6 m). b) Pyrite in the basement in a very fine grained chlorite matrix.

5.1.2 Smith Bank Formation

In general Smith Bank Formation consists of red arenaceous mudstones, with few sandstone streaks. Mudclasts of reddish brown and pale yellowish to greenish color matrix are observed. These mudclasts have brecciated appearance containing fine clay sized matrix with embedded quartz and feldspar grains. The feldspar grains are altered and sericitized.

From 2800m to 2760m both types of mudclasts with different color of matrix are present i.e. matrix having reddish brown color and pale yellow color. These mud fragments are rich in grains of feldspars and quartz (Fig.26a). Feldspars are usually altered as observed by their scuzzy appearance. A large number of micaceous flakes like muscovite and biotite are perceived clearly incorporated within the clasts. Muscovite flakes show high interference

colors in cross polars (Fig.26b). The intergranular spacing within brecciated mudclasts is low and is occupied by the matrix material.

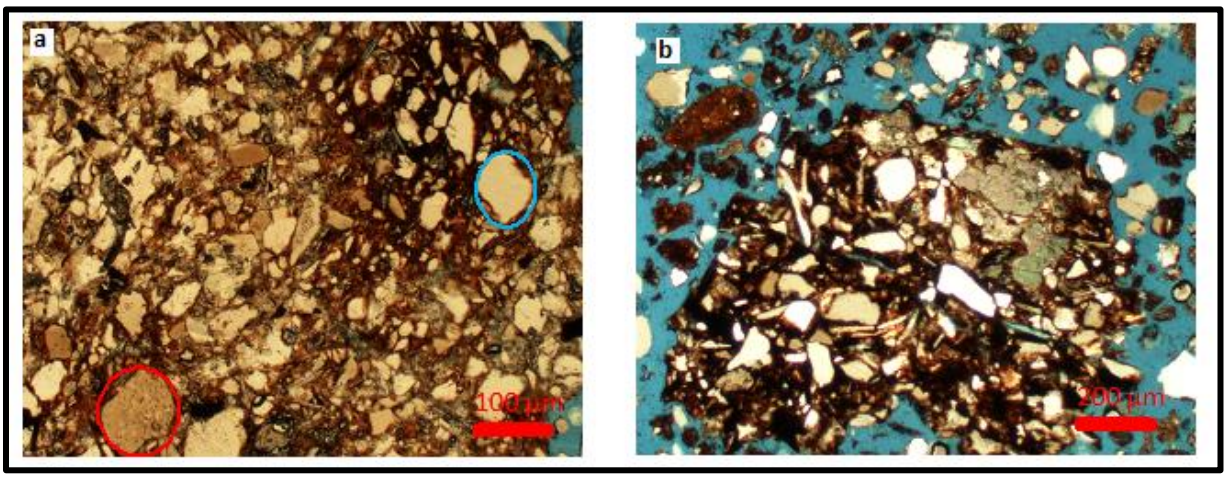

Figure:26 a) Mudclast showing quartz (blue circle) , altered feldspars (red circle), muscovite incorporated in clay matrix(2790m) b) Mudclast showing visible muscovite flakes with angular to subangular quartz grains and striated calcite

From level 2740m to 2570m the observable change is reduction in the ratio of mica flakes entrenched in the mud clasts. The feldspars and quartz grains are less in proportion and size of these grains are also reduced (Fig.27a). The mica flakes are mostly present in mud clasts which are of pale yellowish color (Fig. 27b). From point counting data the average of mud clast fragments is reduced in this zone compared to older succession and on the contrary, the average of shale fragments have increased (Appendix 1).

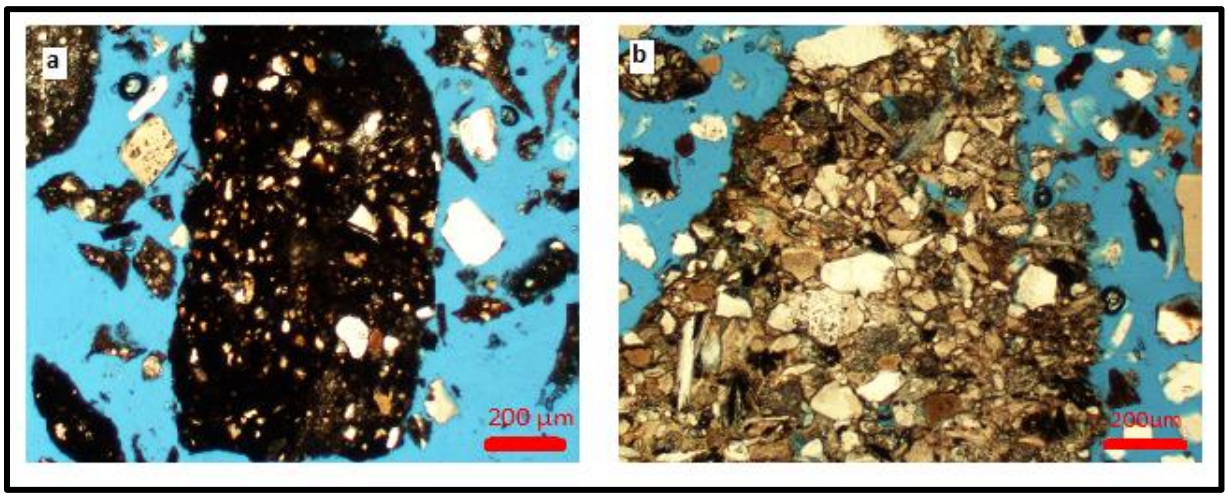

Figure: 27 a) Mudclast showing more clay content highly altered feldspars with no mica flakes observable(2740). b) Pale yellowish colored mudclast with mica flakes(2680m).

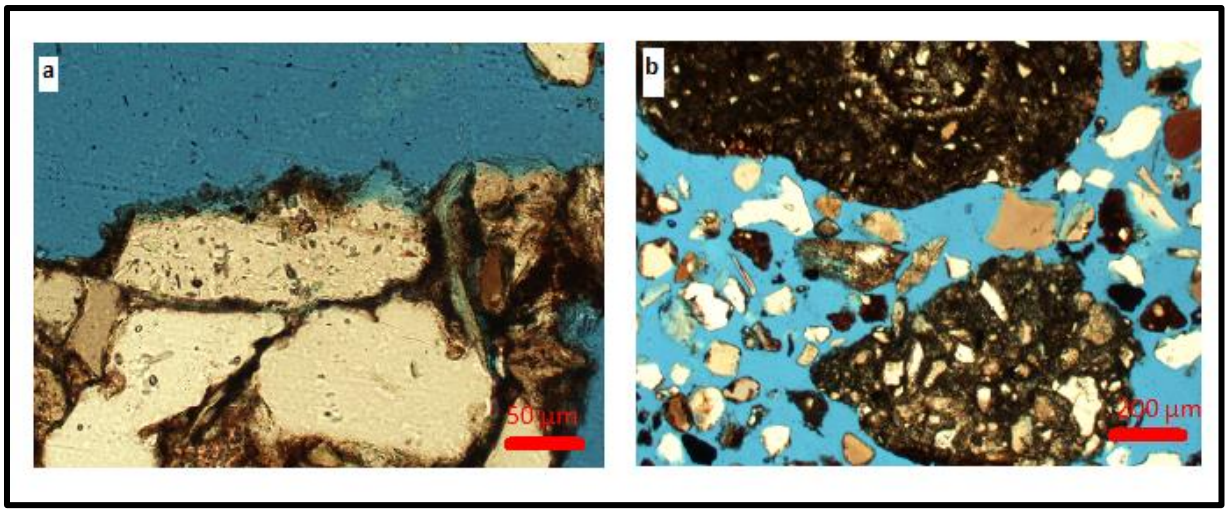

Figure: 28 a) Feldspar grain with sericite on its surface (2720). b) Mud fragment with smaller grains in mud matrix (2660).

From level 2570m to 2445m, mud clasts have mud matrix of mostly greenish color. These fragments are having larger feldspar and quartz grains. Both the type of mudclasts contains very less muscovite flakes. In sample 2540 and 2530 the greenish matrix resembling local amphibolitic basement is dominating the other grains. In many fragment the removal of the matrix and grains can be clearly seen. For the top most few meters reddish brown matrix has very few feldspar grains.

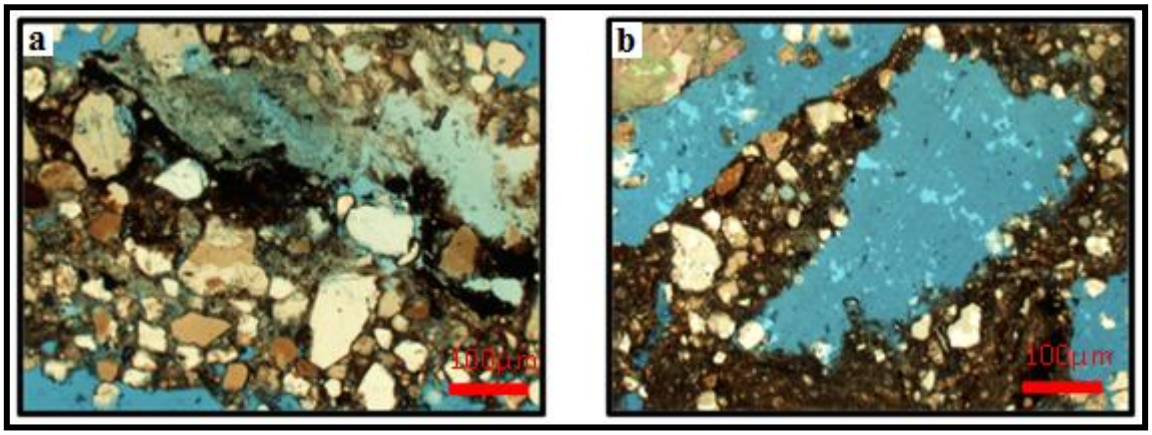

Figure:29 a) Larger constituent grains of mudclast with greenish colored matrix(2530).b) Mud clasts showing removal of matrix

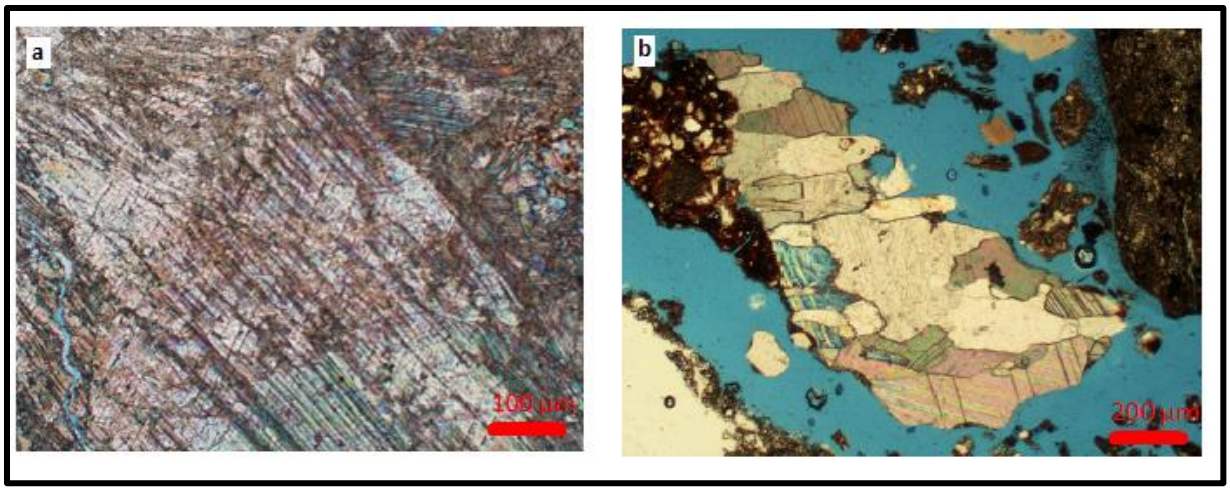

Figure:30 a) Large striated calcite fragment (2800m) b) Calcite fragment (2740)

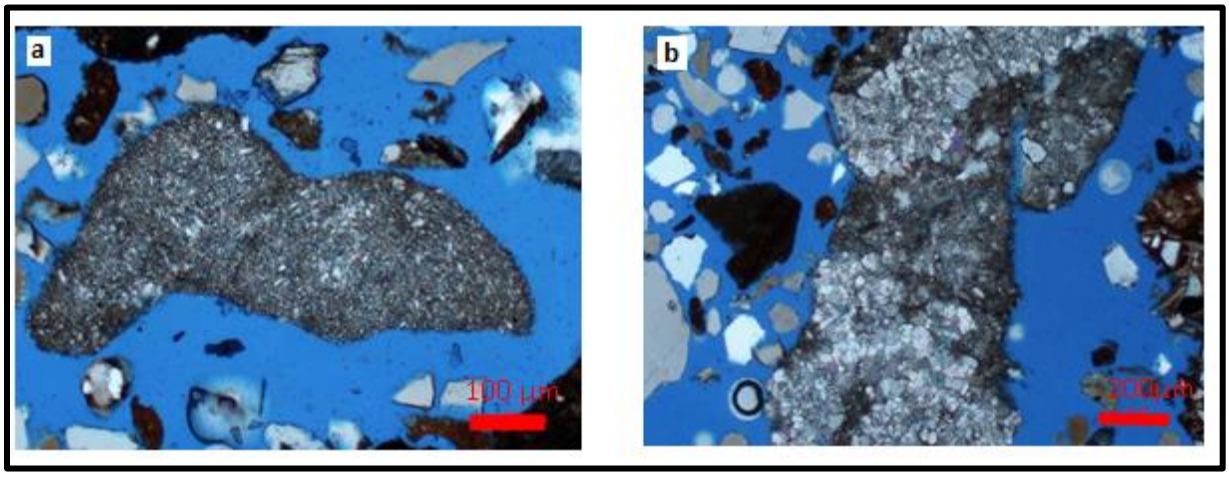

Figure :31 a) Micritic Calcite (2740m) b) Transition zone of micritic and sparitic calcite (2720m)

Calcite fragments showing high birefringence with interference colors (Fig.30a) , which are typically of non-biogenic origin and resemble basement intruded calicitic veins. These fragments are found throughout the succession. From point counting data it is observed that in sample from 2800m and 2790m, the percentile value is 21.4 and 21.1 respectively (Appendix 1). Also the size of the fragments is large. In the two hundred meter zone from 2780m depth to 2580m, there is remarkable decrement in the percentage value and size of the striated calcitic fragments or even the absence of striated fragments. But again in the zone where green mud clasts come up, there is appreciable percentage of striated calcites again (Appendix 1). Fig 31a shows the occurrence of micritic calcite and 31b shows a fragment containing micritic to sparitic transition at a carbonate cemented zone.

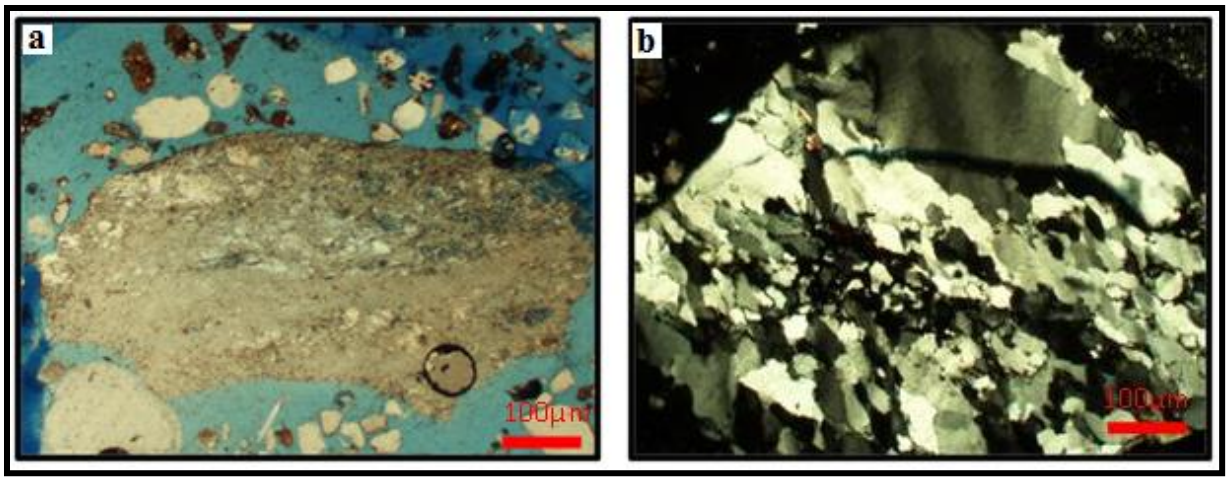

Figure: 32 a) Rock fragment consisting of greenish chlorite matrix resembling basement (2790). b) Polycrystalline quartz crystals

Rock clasts of greenish color resembling the amphibolitic basement in color are here named as amphibolite clasts (Fig .32a). Fine grain size of chlorite matrix and smaller feldspar grains show that these fragments bear a resemblance to basement. In the samples just above the basement these clasts are present in higher proportions. In zone from 2780m to 2580m very few such clasts are identified in thin sections, even if there are any, they are mostly weathered. In the depths ranging from 2580 to top of the Smith Bank Formation an increase is observed. These ratios follow almost the same trend as striated calcite fragments.

Polycrystalline quartz clasts shown in Fig 32b are also observed in various thin sections (Appendix 1). Number of crystals in a single polycrystalline quartz have also been counted (Appendix 1).

Rock fragments of shale shown in Fig.33b, siltstone and sandstone are found to be observed throughout the sequence in all the sections (Appendix 1). These rock fragments are distinguished on the basis of the grain size of material forming these clasts. Rock clasts of dolomite having rhombohedral crystals showing birefringence in cross polars. Carbonate fragments are also distinguishable grains among other clasts. Framboidal pyrite is present in few sections and observed as well.

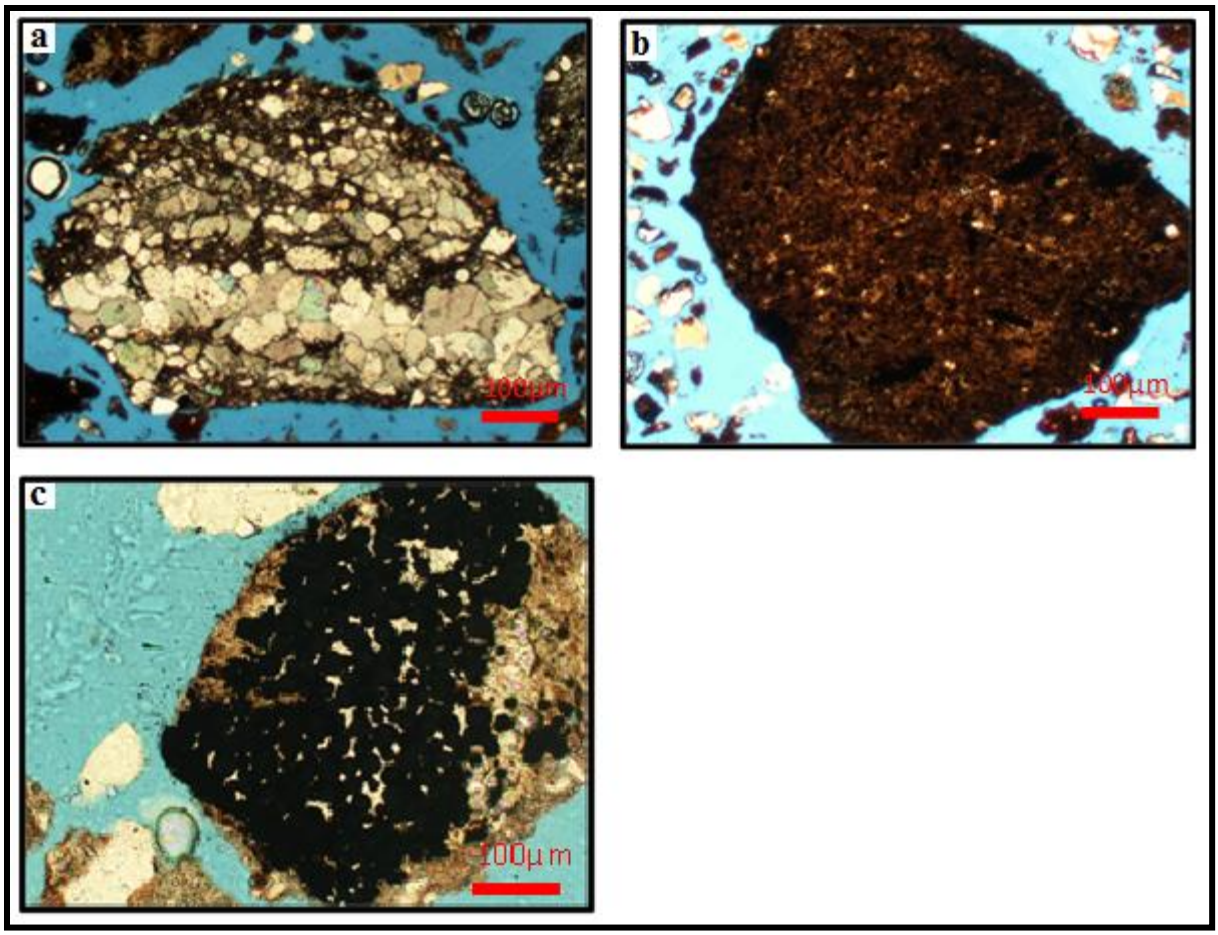

Figure:33 a) Sparitic carbonate fragment (2740) b) Shale fragment (2780) c) Framboidal pyrite

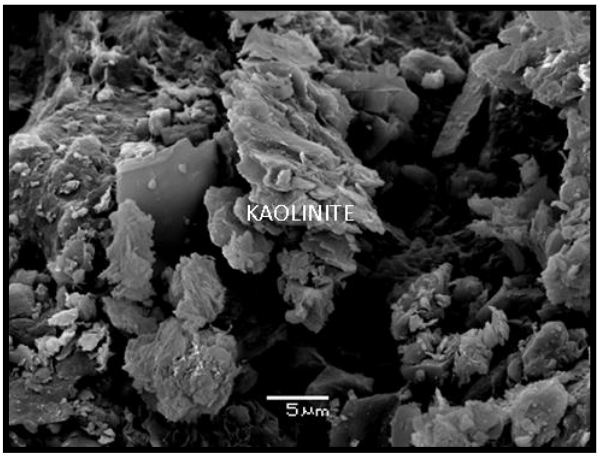

Figure 34: Detrital kaolinite 2745m depth under Scanning Electron Microscope

The stubs observed under SEM revealed the presence of detrital kaolinite. Detrital kaolinite can be recognized by the absence of stacked booklet morphology which is characteristic of authigenic kaolinites.

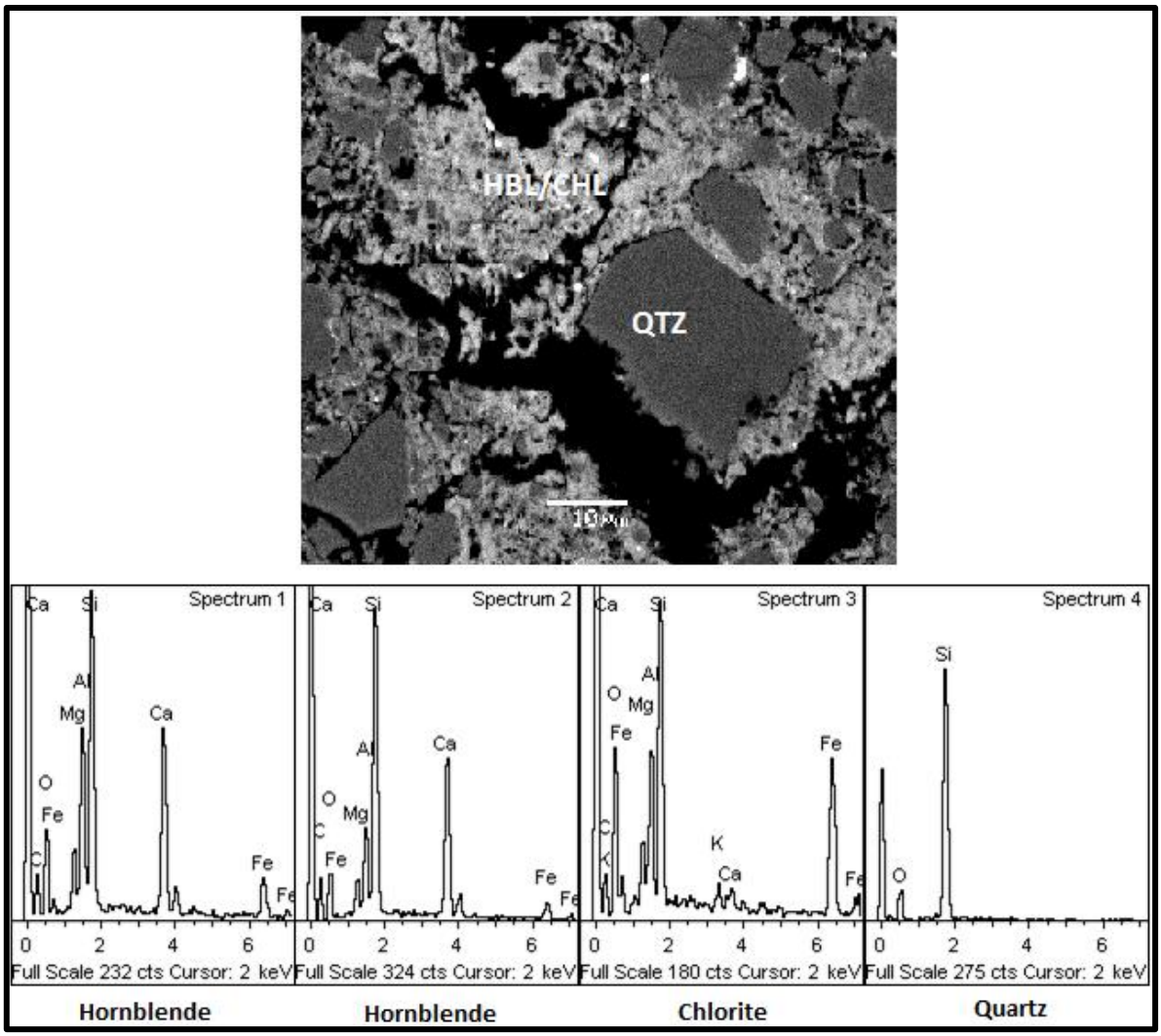

Figure 35: Quartz grain surrounded by hornblende or chlorite at 2790m observed under Scanning Electron Microscope.

Due to heterogeneous mixture in the cutting samples it was difficult to distinguish between hornblende and chlorite shown in (Fig. 35). The various energy spectrums shown in Fig 35 show a mix of chlorite and hornblende. The characteristic spectrum for each of these mineral is different than shown here. But due to close resemblance to the relevant energy dispersive X-Ray Spectrum impure hornblende and chlorite are identified and marked.

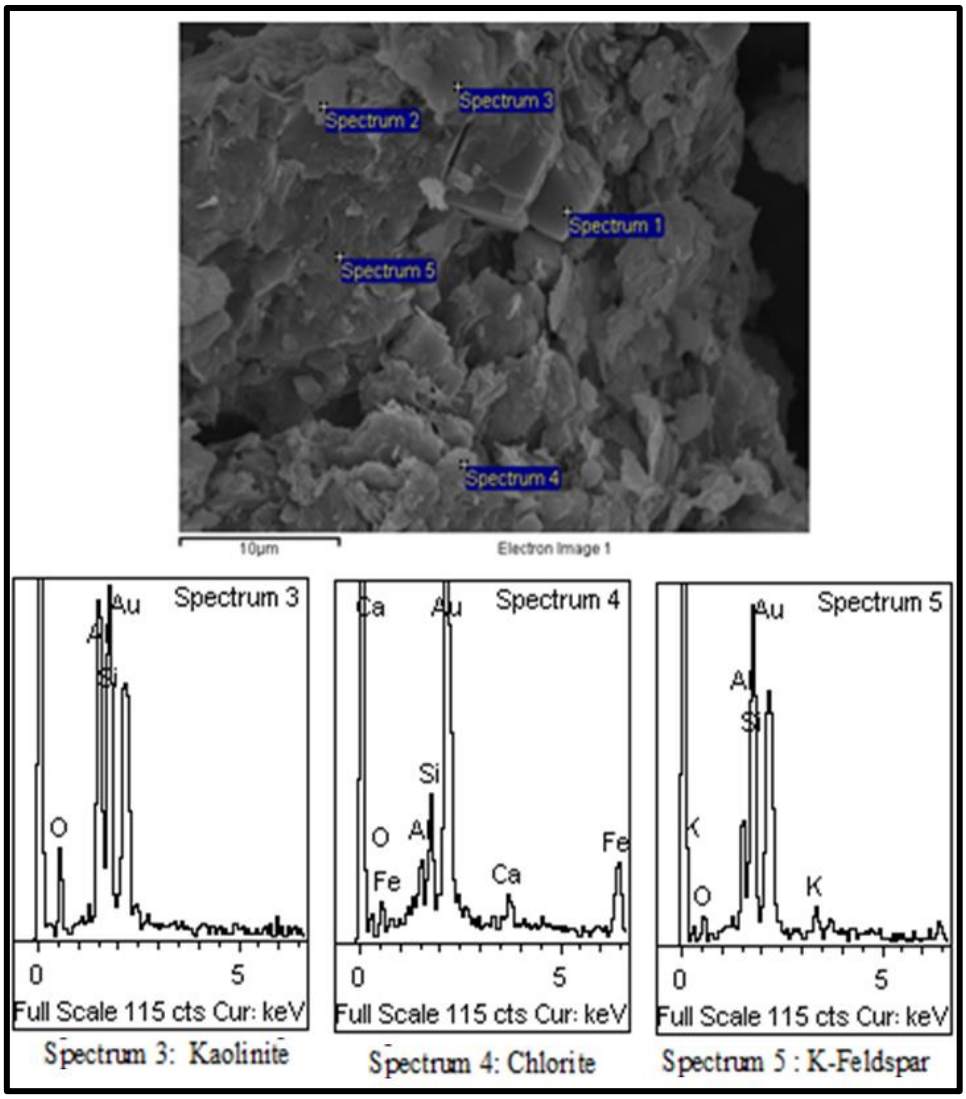

Figure 36: Showing various energy dispersive X-Ray spectrum of different minerals

5.1.3 Bryne Formation

The thin sections from Bryne Formation generally consist of silty to medium grained sandstones along with shale intercalations. The observed thin sections at 2417,6m has angular to sub-angular quartz grains embedded in clay rich matrix. The framework is mainly matrix supported. Quartz has undulose extinction. Concavo-convex grain contacts are commonly identified between grains. Porosity is very low because of the clay matrix. Coal fragments are present in the observed thin section. From point counting data quartz appears to be the dominant mineral with abundant kaolinite clay. Coal is also present in appreciable amounts (Appendix 2). Flakes of mica are also observable, present in place between grains but most of them have almost been altered to clay minerals. The thin section at the 2412,9m has fine to medium size grains with angular to subangular shape. Quartz is the dominant mineral from

point counting, which is mostly monocrystalline (Appendix 2). Calcite cement, pyrite are also observed and this portion of Bryne Formation has higher porosity.

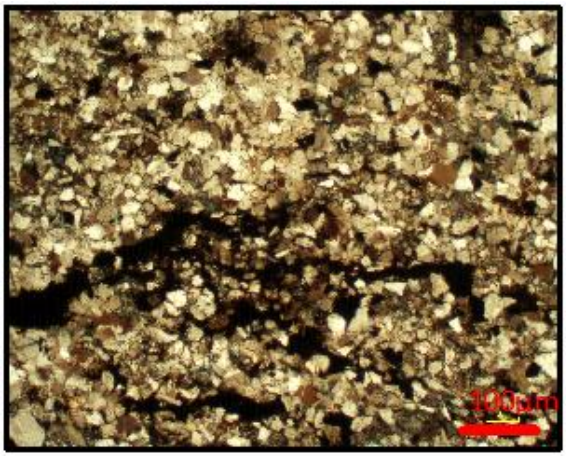

Figure 37: Showing silty sand with coal 2417,6m

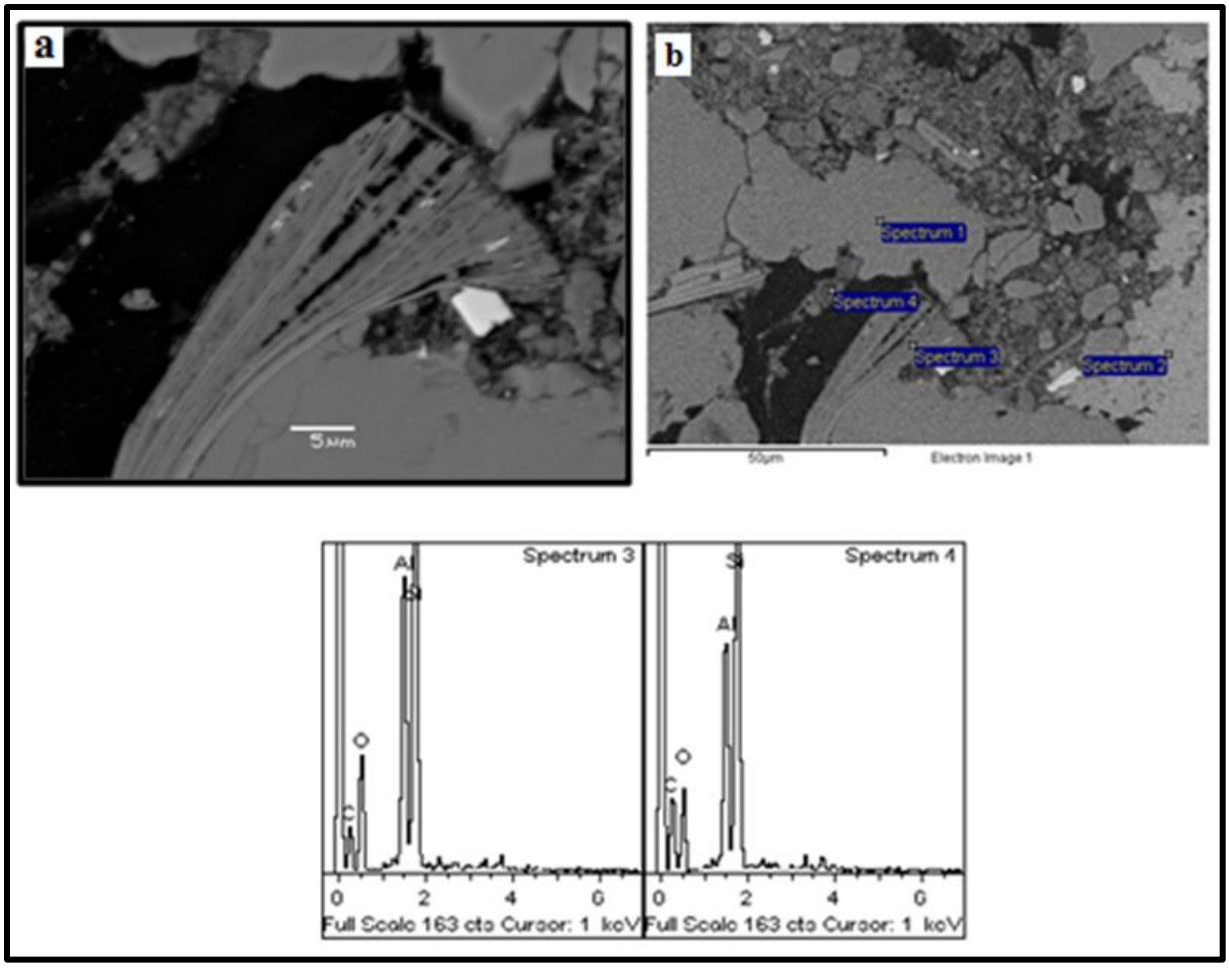

Figure 38: a) Showing morphology resembling to micaceous flakes (2417, 6m) . b) Showing various energy dispersive X-Ray spectrum of the same sample (2417, 6m).

The observation from Fig 38 shows the diagenetic conversion of mica flakes to kaolinite. In Fig 38a it resembles to a mica flake but energy spectrum displays it as a kaolinite.

5.1.4 Sandnes Formation

In general, Sandnes Formation consists of fine to medium grained sandstones with few shale beds as well. The framework of these sandstones is mainly grain supported and clay matrix (kaolinite) is present between the sand grains. Porosities of these sandstones also varies alot in different intervals (Appendix 2). The sands of Sandnes have calcite and quartz cement present in various sections with authigenic dolomite and framboidal pyrite.

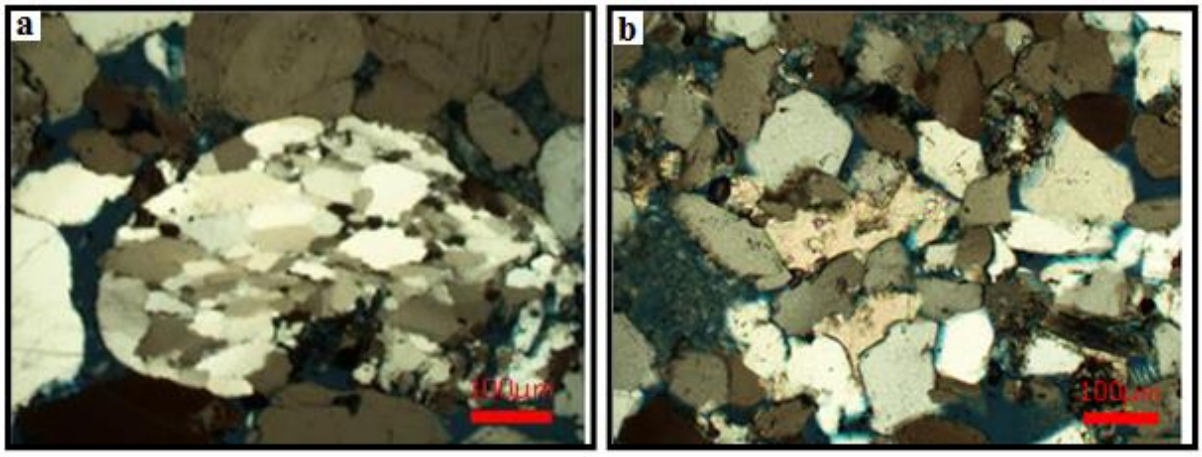

Figure 39: a) Weathered Gneiss in Sandnes Formation (2399,6).b) Quartz grains, clay matrix and calcite cement (2405,1)

Thin section from sand rich unit (2399,6m) is grain supported. Quartz is dominant mineral and quartz overgrowth is also observed. Polycrystalline quartz grains are also present shown in Fig.39a. This interval shows higher porosities from point counting data (Appendix 2). Thin section from 2405,1m is medium grained sandstone and calcite cement is also noticed. This unit is grain supported and from point counting data matrix percentage is 22% and consequently it shows very low primary porosities. The thin section from clay rich interval(2391,5m) is matrix supported. It shows dark brown to black color. Few clastic and quartz grains are noticed inside the matrix. Clay is mostly homogenous without lamination (Fig.40a).The thin section from the top of Sandnes Formation (2388,1m) is medium grained sandstone with authigenic dolomitic growth present between quartz grains (Fig.40b). From point counting data, quartz in most abundant mineral and matrix material is mostly clay.

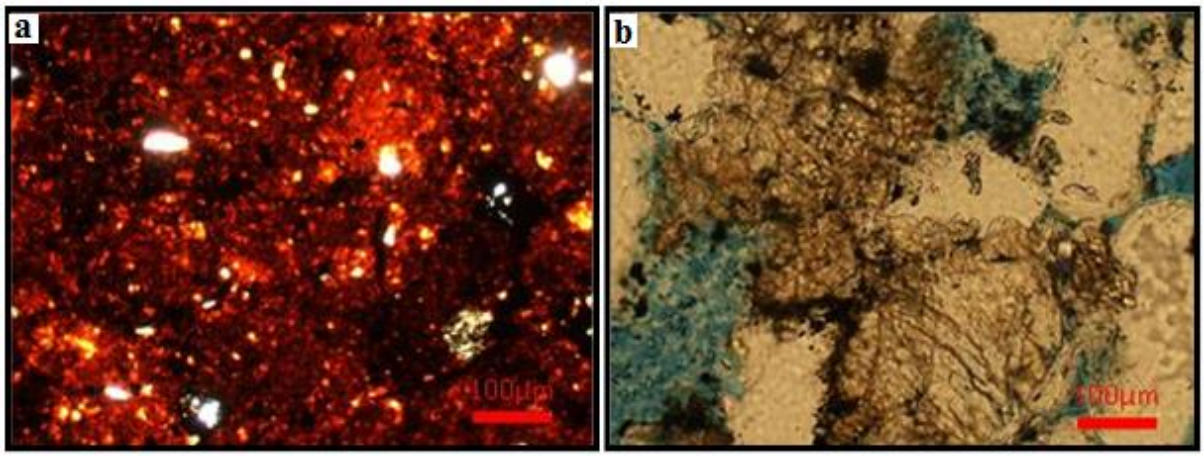

Figure 40: a) Pyrite rich shale of Sandnes Formation (2391, 5). b) Dolomite in the uppermost Sandnes Formation (2388,1).

5.2 X-Ray Diffraction (XRD) analysis

5.2.1 Basement

Bulk XRD analysis of basement samples comprising of both the cuttings and core samples was done in order to make a correlation between basement and overlying strata. Chlorite is the dominating mineral in the basement core samples followed by plagioclase displaying 39 XRD% and 26 XRD% averages respectively. Calcite is also present in large amounts 25 XRD% on average. Quartz makes 8 XRD% on average with pyrite 2 XRD% only.(Appendix 3).

In the cutting samples from the basement the plagioclase appears to be the most dominant mineral with 41 XRD%. Calcite is the second most abundant mineral with 25 XRD%. Chlorite and quartz appear to have averages of 21 XRD% and 10XRD% (Appendix 3).

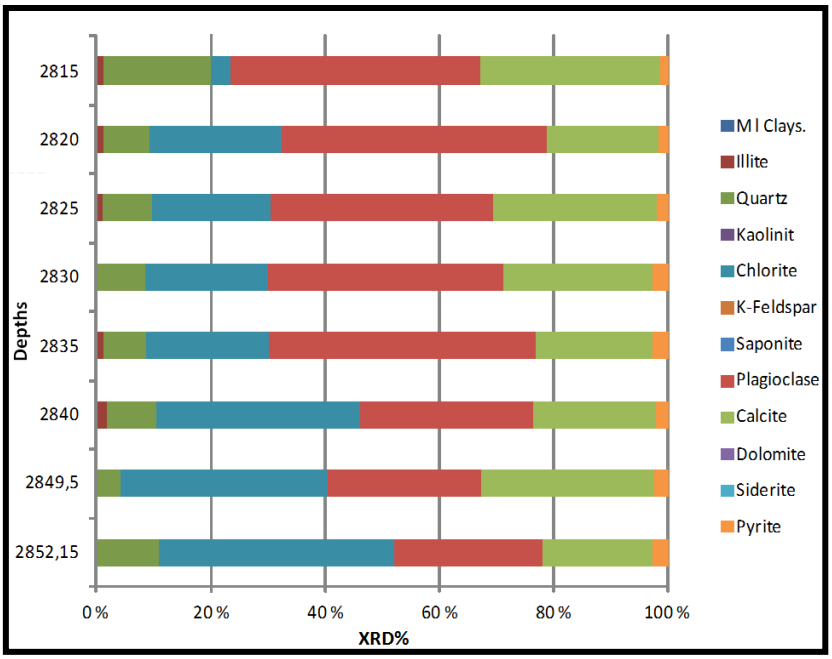

Figure: 41 Showing all the minerals identified in Bulk XRD mineral analysis in basement (Appendix 3).

5.2.2 Smith Bank Formation

Bulk XRD analysis was performed on the cutting samples from Well 17/3-1. These Triassic sediments have been extensively studied. Feldspars are the dominating mineral in the Triassic strata with a total average of 34 XRD%. Plagioclase contributes 29 XRD% , while K-feldspar is 7 XRD%. Quartz is the second most abundant mineral with average 24 XRD% and quartz to all feldspars ratio of 0.41. Calcite makes a significant contribution in XRD mineral percentage i.e 17%, whereas dolomite, pyrite and siderite are 6 XRD%, 3 XRD%, 1 XRD% respectively. Among the clay minerals the most prominent is kaolinite with 6 XRD% followed by chlorite and illite with 4 XRD% and 3 XRD% respectively. A bar graph showing comparisons of different mineral XRD% and the related changes with changing depth are shown in Fig 42 and Fig 43.

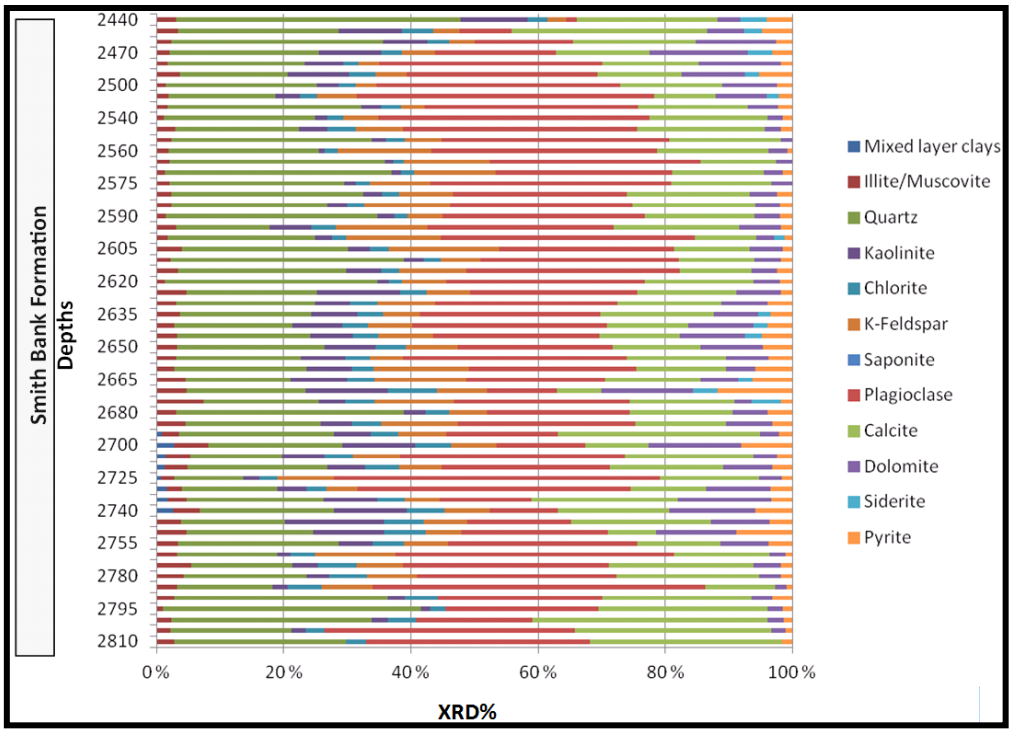

Figure 42 : Showing all the minerals identified in Bulk XRD mineral analysis in SmithBank Formation

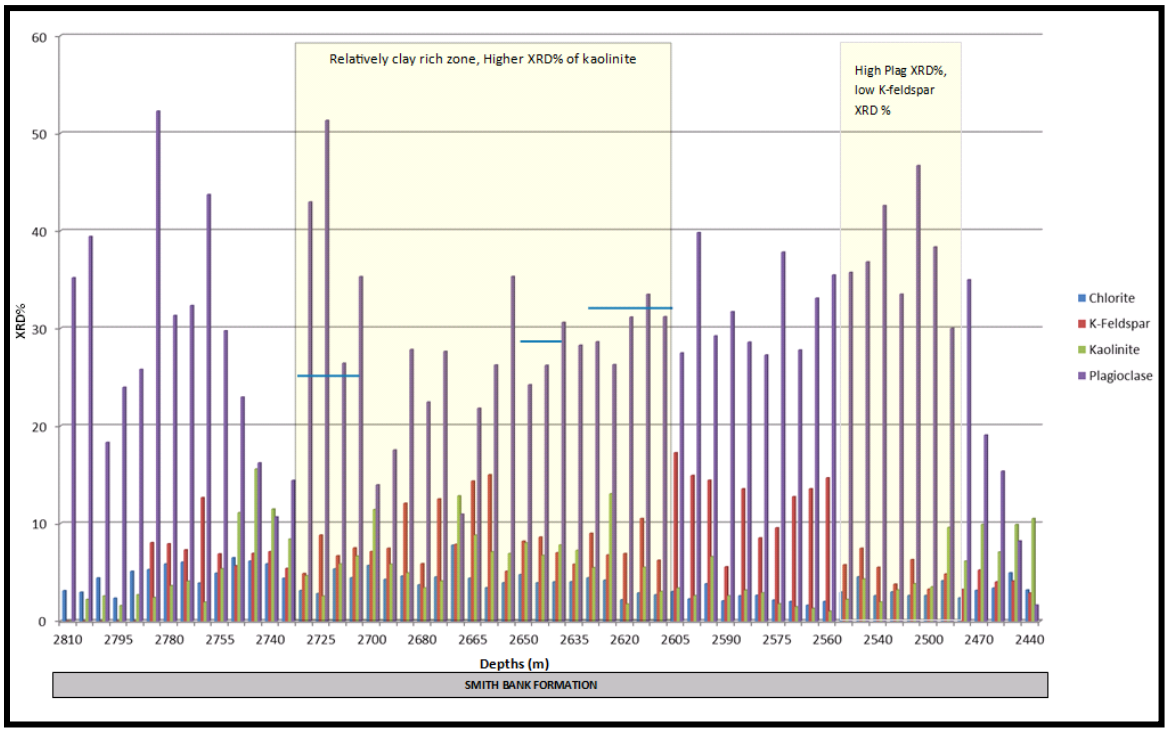

Figure 43: showing percentages of XRD in Triassic succession.

In Figure 43, a relatively clay rich zone is identified from 2750m to 2625m. This clay rich zone is also identified on geophysical log shown in Fig 24. From 2555m to 2470 a higher values of plagioclases is seen and but k-feldspar and kaolinite has very low values.

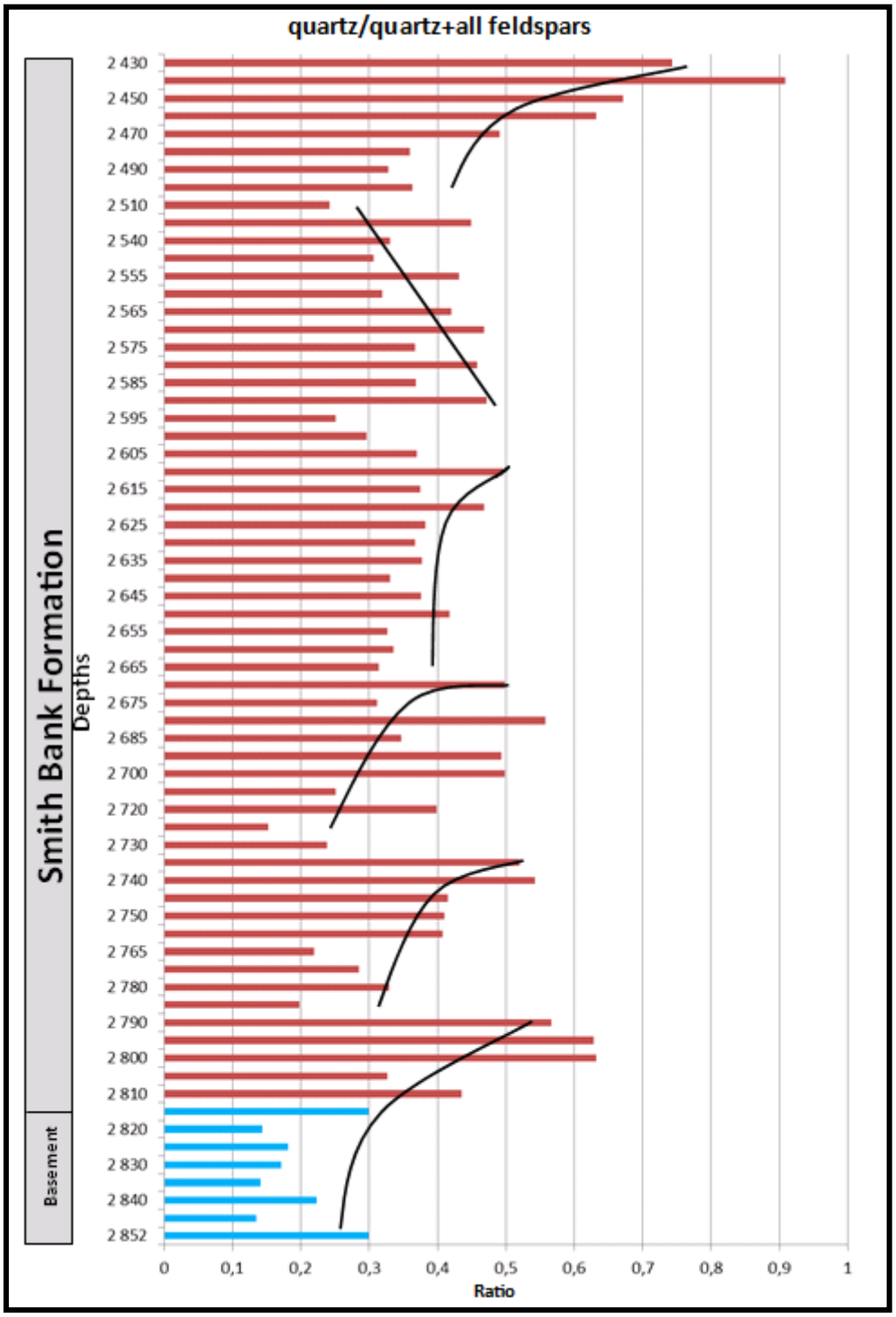

Figure 44: showing Quartz / (Quartz + All feldspar) in basement (blue) and Smith Bank formation(red).

The quartz to feldspars ratio in the lowest part of sedimentary succession reveals an increase in quartz content (Fig 44), compared to the basement presented in blue bars up to 2785m. The

increase in ratio i.e upto 0.5 is noticed due to increase in XRD% of quartz and decrease in plagioclase values. The other interval with higher quartz to feldspars ratio is the top of the Smith Bank Formation, which shows a progressive increase in the ratio towards top. Variation in trends is observed in Smith Bank Formation (Fig 44).

Fig 45 showing a comparison of plagioclase/k-feldspar and gamma ray value trend from basement to the top of investigated section.. The basement samples are completely dominated by plagioclase showing 100 XRD% among feldspar. The first sample where we find induction of k-feldspar is at 2785m depth which is almost 25 meters above the top basement (Appendix 4). This decrease in ratio due to increased XRD% of k-feldspar up to 2750m. At this interval the gamma ray value also show an increase due to potassium in feldspars which is radioactive and results in high gamma ray values.. After 2750m the ratios follow different trends that can be small trends marked in Fig.45. With increasing plagioclase/(plagioclase+K-feldspar) , the gamma ray value decreases and vice versa. However this trend does not strictly follow throughout the succession possibly due to variation in depths for cutting samples and also by the presence of other radioactive minerals. Then from 2550, higher ratios are recorded due to decrease in potassium feldspar XRD% values and this increase continues up to 2480m (Fig.45).

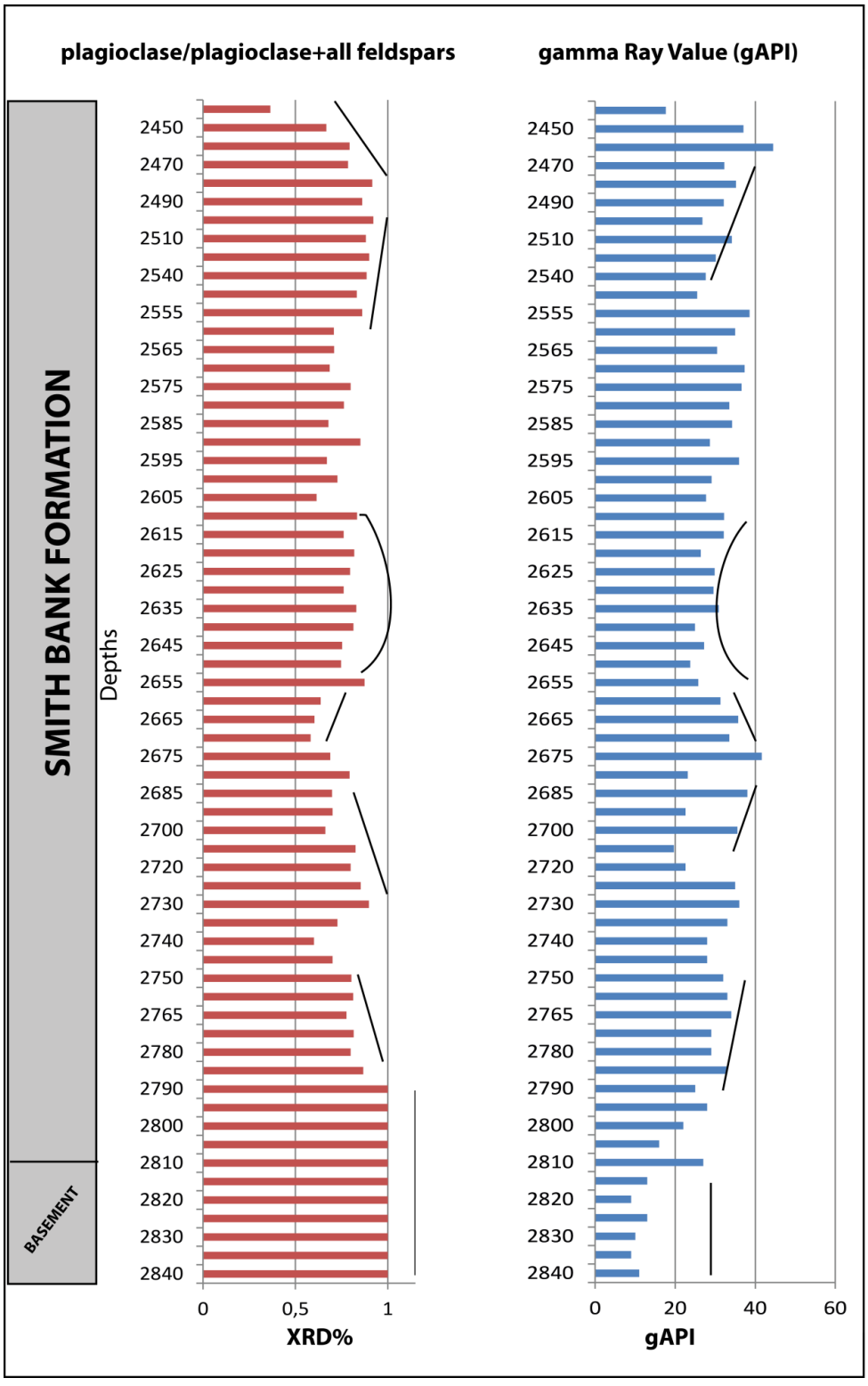

Figure 45: showing comparison of plagioclase/(plagioclase+k-feldspar) and gamma ray values.

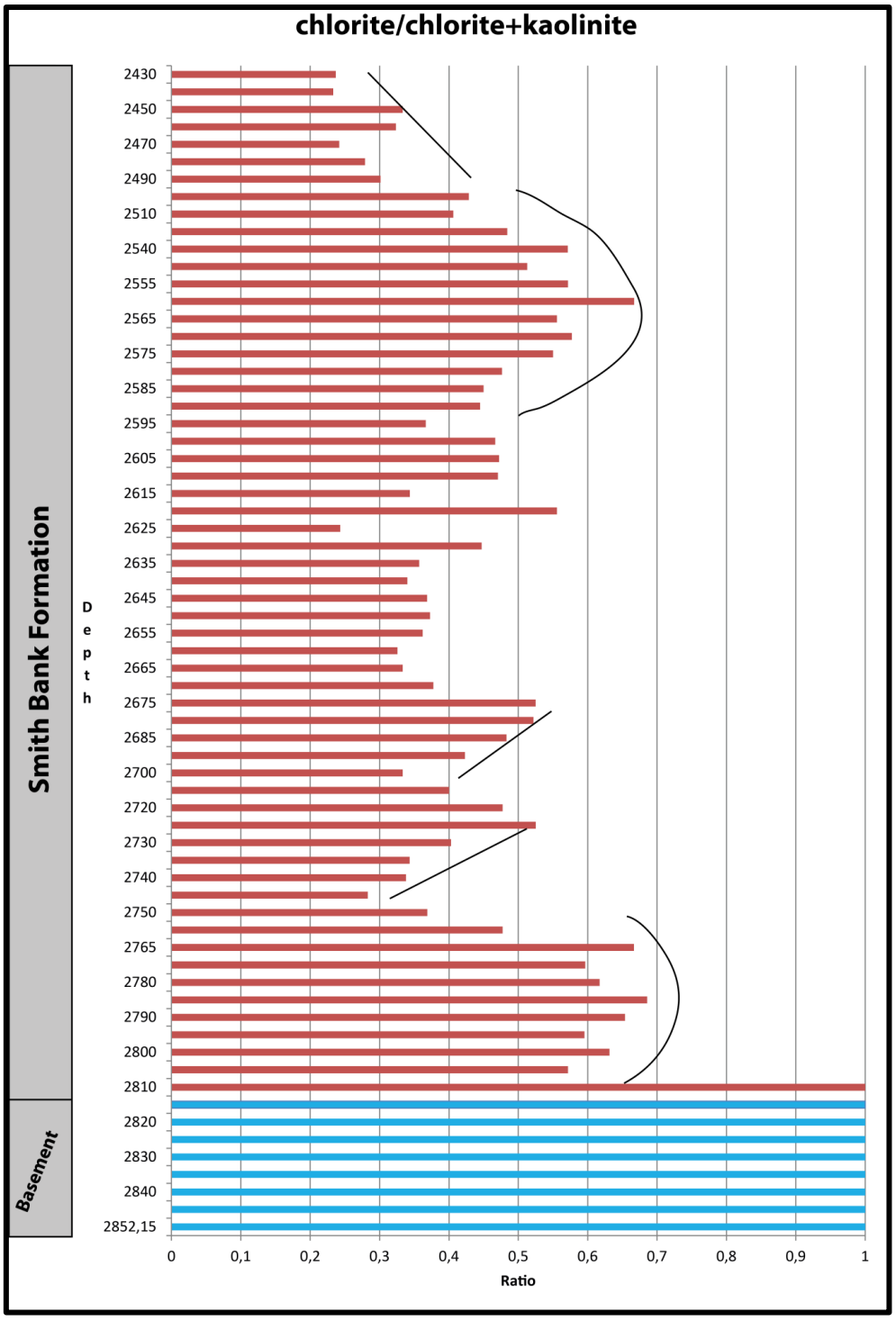

Fig 46 : Chlorite/ chlorite + kaolinite ratio in basement (blue) and Smith Bank formation (red) .

Fig 46 shows the ratio between the two dominating clay minerals. In the metamorphic basement samples the chlorite is present. But the alteration of primary minerals like feldspars results as soon as the basement encounters the atmosphere. With the introduction of kaolinite the ratio decreases. The ratio remained less than 0.5 throughout the Smith Bank formation except for two identifiable zones where ratios are greater than 0.5 i.e. i) from 2805m depth

samples to 2765m depth sample and ii) from 2575m sample to 2520m. In both the zones the higher ratio is the result of low XRD% of kaolinite.

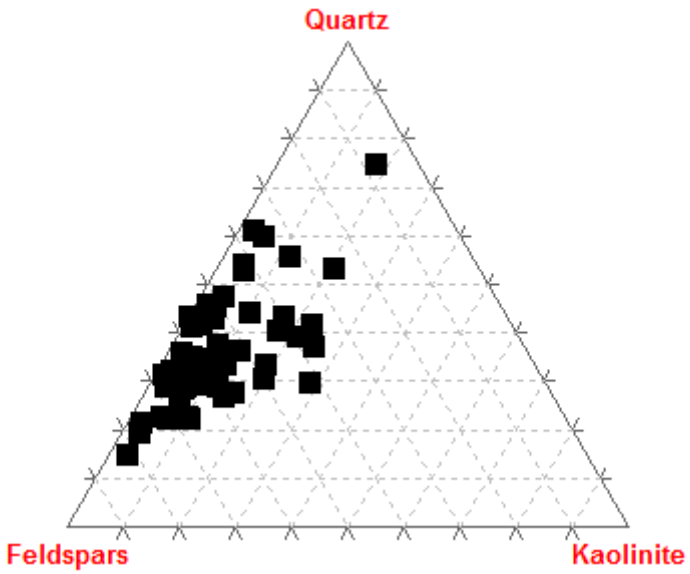

Figure 47 Ternary diagram showing relative XRD% percentages of Quartz, Feldspars and Kaolinite in Smith Bank Formation

The cutting samples from the Smith Bank formation make a cluster on the left of triangle showing higher percentages of feldspars and quartz with very little diagenetic or detrital kaolinite (Fig 47).

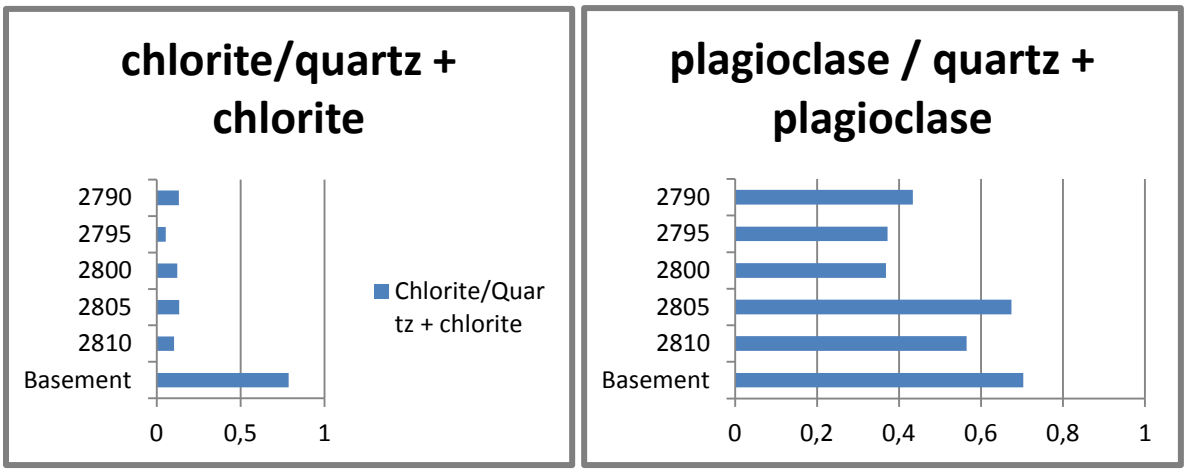

Figure 48: a) chlorite/(quartz+chlorite) above basement .b) Showing plagioclase/(plagioclase+quartz)

Fig 48a shows the decrease in chlorite XRD% in the lowermost Triassic sediments compared to basement and plagioclase to quartz ratio in Fig 48b shows the change in the plagioclase in regards to quartz from basement to lower Triassic sediments up to 2790m depth.

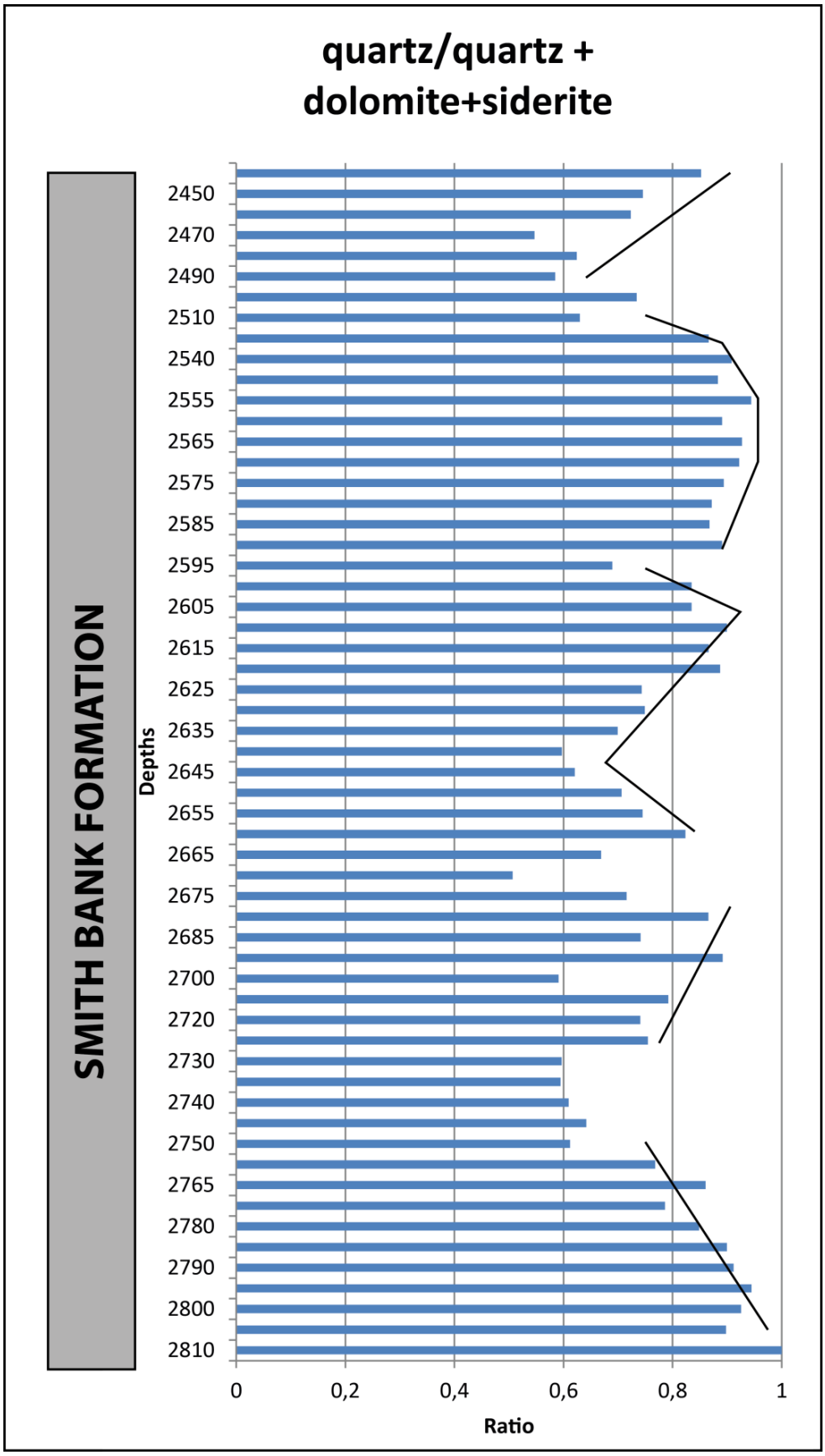

Figure 49 : quartz/ (quartz+dolomite+siderite) for Smith Bank Formation, a measure of allogenic vs authigenic minerals

Fig 49 unveils the fact that Triassic Smith Bank formation has a higher proportion of quartz compared to authigenic minerals.

5.2.3 Jurassic Formations

Sandnes and Bryne Formation:

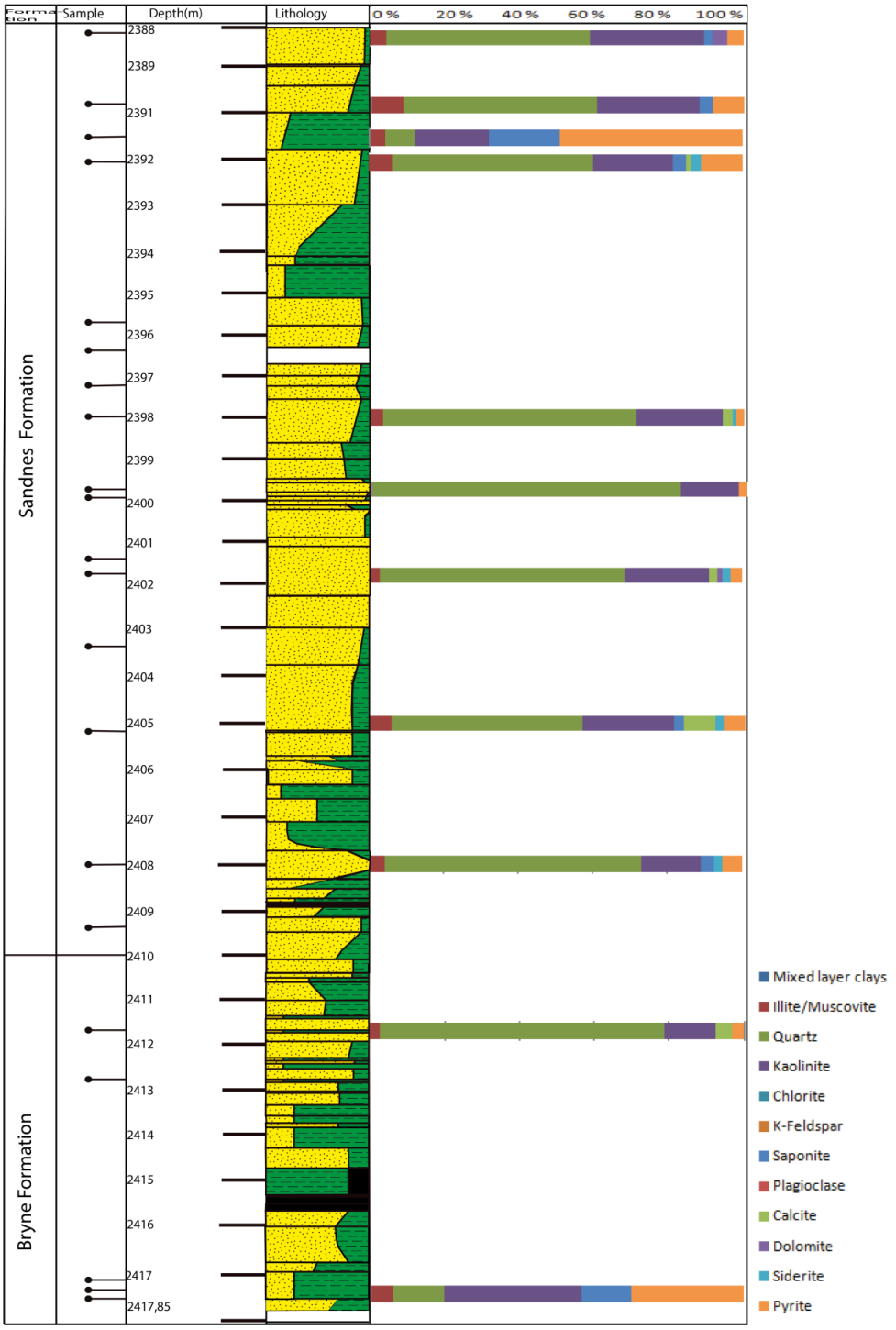

Figure 50: Showing all the minerals identified in bulk XRD mineral analysis in Smith Bank Formation

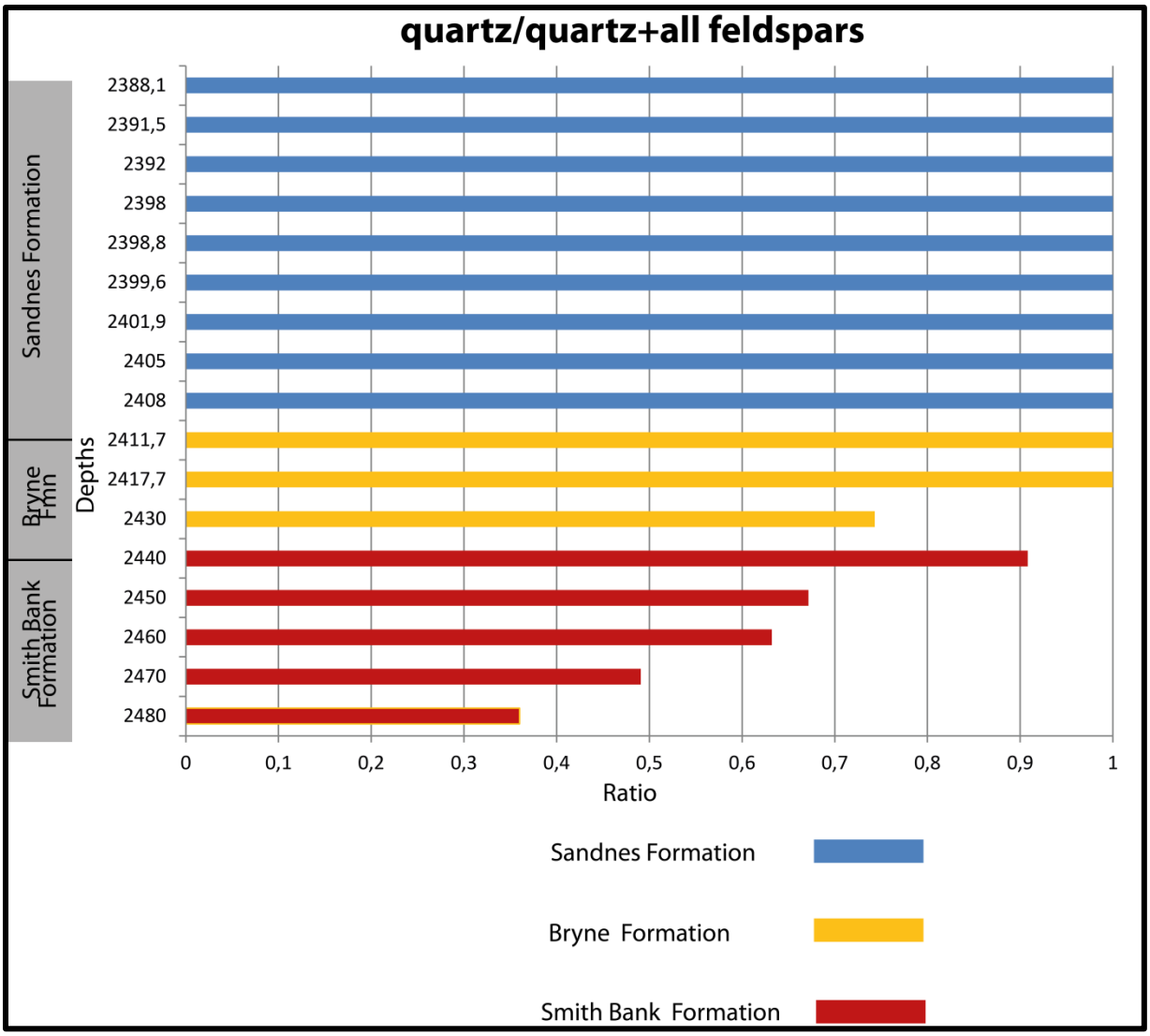

Figure 51: quartz/ quartz+feldspar ratio for top Smith Bank Formation, Bryne Formation and Sandnes Formation

Fig 51 represents the quartz to feldspar ratio of Top Smith Bank formation, Sandnes and Bryne Formation. Top Smith Bank shows a progressive increase in ratio reaching maximum of 1 in Sandnes and Bryne Formation.

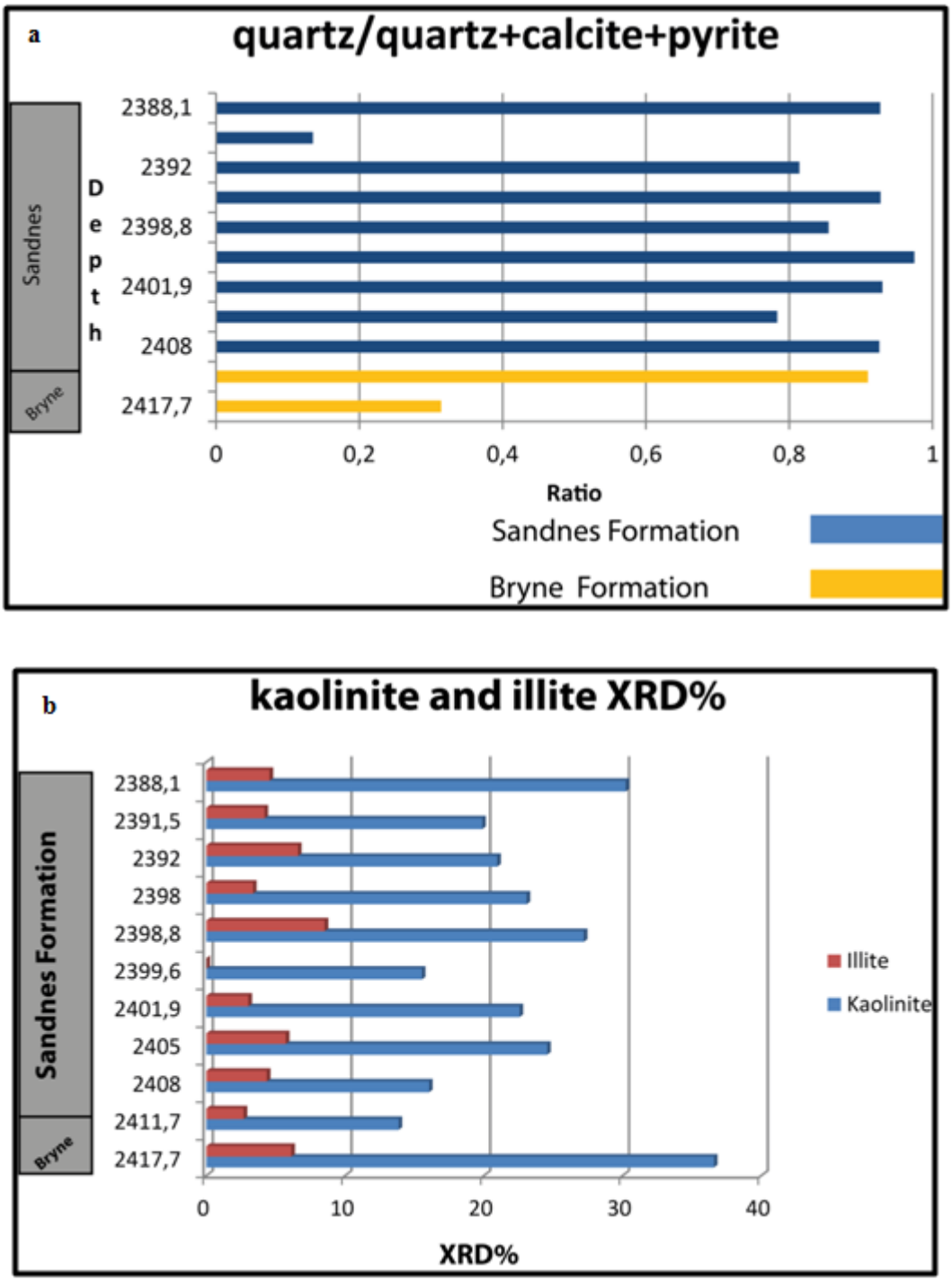

Figure 52 a) quartz/ (quartz+calcite+pyrite) for Bryne Formation and Sandnes Formation, a measure of allogenic vs authigenic minerals. b) Presents the XRD% of clays minerals dominating in the Bryne and Sandnes Formation.

6 Discussion of data:

Weathering involves physical, chemical and biological processes that alter the rock. Physical weathering is the process by which rocks are broken down without significant change in chemical or mineralogical composition, while chemical weathering involves processes that change chemical and mineralogical composition of rocks (Boggs, 1987). Kaolinite is formed in humid environments and acid rich waters within intensely leached bedrock lithologies like granite (Danuor et al., 2012).

The Hardangerfjord Shear Zone is a NE-SW trending ductile extensional shear structure that effects the basement, located in Hardangerfjord-inner Sogn area SW of Norway. The zone runs parallel to Caledonian orogenic belt and lines up with regional lineament offshore (Fig.2). This lineament has brittle faults (showing deformation at shallow crustal levels). Ling depression is the main structural element along this lineament (Fig.2) (Færseth et al., 1995). The brittle faults along this offshore lineament have marked NE-SW orientation which strongly proposes the fact that they represent the reactivation along Hardangerfjord Shear Zone, resembling to onshore Lærdal-Gjende fault system (Fig.2) (Fossen & Hurich, 2005).

Chlorites are very unstable at earth's surface conditions. Chlorites alter rapidly by hydration of hydroxide sheet accompanied with loss of iron and magnesium. This alteration may be related to oxidation of iron. The weathering of chlorite results in mixed layer chlorite-vermiculites, further changing to vermiculite (Proust, 1982). Pyriboles also weather quickly under favorable weathering conditions and result in the source for Mg and Fe for clay mineral formation in saprolites and soils (Proust et al., 2006). Sediments deposited in rift basins have short transport distance in between the site of erosion and deposition. The presence of unstable minerals like chlorite and biotite are good indicators of rapid erosion, otherwise it is unlikely for these minerals to survive (Bjørlykke, 2010).

Basu et al., 1975 suggested for Holocene sands that larger amount of polycrystalline quartz have metamorphic origin compared to sands having plutonic provenance. Sands originating from low grade metamorphic rocks have more polycrystalline quartz than from sands derived from higher rank metamorphic rock (Basu et al., 1975).

6.1 Basement:

Well 17/3-1 is located on the offshore lineament of Hardangerfjord shear zone (Fig 2 & 8). Calcite veins are found to be filling the fractures in the amphibolitic basement. Calcite

probably have precipated as secondary mineral from the circulating groundwater filling the fractures. The presence of microfolds and fractures observed during core logging indicates that basement is effected by both ductile and brittle shearing. This brittle and ductile shearing probably have formed in response to post caledonian extensional activity of Devonian age (Torgeir et al., 1999).

Striations observed on the basement and on the calcitic veins can be attributed to various other reasons.The strike slip displacements related to Sorgenfrei-Tornquist Zone (Variscan Orogeny) is one of the possible reasons for the striations on the basement . Fig 2 and 8 shows that well 17/3-1 is located on offshore lineament of Hardangerfjord Shear Zone which onshore coincides with Lærdal-Gjende Fault system. Translational movements on the faults in Lærdal-Gjende Fault system are comparable to the movements on major faults in North Sea (Torgeir et al., 1999). NE-SW orientated brittle faults on offshore Hardangerfjord Shear Zone originated also due to movement on major faults in North Sea in Permian. These brittle faults are in assemblance with onshore Lærdal-Gjende fault system onshore, so it is also safe to assume that Permian brittle faulting and related movements most likely have resulted in the striations and fractures which were later filled with calcite veins. However it can be assumed that movement along faults continued and resulted in striations on newly precipitated secondary minerals.

Another possibility can be drawn from the observations that calcite precipitation and striations on the basement and calcite veins can be the result of different phases of stresses induced on basement in different periods of time.

Rosendahl (1987) suggested that features which tend to cease the along strike growth of rift units follow the preexisting grain and exhibit the most shearing. Termination of rift units come about by strike slip faulting in pre-rift zone of weakness (Rosendahl ,1987). Fig 8 shows that most of the N-S faults terminate at Hardangerfjord Shear Zone and does not cross this lineament. So on this basis Hardangerfjord Shear Zone can be regarded as a prerift zone which ceases the growth of faults , hence experiences the strike slip faulting. This strike slip faulting may also have resulted on striations and slickensides on the basement.

The rocks of Hardangerfjorden group can be traced for 100km along NE-SW strike (Faerseth 1982). On this basis it is be probable to assume that basement of Well 17/3-1is an extension of Sågvagen formation of Hardangerfjorden group belonging to Sunnhordland Nappe

Complex. But the age predicted for Hardangerfjorden group by Færseth 1982 is Pre-Ashgill age which is not in accordance with the age of basement (410Ma) in Well 17/3-1(npd.no).

6.2 Absence of weathering profile:

The absence of secondary minerals on the section above basement rock indicates that no weathering profile has developed or that it has been fully eroded before Smith Bank Formation deposited. Progressive weathering can result in the alteration of plagioclases and biotites and the end product for this alteration is kaolinite (Tardy et al., 1973). Also the weathering of amphiboles and chlorites will result in the formation of secondary clay minerals. Proust, 1982 suggested that saponite would be the end product of weathering of hornblende in the amphibolite. Nesbitt and Young, 1984 suggested that feldspars commonly weather to kaolinite and illite , mafic minerals and glass probably to smectites and kaolinite , illite as well. Plagioclase is one of the most rapidly weathered silicates and large amount of kaolinite group minerals are formed as a result of plagioclase weathering (Nesbitt and Young, 1989) . The present studies have not disclosed any such findings of secondary clay minerals. The amount of plagioclase did not decreased much above basement (Fig. 48b). So it can be infered that probably physical weathering and resulting deposition has played its part in the accumulation of sediments above basement rather than chemical alteration. The other possibilty can be the presence of a weathering profile which may have eroded down. As this zone, according to Heermans and Faleide, 2004 was a high relief accommodation zone, a relatively elevated zone which might have resulted in erosion of weathering profile to low lying adjacent basins.

6.3 Smith Bank Formation:

The Smith Bank Formation was deposited directly over the metamorphic basement in Well 17/3-1(npd.no). The thickness of Triassic sediments is 311m in well 17/3-1, observed less than adjacent grabens of Stord Basin and Åsta Graben (Fig 3). The well is located on the margins of boundary faults away from the locus of maximum hanging wall subsidence and maximum footwall uplift and most of the fault segments terminate here. Considering the orientations of faults around this area which are dipping in opposite direction and have moderate overlapping zone (Fig 1) it is plausable to classify this horst structure as an oblique accomodation zone defined by Faulds et al, (1998). Accommodation zones are formed in between overlapping zones of normal faults. Also called as rupture barriers (King, 1986).

Smith Bank Formation is deposited in evolving rift basin in Triassic. The depositional environments of Smith Bank Formation vary from alluvial fans to stream/floodplain deposits. The source, mode of transportation and depositional settings are discussed further in detail.

Smith Bank Formation is divided into four zones on the basis of differences observed in depositional settings and probable provenance.

6.4 From 2810m-2785m (Lower Part)

The petrographic and XRD studies of lower part of Smith Bank formation are in accordance with each other. Thin section study of the sediments show mica rich mudclasts, also rich in quartz and feldspar grains embedded in mudclasts (Fig.26a). The XRD% for the plagioclase is high and conversely the kaolinite XRD% is very low i.e only 2%. The minimal values of kaolinite and high XRD% of plagioclase shows that sediments were transported short distances before deposition or the provenance for these sediments is plagioclase rich (Boggs 2006). The higher plagioclase values show that diagenetic alterations due to meteoric water flushing were also negligible. In that case, kaolinite would have precipitated by dissolutioning of feldspar (Lanson, 2002). This is why the alteration of feldspars to secondary minerals is limited. Striations and slickensides on calcite veins were observed on the basement during core logging. SEM analysis showed the presence of hornblende in this zone (Fig.35). The higher XRD% of calcite in this zone and high average number of striated calcite fragments in thin sections makes a logical indication for the amphibolitic basement being one of the main provenance for the sediments. From point counting it was noticed that amphibolite clasts resembling to basement has high percentage in this zone (Appendix 1). Chlorite to kaolinite ratio is higher than 0.6. These numbers cease the fact that very less chemical alteration of the minerals took place place. Also the climate in the early Triassic is arid which did not favor much of the chemical alteration of minerals.

The deposition of sediments in this zone presents the stage of rifting on numerous fault bounded depocentres which were only partly connected and individual fault blocks were not linked together allowing axial transport. Isolated depressions have local interior-drainage basins resulting in no outlet connection to adjacent structures. Though due to rifting tectonic slopes are produced by hanging wall subsidence and foot wall uplift. The foot wall area acts as main source of sediments for basin, although sediments derived from hanging wall are more extensive spatially (Leeder and Gawthorpe, 1987). The sediments deposited in this zone

are predicted to be sourced from locally uplifted amphibolitic basement and deposited as transverse fan deposits in arid to semi-arid climate.

The percentage of polycrystalline quartz is 2.3% from point counting data. Amphibolite facies is a medium grade metamorphic facies so the polycrystalline quartz ratio is also low in this zone. This observation also depicts that sediments were derived from local amphibolitic basement.

Chlorite is very unstable and is changed to regularly interstratified chlorite/vermiculite, afterwards into irregularly interstratified chlorite and then vermiculite (Takashi et al., 1996). In the sediments above basement the XRD% of chlorite shows very much decrement. Chlorite has average percentage of 30XRD% in basement and reduced to only 3XRD% in Triassic sediments (Appendix 4). This might be the only reason to believe that local basement or near source were not the only provenance for this zone and sediments may have travelled enough for the alteration of chlorite to occur.

Various scenarios can be erected to support this proposition like antecedent drainage incising into uplifted hinterland and depositing sediments in the hanging wall. The transverse drainages which supply sediments to margins of hanging wall may originate beyond the region of active tectonism, far into hinterland (Ebinger et al., 2011). So on these assumptions this zone may by directly fed by the uplifted Fennoscandian shield. The sediments are also deposited as alluvial fans but sourced from mainland (Fig.15b). Also as the well 17/3-1 is located on Hardangerfjord shear zone and most of fault units terminate at this zone of weakness so streams enter into this zone directly sourced from Fennoscandian Shield from the east.

Hardangerfjorden Group on the islands of Stord, Bømblo and Tysnesøy can be the possible source for the sediments in this interval. Sagvågen Formation of the Hardangerfjorden Group of volcanic origin has albite, chlorite, calcite, muscovite and quartz (Færseth,1982). The presence of dominant minerals (Fig 42 & 43) in zone from 2810m to 2785m shows that it might have been sourced by the greenschist of Sågvagen Formation.

6.5 From 2780m-2580m (Middle Part)

This zone is demarcated by change in mineral assemblage and XRD% (Fig 37 and Fig 38). The first sample where the induction of K-feldspar is noticed in XRD analysis is 2785m, an

indicative of a new source other than the amphibolitic basement or greenschist facies of Hardangerfjorden Group. The quartz to all feldspar ratios have also decreased with the introduction of K-feldspar (Fig 44). The decrease in striated calcite% and amphibolite fragments% from point counting data also seconds the reason that local amphibolitic basement is not the only provenance for the sediments in this interval. Chlorite to kaolinite ratio is less than 0.5. Petrographic analysis apprising the fact that mudclasts having feldspar grains are more altered, less feldspar grains embedded, less muscovite flakes are noticed, more clayey content proving that sediments may have travelled longer distances before deposition/originating from a distal source or the source material itself is degraded by weathering reactions (Fig.27a). The percentage of polycrystalline quartz is very low or even absent in various sections studied. This low percentage of polycrystalline quartz is indicative of volcanic origin (Basu et al., 1975). Number of crystals in a single polycrystalline grain is also low (< 5) in this zone. This can also be a crude indicative of plutonic origin as suggested by (Basu et al., 1975). The main alteration reactions for formation of kaolinite are given below after (Bjørlykke, 2010)

$2K\ (Na)\ Al_2\ AlSi_3O_{10}(OH)_2$ (muscovite) + $2H^+ + 3H_2O = 3Al_2Si_2O_5(OH)_4$ (kaolinite) + $2K^+(Na^+)$

$2K\ (Mg, Fe)_3\ AlSi_3O_{10}(OH)_2$ (biotite)+ $12H^+ + 2e + O_2 = Al_2Si_2O_5(OH)_4$ (kaolinite) + $4SiO_2$ (in solution) + $Fe_2O_3 + 4Mg^{++} + 6H2O + 2K^+$

$2K\ (Na)\ AlSi_3O_8$ (feldspar) + $2H^+ + 9H_2O = Al_2Si_2O_5(OH)_4$ (kaolinite) + $4H_4SiO_4 + K^+(Na^+)$

Plagioclase to all feldspars ratio (Fig.45) is relatively low in this zone , also the chlorite to kaolinite ratio is low (Fig.46). This can lead to the fact that more chemical alteration of plagioclase has taken place in this zone resulting in the deposition of more kaolinite. Kaolinite is mostly detrital so it can also be assumed that the chemical weathering may have affected the source rocks for this zone or alteration may have taken place during transportation. . Worden and Sadoon, 2003 suggested that kaolinite in sands of Triassic and Jurassic is detrital. The degradation of biotite and muscovite flakes also adds to the point that more chemical alteration of the source rock material took place or sediments travelled enough distance for the alteration to take place.

The westward dipping normal faults along Øygarden fault complex shown in Fig 8 have a throw of more than 3km. Footwall sourced fans are deposited in the lower margins of adjacent hanging wall. The sediments deposited in the hanging wall margins of Stord basin

originated from the uplifted footwall block i.e. Norwegian Mainland. Largest amounts of sediments will enter from relay ramps or where major faults terminate (Ebinger et al., 2011). The increasing rifting will result in the linkage of adjacent fault segments and topography of intrabasinal highs are reduced and axial drainage flow will start (Leeder & Gawthorpe, 2000). This stage is predicted as being in rifting where most of the faults have linked together and axial flow of rivers have started. Meandering axial river system has developed, having close interaction with footwall fans (Fig.15c). In open rift basins axial rivers easily interact with transverse drainages and also react to tilting stimulated by fault activity (Leeder & Gawthorpe, 2000). Contribution from transverse sedimentation is also predicted to be present. The flow direction of meandering river belt is from north to south. Ryseth, (2001) predicted southwardly drainage direction for Triassic alluvial system of North Sea. Streams flowing in southward direction laden with sediments sourced from mainland are the main provenance for this interval. The sediments are predicted to be deposited as stream and stream flood deposits/floodplains by lateral migration and avulsion of axial channel. The gamma ray trends also show the deposition as channel sands and muddy alluvial floodplain facies. Point counting data also depicts the fact that shale and silt percentage fragments in this zone have also increased. Within this interval various small zones of increasing clay contents and decreasing plagioclase content are identified. These zones are deposited as a result of flooding. The episodic occurrence of clay rich intervals shows the deposition in overbank areas of a channel (Fig.43). The monsoonal or seasonal precipitation prevailed in the Triassic and resulted in floods and deposition of clay rich sediments in overbank areas.

The petrophysical log of this zone show two dominating carbonate cemented zone probably calcrete horizons (Fig.24). Between the floods, floodplains dry out and features related to subaerial exposures may develop (Readings, 2003). The sediments on the floodplain were periodically exposed to sub aerial conditions. As the monsoonal conditions prevailed in Triassic and alternating wetting and drying resulted in the downward leaching of the calcium carbonate. This calcium carbonate precipitated in accumulation zones of soil profile on floodplain alluvium forming calcrete horizon. Micritic to sparitic texture observed in thin section in the calcrete horizon (Fig.31a and 31b). Micritic texture is formed from rapidly drying vadose solution while the occurrence of sparite shows there was enough supply of ions for the larger growth of crystals (Durand et al., 2010). Transition zones can be observed between sparry calcitic and micritic textures (Fig.31b). Sparry calcite may have formed by later transformation by consistent supply of ions by phreatic groundwater. The presence of

these calcium carbonate cemented zones indicates that soil forming processes were occurring at the time in the dry intervals between flooding.

The presence of K-feldspars indicates a probable granitic or rhyolitic source. Slagstad et al, (2011) suggested the granitic and dacitic composition of basement on Utsira High. Utsira High can act as a provenance for sediments in this zone. Considering the structural setting of the Utsira high in context to Well 17/3-1 this proposition seems to be implausible. In Fig.53a it can be observed that Utsira high has major bounding fault dipping to east. An overlapping fault having similar polarity but with different throw can also be observed. Though the eastern part of Utsira High can act as footwall uplift and has a high gradient Fig 53a. The sediments from footwall will be deposited as small alluvial fans on lower gently sloping hanging wall in adjacent basin (Fig.53b). In this particular case these sediments would be trapped in the overlapping half graben. Conversly, spatially most of the sediments would be deposited westwards as broad alluvial cones (Fig.53b). The dip would be gentle and a larger area for incision and be exploited by stream erosion (Prosser, 1993). So based on these assumptions basement of Utsira High seems not to be the probable provenance for the sediments in Well 17/3-1.

Most likely alternative source for the Smith Bank Formation in this interval were the volcanic rocks rich in alkali feldspars and plagioclases on the Mainland Norway. Precambrian granitic basement in Hardangerfjorden area (Fig. 13 & 14) and in the east to Hardangervidda area can be provenance of sediments in rift basin. The Pre-Ashgillian Sunnhordland Igneous Complex occupying the northern parts of islands of Bømblo, Stord and Tysenøy has thick sequences of rhyolitic lavas in its upper part (Andersen and Færeseth, 1982) , can also be other possible predicted source for alkali rich sediments (Fig. 13 & 14).

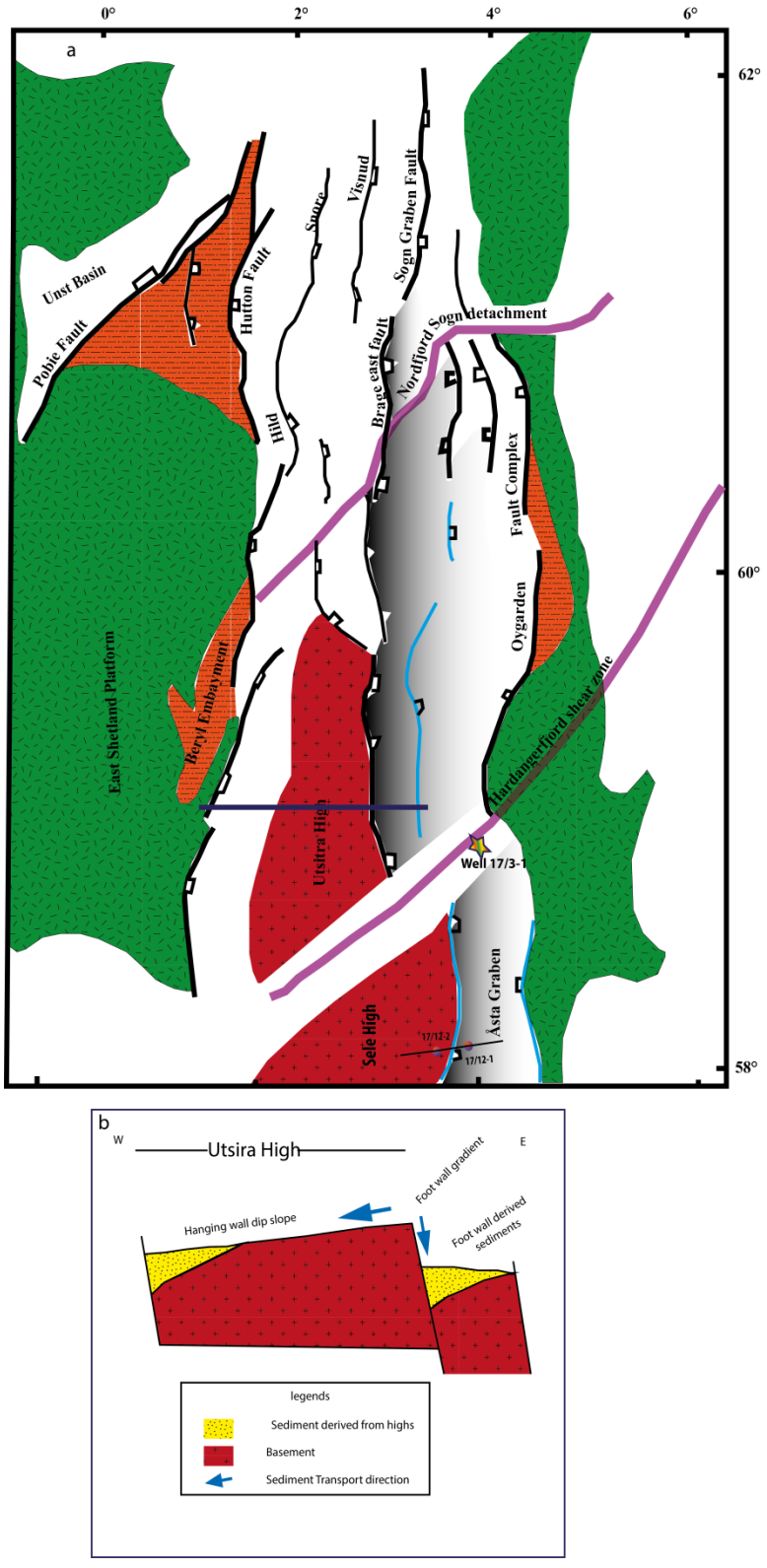

Figure: 53a Main Permo-Triassic structural and tectonic features resulting from extensional tectonics modified from Færseth (1996) and Smith et al. (1993). b : Assumed depositional settings in rift basin around Utsira high profile cutting across Utsira High. Well 17/3-1 is also shown

6.6 From 2580m-2490m (Upper Part)

Petrographic analysis of this zone showed that mudclasts have matrix of greenish color resembling basement with large feldspar and quartz grains and less mica flakes embedded. From point counting data it can be observed that percentages of striated calcite fragments, amphibolite clasts fragment and weathered gneisses have also increased in this zone (Appendix.1) which also is indicative of amphibolitic basement as major sediment source for this zone. Upwards increasing values in the plagioclase to K-feldspar ratio are also evident. The polycrystalline quartz percentage is very high indicative of low grade metamorphic rocks (Basu et al., 1975). Chlorite to kaolinite ratio also increases progressively in this interval with a peak value at 0.65.

These observations reflect increased input of sediments from amphibolitic or greenschist facies of Hardangerfjord group. Various scenarios can be erected for the deposition in this zone. Steel and Ryseth, 1990 suggested intra-basinal tectonics in late triassic as well. This may have resulted in another phase of uplift of local basement. This tectonic activity, uplifting of hinterland or local basement and related increased trasnverse input of sediments resulted in choking and forced migration of axial river. So decrease in kaolinite XRD%, K-feldspar XRD% and shale and silt percentage fragments can be attributed to less sediment input by axial rivers due to lateral shift away from the point of study by proximal alluvial fan deposits sourced from uplifted blocks. The increase in plagioclase to K-feldspar ratio can be the result of decreased input of K-feldspar rich sediments, not the result of alteration of K-feldspars. Nesbitt and Young, 1989 suggested that as K-feldspars usually weather slowly than plagioclase so if axial transportation would resulted in more chemical alteration during transportation or the source rock have started to weather more, in either case the plagioclase values should have also decreased. Plagioclase ratio increased in this zone indicating amphibolitic basement acting as source, which is rich in plagioclase. But at the same time input from axial river transport cannot be completely neglected. Though the amount of sediment input may have reduced in this zone by axial transportation.

Direct input from Fennoscandian shield can be other probability. Increased percentage of polycrystalline quartz indicates that the sediments in this zone are sourced by low rank metamorphic rocks. Various sections of low rank metamorphic rocks are present on the different islands on Mainland Norway shown in Fig 12.

6.7 From 2490m-2440m (Uppermost Part)

This zone marks the progressive decrease in plagioclase XRD% and increase in kaolinite XRD%. Upward increase in quartz to all feldspar ratio in this zone is also noticeable (Fig 44). Plagioclase to K-feldspar (Fig.45) and chlorite to kaolinite ratios (Fig.46) have decreased. The sediments deposited in this are again mostly from axial flowing river . During the deposition of this zone, the basin is assumed to have achieved more tectonic stability with mature relief. Sediments are assumed to go through various cycles of erosion and deposition before finally being deposited so more chances of degradation. Also the climatic conditions may have changed for alteration of feldspars to occur. This tectonic stability and climatic change has resulted in the weathering of provenance and also sediments are more altered during transportation before deposition so more detrital clay rich sediments are deposited.

Overall Smith Bank Formation can be regarded as mineralogically immature unit of sediments. High XRD% of feldspars show that sediments were deposited in tectonically active areas so there was less time for weathering of both insitu bedrock and sediments in transport. Otherwise in tectonically stable areas, the basement rocks would have altered more resulting in the alteration of feldspars. During transportation greater proportions of feldspars would have broken down as sediments would have deposited and eroded various times before final deposition. Fig 49 shows that allogenic minerals are dominating in Smith Bank Formation. Hence very little diagenetic alteration of sediments have resulted in formation of authigenic minerals.

The islands of Bømblo and Stord have complex and heterogenous stratigraphy, but the source for the Triassic sediments can be predicted by lithology comparison. Quartzo feldspathic mylonitic gneisses with bands of amphibolites (Færeseth, 1982) make the Halsnøy complex shown in Fig (13). Dryskard unit of Dryskard-Kvitenut-Revsegg allochton metamorphosed to amphibolite facies but later break down to biotite and chlorite is also noted (Andersen and Færeseth, 1982). This unit is exposed in southern Hardangerfjorden area shown in Fig.(13) and can be probable provenance for continuous chlorite input into Triassic sediments. Kvitenut unit is also exposed to southern part of islands of Bømblo (Fig 13). The erosion and subsequent deposition of these lithologies from Fennoscandian shield may be the main source for sediments in Triassic rift basins.

6.8 Stratigraphic model of Smith Bank Formation in Well 17/3-1 on basis of Petrophysical logs

Rift sequence stratigraphic model presented by Neto and Catuneanu, 2009 is applicable to marine and non-marine (lacustrine settings). The deposition of Smith Bank Formation in this part of the basin is interpreted to be mainly as transverse fan deposits from uplifted blocks and as the floodplain and stream deposits. So the rift sequence stratigraphic model of Neto and Catuneanu,2009 is not accurately applicable in non-marine sub aerial settings. However the depositional model is presented on the basis of depositional tracts marked from gamma ray logs. Various depositional system tracts i.e coarsening upward and fining upward tracts have been identified and marked on the basis of changing patterns of lithology and gamma ray (Fig 54). The fining upward sequence represents periods of fault activation and accommodation space creation. The major portion constitutes of progradational stacking of facies in rift sequence pattern which is coarsening upward in vertical succession. This represents the period of tectonic quiescence (Neto and Catuneanu,2009).

Depositional pattern of Smith Bank Formation starts with the basal sands (Fig 54). In the initial stage of rifting the accommodation space was still limited (Prosser, 1993) so the coarser particles were deposited by alluvial fans. This basal sand can also be a representative of early stages of rift development, where younger basins have smaller depocentres rapidly filled by sediment influx (Schlische & Olsen 1990). The first sequence observed is a fining upward sequence showing the retrogradation of alluvial fan sourced from local basement. The retreat of the alluvial fan may be due to degradation of source area (Gloppen and Steel, 1981) or the ongoing tectonic activity in which sedimentation is outpaced by subsidence.

The following tract is a coarsening upward sequence CU_2. The possible reason for this coarsening upward sequence could be the

1) Period of tectonic inactivity in which no new accommodation space be created and already created accommodation space be filled with sediments by advancing alluvial fan resulting in coarsening upward succession.

2) The previous tectonic activity resulted in a higher relief between provenance and basin so sediment influx would be high, or possibly an induction of sediments from a new source can also result in coarsening upward sequence.

Analyzing the results from XRD data it is revealed that K-feldspar is considered from another source rather than amphibolitic basement. The peaks representing K-feldspar come from depth 2785m from cutting sample. Cutting samples can show up from 5-10m above the original depth being presented. So based on this assumption it is most likely to say that this coarsening upward succession is the strong indicative and result of new source area (Prosser, 1993)

Another phase of coarsening upward sequence CU_2 indicates more sediment infilling to younger basin from multisource, which is tectonically not so active. In this sequence channel fill sandstones are recognized on the basis of gamma ray box car trend (Fig.54).

FU_2 represents the fining upward succession of the basin. This part starting from 2720m depth can be demarcated as a zone which represents the fault activity. This activation has probably resulted in increased accommodation space and in response, rate of sedimentation is less than the rate at which the basin is subsiding so a fining upward sequence is observed. The other possibility can be the degradation of source area which results in reduced sediment input to the basin.

An irregular trend of gamma ray is observed above this zone. It is representative of aggradation of a silty and shaley lithology deposited in alluvial overbank facies from 2670m to 2550m. Point counting data also shows an increase in shale and silt percentage fragments in this zone. The detailed interpretation resulted in marking various coarsening upward and fining upward sequences in this zone as well.

From 2550m another well-defined coarsening upward sequence CU_5 is observed which can be related to increased amount of transverse sediment input from locally uplifted basement. These observations of increased sediment input from amphibolitic basement also resemble to studies based on petrography and XRD data. FU_5 is a fining upward sequence showing increase in shale content and retreat of the fan deposits.

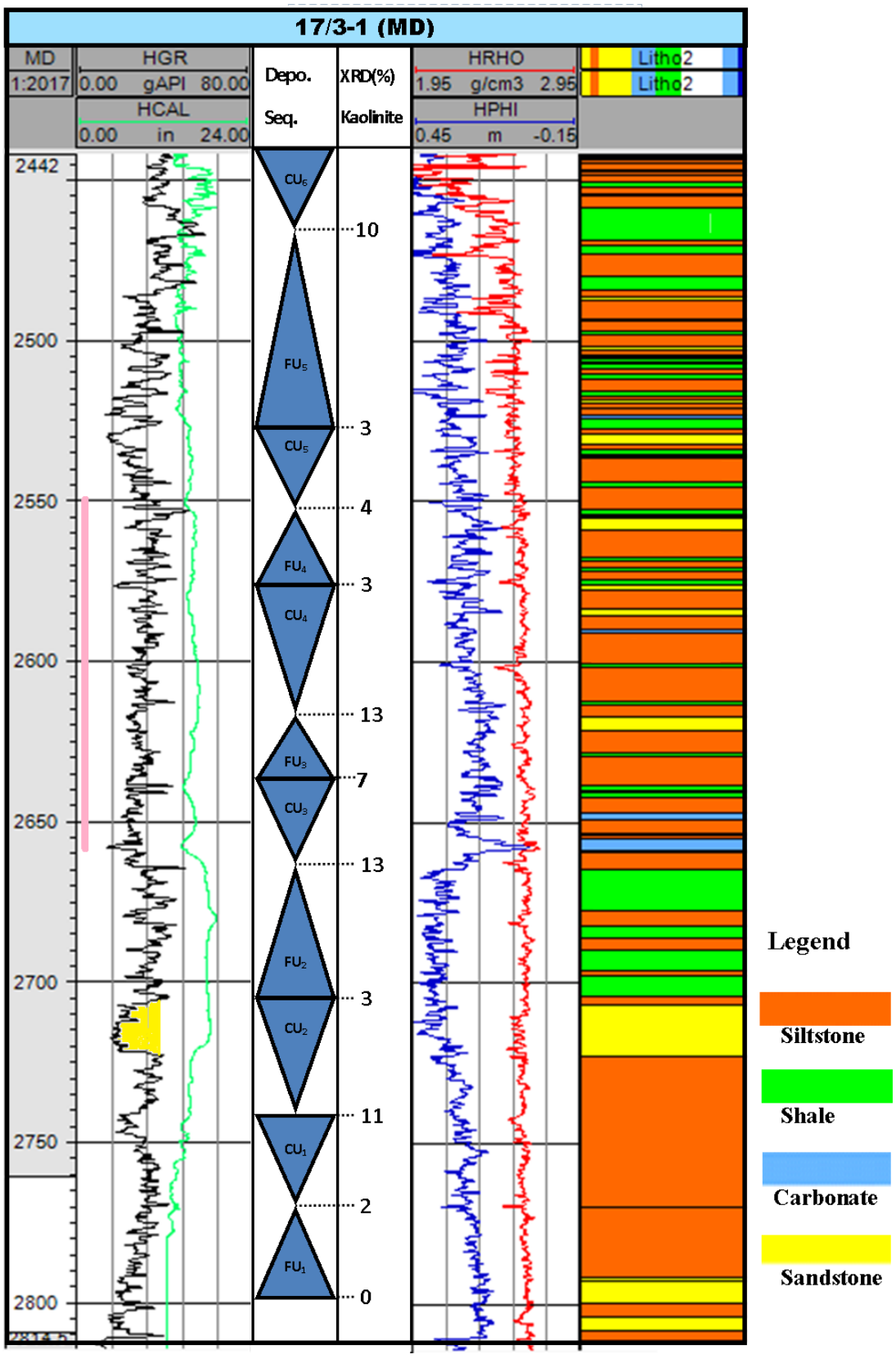

Figure 54: Showing depositional tracts in vertical succession in rift basin and interpreted lithology on the basis of gamma ray log. Pink vertical line demarcates irregular trend. Yellow zone on gamma ray is marked as channel sands.

6.9 Bryne Formation:

The observed sedimentary structures and lithology of Bryne Formation shows the deposition in delta plain/tidal flats where the effects of tides are quite significant. Tidal flats can be divided into supratidal and intertidal flats, above normal high tide and between high and low tide levels respectively (Readings, 2003). The presence of wavy bedding at level 2417.7m indicates deposition in sand dominated mid-tidal flat environment. The occurrence of sand lenses (Fig19b) which are associated to lenticular bedding shows that proportion of mud has increased.

The deposition of coal is interpreted in the interdistributory area of delta plain i.e. in the tidal swamp at level 2415.4(Fig 19).

Ripples are mostly observed in the upper part of Bryne Formation. These current generated sand bedforms usually predominate in low tidal flat zone. So the presence of ripples indicates most probably deposition in low tidal flat zone. Herring bone cross stratification is noticed at the top of Bryne Formation at 2410.2m (Fig.20a), also an indicative of low tidal flat environment where bedload is dominant transport process. In herring bone cross stratification sediments deposited during flood tide dip in opposite direction to ebb tide (Boggs, 1987).

Bryne Formation shows complete transformation of feldspars to clays possibly related to diagenetic alteration. Due to the absence of feldspars it was difficult to come up with source suggestions for these sediments. Petrographic studies of Bryne formation also didn't show any lithic fragments, direct indicators of possible source area. Vestland Group is equivalent to Brent group which is formed by the erosion products of recycled Triassic sandstones (Zeigler, 1970). Bryne Formation of middle Jurassic is directly overlying Triassic sediments, an indication of erosion of Lower Jurassic/Upper Triassic strata. The source of the sediments can be Triassic/Lower Jurassic sediments from the south, eroded as a result of pre volcanic uplift of southern North Sea. SEM studies revealed the presence of both the detrital and authigenic kaolinite. Detrital kaolinite can be attributed to the alteration of feldspars during transportation from pre volcanic domal uplift of area in the south. The lower part of Bryne Formation is dominated by shales rich in pyrite. XRD analysis shows that pyrite is accompanied by saponite. The high pyrite content at the base of Bryne formation is indicative of anoxic environment probably in tidal swamp. Sedimentary logs also show absence of bioturbation in clay rich zones indicative of anoxic environment (Fig.18 and 21).In anoxic

environment Fe is extracted from smectite and replaced by Mg during the process of pyrite formation. Replacement of Fe rich smectite (nontronite) by Mg rich smectite (saponite) is accompanied by formation of pyrite (Breeman, 1979). But the probable occurrence of nontronite and saponite suggest possible altered basic, ultrabasic rocks as the provenance (Dos Anjos et al., 2010). These basic, ultrabasic rocks can be from Fennoscandian Sheild. Weathering of amphiboles can result in saponite and nontronite formation (Proust, 1985). Triassic sediments may contain amphiboles which may have not altered chemically during Triassic. As actinolite/hornblende is observed under SEM analysis in Triassic sediments. So recycling of these sediments can result in the formation of saponite. Another possibility for the smectite precursor mineral which later changed to saponite can be volcano clastic material or volcanic ash. Jurassic domal uplift was accompanied by volcanic activity at different volcanic centres in Forties Volcanic Province (Smith et al,. 1993). Egersund Volcanic Complex located in the south or Fisher Bank Volcanic Centre in southeast of study area can be probable source for the smectite rich clays (Fig.8). The age of the Egersund Volcanic Complex is interpreted as 170±2 Ma (Smith et al,. 1993). On the basis of the age of Egersund Complex and its southward location in close vicinity of study area, it is tempting to suggest that Egersund Complex is one of possible sources for the Bryne Formation. As Bryne Formation is interpreted to be deposited in coastal plain settings and overlain by shallow marine sediments so it can be assumed that this sequence represents the retreat of delta or sealevel rise.

6.10 Sandnes Formation:

The lower part of Sandnes Formation is dominated by coastal/tidal facies like Bryne Formation shown in Fig 16. From 2405m, a more sand dominated interval is observed. The lower part of this sand dominated zone is calcite cemented. The source for the calcite cement in shallow marine sandstones cannot be outside the sandstone due to lack of transport mechanisms for dissolve calcium carbonate. Biogenic carbonate will be the important source of calcite cement in shallow marine environments (Walderhaug and Bjørkum, 2009). The sands in this zone are mostly friable, homogenous dominating the zone upwards from the 2405m to 2401m (Fig.20 & 21). These occurrences of homogenous sands can also be result of fast deposition related to storm waves acting on the sediments on beach and deposit them seaward on the shoreface (Boggs, 1987). However if this sands were deposited from beach deposits, then it would have higher quartz percentage in XRD as well as in point counting. As the beach sands are well sorted by wave activity. The base of this zone has relatively high

calcite values compared to top (Appendix 5) suggesting that this zone was influenced by more terrestrial influx which hindered the carbonate deposition. Quartz cementation in the sandstones analyzed in thin section (Appendix 2) may be due to argillization of volcanic ash (Jeans et al., 2000). The bioturbated sediments with small clay laminae are observed above homogenous sand interval at 2399.8m (Fig.21b). Shale rich interval with sand lenses and rootlets (Fig 22b &22c) again indicates the change of environment to be dominated by deltaic facies at top of the Sandnes Formation showing a possible retreat in sea-level. Fluctuations in sea level can be observed from Bryne to top of Sandnes Formation.

Sandnes formation which is equivalent to Hugin Formation in southern Viking Graben represents the trangression of sea. It is overlying tidal influenced Bryne formation. During core logging an overall upward coarsening sequence is observed, an indicative of marine transgression. Few thin sections from the homogenous sands show the occurrence of polycrystalline quartz (Appendix 2). The polycrystalline quartz shows metamorphic influx. Number of crystal units per single polycrystalline grain is greater than five (Appendix 2), showing gneisses as its parent material (Basu et al., 1975). Feldspars in Sandnes formation have been depleted by mostly diagenetic alteration. Pyrite rich clay with saponite is observed at the top of Sandnes formation. Saponite can have detrital or authigenic origin. The origin of saponite and smectite have already been interpreted. Phlogopite is also observed under SEM studies in pryrite rich clay at 2391.5m . The presence of phlogopite also directs the attention to Egersund sub-Basin as the source material for these sediments. The occurrence of phlogopite/leucite-bearing dykes point to alkaline magmatism which was active in Egersund sub-Basin in Pliensbachian (Furnes et al,. 1982). However the age of magmatism by Smith et al, (1993) on the basis of Ar40-Ar39 analysis phlogopites of Egersund Complex is 170±2Ma. The presence of alkaline magmatic rocks rich in phlogopite and occurrence of phlogopite, saponite in clays of Sandnes Formation makes the Egersund Volcanic Complex a possible source for sediments.

The studied basement has not developed any weathering profile. If there was any it was eroded prior to Triassic deposition.The Triassic strata is deposited in tectonically active rift basin where little time was provided for the weathering of bedrock/provenance in uplifted source areas. Also the climate was arid to semi-arid at the time of deposition of these sediments. Mostly the sediments are predicted to be sourced from proximal provenance, so little chemical alteration during transit, indicating rapid erosion and deposition. The sediments are deposited in continental settings in alluvial fans and floodplains as relatively fine grained

siltstones, shales and few sand beds. On this basis it can be assumed that sediments would have poor sorting and low porosity. Diagenetic alterations are also not remarkable.

7 Conclusions:

Weathering of the amphibolitic basement, the transition from basement to Triassic and Jurassic strata in well 17/3-1, the possible source for Triassic sediments and transportation and deposition of these sediments in rift basins has been studied on the basis of results from mineralogical analysis (Thin sections and XRD) and sedimentary core logging. Following conclusions can be drawn:

1) Basement comprised of amphibolite is fractured and sheared. Both the ductile and brittle shearing has affected the basement. Calcite and quartz veins are interpreted to precipitate as fracture filling secondary minerals. The extensional movement along Hardangerfjord Shear Zone in Devonian,the strike slip movement due to Variscan Orogeny along Sorgenfrei-Tornquist Zone, Permian brittle faulting resulting due to movements on major faults in North Sea can be few reasons for observed striations and fractures on basement.
2) The sediments lying immediately above the basement, revealed no observable signs of weathering profile. The higher XRD% of plagioclase and absence of secondary clay minerals (Kandites) which should have formed at the expense of plagioclase is indicating that weathering profile has not developed.
3) Smith Bank Formation is overlying the basement. The lower 25m of Smith Bank Formation from 2810m-2785m is interpreted to be deposited in an isolated basin as transverse fan deposits. On the basis of high amount of quartz and feldspar grains embedded in mudclasts, higher plagiclase XRD%, higher striated calcite percentage and higher amphibolitic clasts it is assumed that this zone is mostly sourced by proximal, local uplifted amphibolitic basement. Low chlorite XRD% can indicate otherwise. Sediments may have travelled enough distance for chlorite weathering. Greenschist facies of Sågvagen Formation (Volcanic origin) on the Fennoscandian Sheild can be the other possible source.
4) From 2780m-2580m mostly the sediments are deposited as stream and stream flood deposits/floodplains by axially flowing meandering river between linked half grabens. Gamma ray log trends also indicate the similiar depositional conditions. Mudclasts have low muscovite and biotite flakes and more clayey content. Chlorite to kaolinite ratio is also low indicating sediments travelled enough for alteration of primary minerals (proximal source). K-feldspar is not a constituent mineral of basement so its occurrence in this part points to another source than local amphibolitic basement.

Considering the structural setting and basinal position of the well 17/3-1, Utsira High cannot be the provenance of this zone. Precambrian granitic basement rocks and Sunnhordland Igneous Complex can be other probable sources.

5) The zone from 2580m-2490m is again majorly being sourced by local amphibolitic basement. This zone defines an intrabasinal tectonic activity resulting in uplifting of basement. The increased sediment input from local basement as transverse alluvial fans, resulted in choking or forcing lateral change in path of axial river away from the point of study. The increased percentage of amphibolitic clasts, striated calcite fragments and plagioclase to K-feldspar ratio show that amphibolitic basement was main source.
6) From 2490m-2440m the sediments are deposited mostly by axial flowing rivers. The upward decrease in plagioclase XRD% and increase in kaolinite XRD% shows progressive increase of weathering. On this basis, it is interpreted that basin has become tectonically mature and also climate may have changed resulting in deposition of mineralogically more mature sediments and consequent degradation of feldspars.
7) Bryne Formation is composed of interbedded sandstones, coals and shales. It is interpreted to be deposited in delta plain/tidal flat settings. XRD results show complete transformation of feldspars to clays. The shale rich sediments are also rich in pyrite. Saponite is the clay mineral observed in XRD analysis. Saponite may have formed by weathering of amphiboles. Saponite can form by the alteration of nontronite accompanied by pyrite formation. The possible source for smectite can be recyclying of Triassic sediments deposited in south of study area or by alteration of volcanic ash from Egersund Volcanic Complex.
8) Sandnes Formation is dominated by sandstones with ocassional shales and peat beds. It is interpreted to be deposited in shallow marine to tidal settings. It is overlying non marine, tide dominated Bryne Formation thus indicating a rise in sea level. Sands are homogenous and friable resulting due to fast deposition related to storm activity. Feldspars have also been completely transformed. This formation was also being sourced from South, Egersund Volcanic Complex or Triassic recycled rocks.

References

ABRAMOVITZ, T. & THYBO, H. 1998. Seismic structure across the Caledonian Deformation Front along MONA LISA profile 1 in the southeastern North Sea. *Tectonophysics,* 288**,** 153-176.

ANDRESEN, A. & FÆRSETH, R. 1982. An evolutionary model for the southwest Norwegian Caledonides. *American Journal of Science,* 282**,** 756-782

ANDERSEN, T. B., TORSVIK, T. H., EIDE, E. A. OSMUNDSEN, P. T. & FALEIDE, J. I. 1999. Permian and Mesozoic extensional faulting within the Caledonides of central south Norway. *Journal of the Geological Society,* 156**,** 1073-1080.

BASSETT, M. G. 2003. Sub-Devonian geology. 61-63 in The Millennium Atlas: petroleum geology of the central and northern North Sea. *Evans, D, Graham, C, Armour, A,and Bathurst, P (editors and co-ordinators). (London: The Geological Society of London.)*

BASU, A., STEVEN , W. Y., LEE, J., SUTTNER, W., CALVIN, J. AND GRED H.M. re-evaluation of the use of undulatory extinction and polycrystallinity in detrital quartz for provenance interpretation. *Journal of sedimentary petrology,* 45**,** 873-882.

BJØRLYKKE, K. & AAGAARD, P. 1992. Clay Minerals in North Sea Sandstones.

BREEMAN, O., VAN., PIDGEON, R.T. AND JOHNSON, M.R.W. (1974) Precambrian and Paleozoic pegmatites in the Moines of northern Scotland.J. Geol. Soc . London 139, 493-509.

BLAIR, T. C. 1987. Tectonic and hydrologic controls on cyclic alluvial fan, fluvial and lacustrine rift-basin sedimentation, Jurassic-Lowermost Cretaceous Todos Santos Formation, Chiapas, Mexico. *Journal of Sedimentary Petrology*, 57, 845-862.

BOGGS, S. 1995. *Principles of sedimentology and stratigraphy*, Prentice Hall Englewood Cliffs.

BOGGS,S. J. 1987. Principles of sedimentology and stratigraphy. 2nd edition.

BREEMEN, N. V. 1979. Magnesium-Ferric iron replacement in smectite during aeration of pyritic sediments. *Clay Minerals (1980),* 15**,** 101-110.

CLEMMERSEN , L.B., STEEL , R . J. AND JACOBSEN, V.W. 1980: Some aspects of Triassic sedimentation and basin devolpment : East Greenland, North Scotland and North Sea. In, The sedimentation of North Sea Reservoir Rocks. *Norwegian Petroleum Society* , Geilo.

COWARD, M. 1995. Structural and tectonic setting of the Permo-Triassic basins of northwest Europe. *Geological Society, London, Special Publications,* 91**,** 7-39.

CROSSLEY, R. 1984. Controls on sedimentation in the Malawi Rift, Central Africa, Sedimentary Geology, 40, 73-88.

DANUOR, S., DZIRASAH, W. & PECK, J. 2012. Determination of the Source and Depositional Environment of Sediments of Lake Bosumtwi using X-Ray Diffraction (XRD) Techniques.

DEEGAN, C. T. & SCULL, B. J. 1977. *A standard lithostratigraphic nomenclature for the Central and Northern North Sea,* HMSO.

DEEGAN, C. E. & SCULL, B. J. 1977. A proposed standard lithostratigraphic nomenclature for the central and northern North Sea. *Institute of Geological Sciences,* Report, No. 77/25; Norwegian Petroleum Directorate Bulletin, no. 1.

DOS ANJOS, C. W. D., MEUNIER, A., GUIMARÃES, E. M. & EL ALBANI, A. 2010. saponite-rich black shales and nontronite beds of the permian irati formation: sediment sources and thermal metamorphism (paraná basin, brazil). *Clays and Clay Minerals,* 58**,** 606-626.

DURAND, N., MONGER, H. C. & CANTI, M. G. 2010. Calcium carbonate features. *Interpretation of micromorphological features of soils and regoliths. Elsevier, Amsterdam***,** 149-194.

EBINGER, C. & SCHOLZ, C. A. 2011. Continental Rift Basins: The East African Perspective. *Tectonics of Sedimentary Basins.* John Wiley & Sons, Ltd.

EIDE, E. A. 2001. Crystalline basement Ar40/Ar39 ages from North and Norwegian sea cores – reexamination and consequences for the Early Palaeozoic SW Baltica margin. 21 in Abstracts: Early Palaeozoic Palaeogeographies and Palaeobiogeographies of Western Europe and North Africa.

FALT, L.M., HELLAND, R., JACOBSEN .W.V & RENSHAW, D. 1989. Correlation of transgressive-regressive depositional sequence in the Middle Jurassic Brent/Vestland Group megacycle, Viking Graben, Norwegian North Sea. Norwegian Petroleum Society, 191-200.

FÆRSETH, R. B. 1982. Geology of Southern Stord and Adjacent Islands, Southwest Norwegian Caledonides. Nor. Geol, 57-112.

FÆRSETH, R., GABRIELSEN, R. & HURICH, C. 1995. Influence of basement in structuring of the North Sea basin, offshore southwest Norway. *Norsk Geologisk Tidsskrift*, 75**,** 105-119.

FÆRSETH, R. 1996. Interaction of Permo-Triassic and Jurassic extensional fault-blocks during the development of the northern North Sea. *Journal of the Geological Society*, 153**,** 931-944.

FALEIDE, J. I., BJØRLYKKE, K. & GABRIELSEN, R. H. 2010. Geology of the Norwegian continental shelf. Petroleum Geoscience. Springer,467-499.

FAULDS, J. E. & VARGA, R. J. 1998. The role of accommodation zones and transfer zones in the regional segmentation of extended terranes. SPECIAL PAPERS-GEOLOGICAL SOCIETY OF AMERICA, 1-46.

FISHER,M.J. & MUDGE,D.C. Triassic K.W. GLENNIE (eds) FOURTH EDITION, Petroleum Geology of the North Sea, Fourth Edition,212-244.

FÒRSETH, R., KNUDSEN, B.-E., LILJEDAHL, T., MIDBØE, P. & SØDERSTRØM, B. 1997. Oblique rifting and sequential faulting in the Jurassic development of the northern North Sea. *Journal of Structural Geology*, 19**,** 1285-1302.

FOSSEN, H. & HURICH, C. A. 2005. The Hardangerfjord Shear Zone in SW Norway and the North Sea: a large-scale low-angle shear zone in the Caledonian crust. *Journal of the Geological Society,* 162**,** 675-687.

FOSSEN ,H., PEDERSEN, B.R., BERGH,S. & ANDRESEN,A.2008.Creation of mountain chain.RAMBERG, I.B., BRYHNI, I., NØTTVEDT, A. & RANGNES, K. (eds.) 2008, The Making of a Land-Geology of Norway. Trondheim. Norwegian Geological Association,178-231

FROST, R. T. C., FITCH F. J. & MILLER J. A.1981. The age and nature of the crystalline basement of the North Sea Basin. In: Illing L. V., Hobson G. D. (eds) Petroleum Geology of the Continental Shelf of North-West Europe. Heyden, London, 43–57.

FURNES, H., ELVSBORG, A. & MALM, O. A. 1982. Lower and Middle Jurassic alkaline magmatism in the Egersund sub-Basin, North Sea. Marine Geology, 46, 53-69.

GABRIELSEN, R., FÆRSETH, R., STEEL, R., IDIL, S. & KLØVJAN, O. 1990. Architectural styles of basin fill in the northern Viking Graben. *Tectonic Evolution of the North Sea Rifts. Clarendon Press, Oxford***,** 158-179.

GAWTHORPE, R. & LEEDER, M. 2000. Tectono‐sedimentary evolution of active extensional basins. *Basin Research,* 12**,** 195-218.

GOLDSMITH, P., RICH, B. & STANDRING, J. 1995. Triassic correlation and stratigraphy in the south Central Graben, UK North Sea. *Geological Society, London, Special Publications,* 91**,** 123-143.

GIBBS, A. 1987. Development of extension and mixed-mode sedimentary basins. *Geological Society, London, Special Publications,* 28**,** 19-33.

HARALD, B., HANS,I., CHRISTIAN,M., MAGNUS & ROBERT ,W.2001. Sedimentary Environments Offshore Norway-Paleozoic to Recent edited by O.J Martinsen and T. Dreyer. NPF Special Publication 10, pp.7-37, Published by Elsevier Science B.V., Amsterdam.Norwegian Petroleum Society (NPF), 2001.

HEEREMANS, M. & FALEIDE, J. I. 2004. Late Carboniferous-Permian tectonics and magmatic activity in the Skagerrak, Kattegat and the North Sea. *SPECIAL PUBLICATION-GEOLOGICAL SOCIETY OF LONDON,* 223**,** 157-176.

http://epgeology.com/

HUSMO, T., HAMAR, G.P., HØILAND, O., JOHANNESSEN, E.P,, RØMULD, A., SPENCER, A.M., & TITTERTON, R. 2002. Lower and Middle Jurassic. 129-155 in The Millennium Atlas: petroleum geology of the central and northern North Sea. Evans, D, Graham, C, Armour, A, and Bathurst, P (editors and co-ordinators). (London: *The Geological Society of London*).

JEANS, C., WRAY, D., MERRIMAN, R. & FISHER, M. 2000. Volcanogenic clays in Jurassic and Cretaceous strata of England and the North Sea Basin. *Clay Minerals,* 35**,** 25-25.

LARSEN , B.T., OLAUSSEN, S., SUNDVOLL, B & HEEREMANS, M. 2008 Volcanoes and faulting in an arid climate. RAMBERG, I.B., BRYHNI, I., NØTTVEDT, A. & RANGNES, K. (eds) 2008. *The making of land - Geology of Norway.* Trondheim. Norwegian Geological Association**,** 260-303.

LEEDER, M.R. 1975. Pedogenic carbonates and flood sediment accretion rates: a quantitative model for alluvial arid-zone lithofacies. *Geol. Mag. 112,* 3**,** pp. 257-270.

LEEDER, M. & GAWTHORPE, R. 1987. Sedimentary models for extensional tilt-block/half-graben basins. *Geological Society, London, Special Publications,* 28**,** 139-152.

LIPPARD, S. & MITCHELL, J. 1980. Late Caledonian dolerites from the Kattnakken area, Stord, SW Norway, their age and tectonic significance. *Nor. Geol. Unders,* 358**,** 47-62.

MARTINS-NETO, M. & CATUNEANU, O. 2010. Rift sequence stratigraphy. *Marine and Petroleum Geology,* 27**,** 247-253.

MCCANN, T., KIERSNOWSKI, H., KRAINER, K., VOZÁROVÁ, A., PERYT, T., OPLUSTIL, S., STOLLHOFEN, H., SCHNEIDER, J., WETZEL, A. & BOULVAIN,

F. The Geology of Central Europe. Volume 1: Precambrian and Palaeozoic. Geological Society, London, 2008.pp. 419.

MOORE, D.M. & REYNOLDS, R.C., 1997, X-ray diffraction and the identification and analysis of clay minerals: Oxford, Oxford University Press, xviii, 378 s. p.

NESBITT, H. & YOUNG, G. 1984. Prediction of some weathering trends of plutonic and volcanic rocks based on thermodynamic and kinetic considerations. *Geochimica et Cosmochimica Acta,* 48**,** 1523-1534.

NESBITT, H. & YOUNG, G. M. 1989. Formation and diagenesis of weathering profiles. *The Journal of Geology***,** 129-147.

NØTTVEDT, A., JOHANNESSEN, E. P. & SURLYK, F. 2008. The mesozoic of western Scandinavia and East Greenland. *Episodes,* 31**,** 59-65

NPD factpages: http://factpages.npd.no/factpages/

NYSTUEN, J.P., MORK, A., MULLER.R & NOTTVEDT.A. 2008. From desert to alluvial plain-from land to sea. RAMBERG, I.B., BRYHNI, I., NØTTVEDT, A. & RANGNES, K. (eds.) 2008, The Making of a Land-Geology of Norway. Trondheim. Norwegian Geological Association, pp. 330-335.

OLA, F., RONALD, S., ODLEIV, O., JAN, L., JOCHEN,K., ELSE, M.G., MACRO, B., HORST, Z., AXEL, M. & CHRISTOPH ,V.2013. Chemical weathering of basement rocks in Norway. What do we know and what are the implications for the petroleum industry? NGF Abstracts and Proceedings, No 2, 2013.

PARRISH, J.T. ZIEGLER,A.M. SCOTESE,C.R.1982.Rainfall patterns and the distribution of coals and evaporites in the Mesozoic and Cenozoic. Palaeogeography Palaeoclimatology,Palaeoecology 40, 67–101.

PRETO, N. KUSTATSCHER, E. & WIGNALL, P. B. 2010. Triassic climates—State of the art and perspectives. *Palaeogeography, Palaeoclimatology, Palaeoecology,* 290**,** 1-10.

PROUST, D. CAILLAUD, J. FONTAINE, C. 2006. Clay minerals in early amphibole weathering: tri- to dioctahedral sequence as a function of crystallization sites in the

amphibole, the clay Minerals Society, Clays and Clay Minerals, Vol. 54, No. 3, 351-362.

PROUST, D. 1982. ALTERATION OF METAMORPHIC AN AMPHIBOLITE FROM MASSIF CENTRAL, FRANCE. *Clay Minerals,* 17**,** 159-173.

PROUST, D. 1985. Amphibole weathering in a glaucophane-schist (Ile de Groix, Morbihan, France). *Clay Minerals,* 20**,** 161-170.

READING, H. G. 2009. *Sedimentary environments: processes, facies and stratigraphy,* Wiley-Blackwell.

ROBERTS, A., YIELDING, G., KUSZNIR, N., WALKER, I. & DORN-LOPEZ, D. 1995. Quantitative analysis of Triassic extension in the northern Viking Graben. *Journal of the Geological Society,* 152**,** 15-26.

ROSENDAHL, B. R. 1987. Architecture of continental rifts with special reference to East Africa. *Annual Review of Earth and Planetary Sciences,* 15**,** 445.

PROSSER, S. 1993. Rift-related linked depositional systems and their seismic expression. *Geological Society, London, Special Publications,* 71**,** 35-66.

RIDER, M. A. M., K 2011. The Geological Interpreted of Well logs. *Rider-French Consulting Limited,* 3.

STEEL, R. & RYSETH, A. 1990. The Triassic—Early Jurassic succession in the northern North Sea: megasequence stratigraphy and intra-Triassic tectonics. *Geological Society, London, Special Publications,* 55**,** 139-168.

RYSETH, A. 2001. Sedimentology and palaeogeography of the statfjord formation (Rhaetian-Sinemurian), North Sea. *In:* OLE, J. M. & TOM, D. (eds.) *Norwegian Petroleum Society Special Publications.* Elsevier.

TARDY, Y., BOCQUIER, G., PAQUET, H. & MILLOT, G. 1973. Formation of clay from granite and its distribution in relation to climate and topography. *Geoderma,* 10**,** 271-284.

THOREZ, J. & THOREZ, J. 1976. *Practical identification of clay minerals: a handbook for teachers and students in clay mineralogy*, Lelotte.

TORSVIK, T., STURT, B., SWENSSON, E., ANDERSEN, T. & DEWEY, J. 1992. Palaeomagnetic dating of fault rocks: evidence for Permian and Mesozoic movements and brittle deformation along the extensional Dalsfjord Fault, western Norway. *Geophysical Journal International,* 109**,** 565-580.

SCHLISCHE, R. W. & OLSEN, P. E. 1990. Quantitative filling model for continental extensional basins with applications to early Mesozoic rifts of eastern North America. *The Journal of Geology***,** 135-155.

SMITH, K. & RITCHIE, J. Jurassic volcanic centres in the Central North Sea. Geological Society, London, Petroleum Geology Conference series, 1993. Geological Society of London, 519-531.

SLAGSTAD, T., DAVIDSEN, B. & DALY, J. S. 2011. Age and composition of crystalline basement rocks on the Norwegian continental margin: offshore extension and continuity of the Caledonian–Appalachian orogenic belt. *Journal of the Geological Society,* 168**,** 1167-1185.

WALDERHAUG, O. & BJØRKUM, P. 1998. Calcite cement in shallow marine sandstones: growth mechanisms and geometry. *Carbonate Cementation in Sandstones: Distribution Patterns and Geochemical Evolution***,** 179-192.

WARR,L.N. 2012 Geological History of Britain and Ireland, Second Edition. Edited by Nigel Woodcock, Rob Strachan.

VAN STAAL, C.R., DEWEY, J.F., MAC NIOCAILL, C. & MCKERROW, W.S. 1998. The Cambrian-Silurian tectonic evolution of the northern Appalachians and British Caledonides: History of a complex west and southwest Pacific-type segment of Iapetus. In: BLUNDELL, D.J & SCOTT, A. C. (eds) Lyell: the Past is the Key to the Present. Geological Society, London, Special Publications,143,199-242.

VAN WAGONER, J., MITCHUM ,J. R., CAMPION, K., & RAHAMANIAN, V.1990. Siliciclastic sequence stratigraphy in well logs, core sand outcrops: concepts for high-resolution correlation of time and facies. *Tulsa: American Association of Petroleum Geologists*. Methods in Exploration Series 7, p. 55.

VOLLSET, J., DORE, A. G. 1984. *A revised Triassic and Jurassic lithostratigraphic nomenclature for the Norwegian North Sea*,38-40.

WATSON, M. P., HAYWARD, A. B., PARKINSON, D. N. & ZHAN6, Zh. M. 1987. Plate tectonic history, basin development and petroleum source rock deposition inshore China. Marine and Petroleum Geology, 4, 205-225.

WATTERSON, J. 1986. Fault dimensions, displacements and growth. *Pure and Applied Geophysics*, 124**,** 365-373.¨

WEIMER, P. POSAMENTIER, H.W. (EDS.), 1993. Siliciclastic Sequence Stratigraphy. AAPG Memoir 8, p. 292.

WILLIAMS, G. D. 1993. Tectonics and seismic sequence stratigraphy: an introduction. *Geological Society, London, Special Publications*, 71**,** 1-13.

WILLIAMS, T. J. A NEEDLE IN THE X-RAY HAYSTACK: DETECTION LIMITS IN POWDER X-RAY DIFFRACTION OF GEOLOGIC MATERIALS. 2007 GSA Denver Annual Meeting, 2007.

WORDEN, R. & MORAD, S. 2003. *Clay minerals in sandstones: controls on formation, distribution and evolution*, Wiley Online Library.

ZIEGLER, P. A. 1990. Tectonic and palaeogeographic development of the North Sea rift system. *In: Blundell D. J., Gibbs A. D. (eds) Tectonic Evolution of the North Sea Rifts. Oxford University Press, Oxford***,** 1–36.

Appendices

Appendix 1: Thin Section mineral counting results for Smith Bank Formation

Smith Bank Formation											
Depth (m)	Shale (%)	Siltstone (%)	Sandstone (%)	Mudclast (%)	Q(P) Fragments (%)	Number of crystals in 1 Q(P)	Striated Calcite (%)	Calcite (%)	Dolomite (%)	Amphibolite clasts (%)	Pyrite (%)
2445	72.6	5.5	8	6.7	1.8			1.8		0.4	0.6
2465	14.9	0.5	6.3	71.1			2.2		0.5	4	
2490	12.2	6.3	43.4	37.5				0.4			
2510	3.5	1.7	26.1	55.2	0.4		2.2	3.5	2.2	4.8	
2530	3.2		8.8	68	12		0.8	3.2		4	
2540	10.6		18.9	48.4	6		1.5	6.8		7.5	
2560	2.1	7.3	15.7	28.4	12.6	>5	5.2	8.4	1	16.8	
2570	3.5	0.7	28.3	36.5	12.7	>5	4.9			12	
2580	6.6	1.8	9.4	61.3			3.7	0.9		15	
2600	30.7	4.6	33.8	24.6	4.6	2-5				1.5	
2620	21.1	9.9	32.9	24.8			0.6	3.7	4.3	1.2	
2640	12.5	7	44	28.8				4.3	2.1	1	
2660	24.8	23.7	37.2	10.7	2.2	5			1.1		
2680	21.1	10.2	41.6	17.5				6.5	2.9		
2700	16.4	18.7	36.9	20.4				3.9	3.4		
2720	15.7	20	35.8	34.4			0.3	3.5			
2740	31.8	22.3	30.7	6.7	1.1		1.6	5	0.5		
2760	8.9	1.1	45.1	31.6	3.9	>5	1.6	5.6	1.8		
2780	15	3.2	37	33			3.2	5.1		0.6	0.6
2790	12.05	10.2	36	31	2.3	>5	21.1			5.8	
2800	8.7		19	36.5	2.3	>5	21.4			11.9	

Appendix 2: Thin Section mineral counting results for Bryne and Sandnes Formation

Bryne Formation											
Depth	Quartz (M) (%)	Quartz (P)(%)	Matrix(%)		Cement(%)		Muscovite (%)	Coal(%)	Pyrite(%)	Porosity (%)	Dolomite(%)
			Kaolinite	Illite	Quartz	Calcite					
2412.9	71.5	1	5.2	3.5		3.5	0.7			11.2	
2417.6	57.6		11.3			17.9		6.6	4.3	0.3	

Sandnes Formation											
Depth	Quartz (M) (%)	Quartz (P)(%)	Number of crystals in 1 Q(P)	Matrix(%)		Cement(%)		Muscovite (%)	Coal(%)	Pyrite(%)	Primary (%)	Dolomite(%)
				Kaolinite	Illite	Quartz	Calcite					
2388.1	60.6			23.9				0.3		3.6	7	3.5
2396	68	4.2	>5	8.4		0.8						
2399.6	69.7	3	>5	7.5		2.2				2.2	16.2	
2405.1	61			22.6			3.1	4.3	1	5	2	

Appendix 3 Mineral estimation from bulk XRD for Basement

Basement											
Depths	Mixed layer minerals	Illite/Muscovite	Quartz	Kaolinite	Chlorite	K-Feldspar	Plagioclase	Calcite	Dolomite	Siderite	Pyrite
2815	0	1	19	0	4	0	44	32	0	0	1
2820	0	1	8	0	23	0	46	19	0	0	2
2825	0	1	9	0	21	0	39	29	0	0	2
2830	0	0	9	0	22	0	41	26	0	0	3
2835	0	1	8	0	21	0	47	21	0	0	3
2840	0	2	9	0	36	0	30	21	0	0	2
2849.5	0	0	4	0	36	0	27	30	0	0	2
2852.15	0	0	11	0	41	0	26	19	0	0	3
Average	0	1	9	0	26	0	37	25	0	0	2

Basement core samples												
Depths(m)	M layer Clays.	Ill.	Qtz.	Kaol.	Chlor.	K-feld.	Saponit.	Plag.	Calcite	Dolo.	Siderite	Pyrite
2852,15	0	0	11	0	41	0		26	19	0	0	3
2849,5	0	0	4	0	36	0		27	30	0	0	2
Average	0	0	8	0	39	0		26	25	0	0	3

Basement cutting samples												
Depths(m)	M layer Clays.	Ill.	Qtz.	Kaol.	Chlor.	K-feld.	Saponit.	Plag.	Calcit.	Dolo.	Siderite	Pyrite
2840	0	2	9	0	36	0		30	21	0	0	2
2835	0	1	8	0	21	0		47	21	0	0	3
2830	0	0	9	0	22	0		41	26	0	0	3
2825	0	1	9	0	21	0		39	29	0	0	2
2820	0	1	8	0	23	0		46	19	0	0	2
2815	0	1	19	0	4	0		44	32	0	0	1
Average	0	1	10	0	21	0		41	25	0	0	2

Appendix 4: Mineral estimation from bulk XRD

Smith Bank Formation												
Depths	**Mixed layer Minerals**	**Illite/Muscovite**	**Quartz**	**Kaolinite**	**Chlorite**	**K-Feldspar**	**Saponite**	**Plagioclase**	**Calcite**	**Dolomite**	**Siderite**	**Pyrite**
2440	0	3	45	11	3	3	0	2	22	4	4	4
2450	0	3	25	10	5	4	0	8	31	6	3	5
2460	0	2	33	7	3	4	0	15	19	13	0	3
2470	0	2	23	10	3	5	0	19	15	16	4	3
2480	0	2	22	6	2	3	0	35	15	13	0	2
2490	0	4	17	10	4	5	0	30	13	10	2	5
2500	0	1	24	4	3	3	0	38	16	9	0	2
2510	0	2	17	4	3	6	0	47	10	8	2	2
2520	0	2	30	3	3	4	0	34	17	5	0	2
2540	0	1	24	2	3	6	0	43	19	2	0	2
2550	0	3	20	4	5	7	0	37	20	3	0	2
2555	0	2	32	2	3	6	0	36	18	2	0	0
2560	0	2	24	1	2	15	0	35	18	3	0	1
2565	0	2	34	1	2	14	0	33	12	3	0	0
2570	0	1	36	1	2	13	0	28	14	3	0	2
2575	0	2	28	2	2	10	0	38	16	3	0	0
2580	0	2	30	3	3	9	0	27	19	4	0	2
2585	0	2	25	3	3	14	0	29	19	4	0	2
2590	0	1	33	3	2	6	0	32	17	4	0	2
2595	0	3	15	7	4	14	0	29	20	7	0	2
2600	0	2	23	3	2	15	0	40	10	3	2	1
2605	0	4	26	3	3	17	0	27	12	5	0	2
2610	0	2	37	3	3	6	0	31	12	4	0	2
2615	0	3	26	6	3	11	0	33	11	4	0	2
2620	0	1	33	2	2	7	0	31	17	4	0	2

Smith Bank Formation												
Depths	**Mixed layer Minerals**	**Illite/Muscovite**	**Quartz**	**Kaolinite**	**Chlorite**	**K-Feldspar**	**Saponite**	**Plagioclase**	**Calcite**	**Dolomite**	**Siderite**	**Pyrite**
2625	0	5	20	13	4	7	0	26	16	7	0	2
2630	0	3	22	5	4	9	0	29	16	7	0	4
2635	0	4	21	7	4	6	0	28	18	7	2	3
2640	0	3	19	8	4	7	0	31	13	10	2	4
2645	0	3	21	7	4	9	0	26	13	10	3	5
2650	0	3	23	8	5	8	0	24	14	10	0	5
2655	0	3	20	7	4	5	0	35	15	7	0	4
2660	0	3	21	7	3	15	0	26	14	4	0	6
2665	0	5	17	9	4	14	0	22	15	6	2	6
2670	0	5	19	13	8	8	0	11	7	14	4	12
2675	0	7	18	4	5	13	0	28	16	3	5	2
2680	0	3	36	3	4	6	0	22	16	6	0	4
2685	0	5	21	5	5	12	0	28	14	7	0	3
2690	1	3	24	6	4	7	0	18	32	3	0	2
2700	3	5	21	11	6	7	0	14	10	15	0	8
2715	1	4	14	7	4	8	0	35	20	4	0	2
2720	1	4	22	6	5	7	0	26	18	8	0	3
2725	1	2	11	3	3	9	0	51	16	4	0	2
2730	2	2	15	5	3	5	0	43	12	10	0	4
2735	2	3	22	8	4	5	0	14	23	15	0	3
2740	3	4	21	11	6	7	0	11	18	14	0	6
2745	0	4	16	16	6	7	0	16	22	9	0	4
2750	0	5	20	11	7	6	0	23	8	13	0	9
2755	0	3	25	5	5	7	0	30	13	8	0	4
2765	0	3	16	2	4	13	0	44	15	3	0	1
2775	0	5	16	4	6	7	0	32	23	4	0	2
2780	0	4	19	4	6	8	0	31	22	3	0	2

Depths	Mixed layer Minerals	Illite/Muscovite	Quartz	Kaolinite	Chlorite	K-Feldspar	Saponite	Plagioclase	Calcite	Dolomite	Siderite	Pyrite
2785	0	3	15	2	5	8	0	52	11	2	0	1
2800	0	2	31	3	4	0	0	18	37	3	0	1
2805	0	2	19	2	3	0	0	39	31	2	0	1
2810	0	3	27	0	3	0	0	35	30	0	0	2
Average	**0**	**3**	**22**	**6**	**4**	**7**	**0**	**28**	**19**	**6**	**0**	**3**

Appendix 5: Mineral estimation from bulk XRD

Sandnes Formation												
Depths	Ml Clays.	Ill/Mus.	Qtz.	Kaol.	Chl.	K-Felds.	Sapo.	Plag.	Calc.	Dolo.	Sider.	Pyr.
2388.1	0	5	54	30	0	0	3	0	0	4	0	4
2391.5	0	4	8	20	0	0	19	0	0	0	0	49
2392	0	7	54	21	0	0	4	0	1	0	3	11
2389.8	0	9	52	27	0	0	4	0	0	0	0	9
2398	0	3	67	23	0	0	0	0	3	0	1	2
2399.6	0	0	82	16	0	0	0	0	0	0	0	2
2401.9	0	3	66	23	0	0	0	0	2	1	2	3
2405	0	6	51	25	0	0	3	0	8	0	2	6
2408	0	4	69	16	0	0	3	0	0	0	2	6

Bryne Formation												
Depths	Ml Clays.	Ill/Mus.	Qtz.	Kaol.	Chl.	K-Felds.	Sapo.	Plag.	Calc.	Dolo.	Sider.	Pyr.
2411.7	0	3	76	14	0	0	0	0	4	0	0	3
2417.7	0	6	14	37	0	0	13	0	0	0	0	30

Appendix 6: Mineral estimation from bulk XRD

Bryne Formation					
Depth(m)	Lithology	Framework configuration	Grain Size	Grain Shape	Sorting
2417.6	Sandy shale	Matrix supported	Silt to very fine	Angular to subangular	Poor
2411.6	Shaly sand	Grain supported	Fine	Angular to subangular	Medium

Sandnes Formation					
Depth(m)	Lithology	Framework configuration	Grain Size	Grain Shape	Sorting
2388.1	Sandstone	Grain supported	Medium	Angular to sub angular	Medium
2391.5	Shale	Matrix supported	Clay		Medium
2399.6	Sandstone	Grain supported	Medium	Angular to subangular	Medium
2405.1	Sandstone	Grain supported	Medium	Angular to subangular	Medium

Appendix 7

Logging sheet used for current study

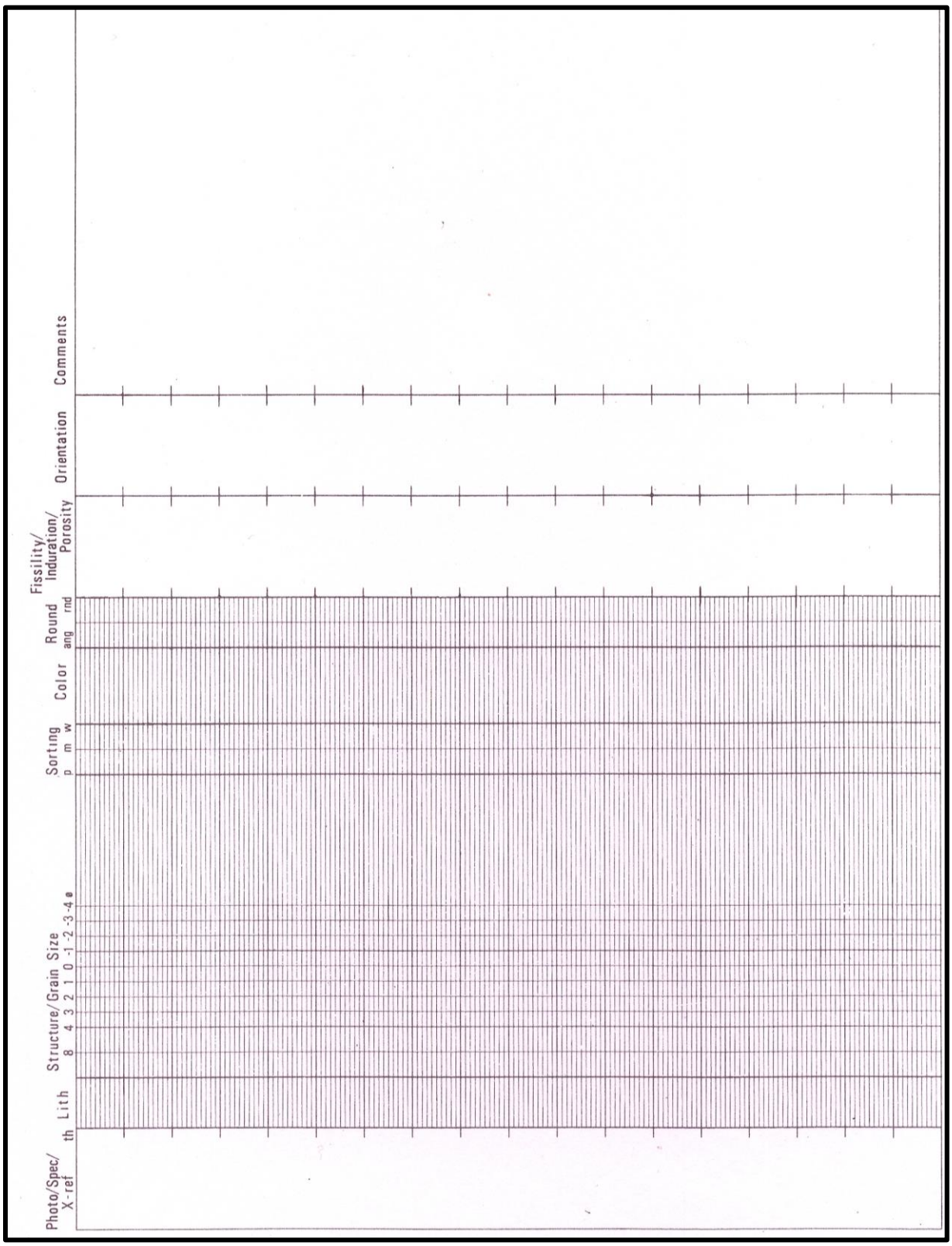

Acknowledgements

First of all I am thankful to ALMIGHTY ALLAH for giving me enough strength and patience to complete my thesis. Blessings of peace on Prophet Muhammad (P.B.U.H).

I would like to express my sincere gratitude to my supervisor Professor Henning Dypvik and Co-supervisor Lars Riber, Department of Geosciences, University of Oslo for their continuous supervision throughout the research with valuable suggestions, guidance and encouragement. I am also thankful to them for their constructive and valuable criticism during reviewing the manuscript.

I wish to express my special gratitude to Martin Aerts for the preparation of samples and his guidance in XRD analysis. Thanks to Berit Løken Berg for her help in SEM analysis.

Many thanks are dedicated to people who worked along me on Utsira project specially Asmar Naqvi, Nicolas Oberhardt for their constructive discussions in this research.

Thanks to Lundin A/S for their financial support during core logging trip to Stavanger and to Norwegian Petroleum Directorate for providing me their core storage unit in Stavanger.

I would like to thank all my class fellows for their support and help during my thesis.

At last, I would like to convey my special gratitude and love to my family, loved ones especially to my mother who have always been supporting and encouraging me throughout my life.

Lastly, thanks to my all friends who came from different countries around the world. Your moral and emotional supports relish me throughout my life.

P.S. ‘‘ Choury kam nae rukde, kam ho he jande ne ☺’’